8-2022

The Development and Analysis of Methods Used to Evaluate American Football Facemasks

Alexander Bina
abina@g.clemson.edu

The Development and Analysis of Methods Used to Evaluate American Football Facemasks

---

A Dissertation
Presented to
the Graduate School of
Clemson University

In Partial Fulfillment
of the Requirements for the Degree
Doctor of Philosophy
Bioengineering.

---

by
Alexander J. Bina
August 2022

Accepted by:
Dr. John D. DesJardins, Committee Chair
Dr. Gregory S. Batt, Committee Chair
Dr. Martine LaBerge, Committee Member
Dr. William Bridges, Committee Member

ABSTRACT

The motivation for this Ph.D. dissertation is to provide football equipment managers, coaches, parents, athletes, and relevant industry personnel with an understanding of the implication a chosen football facemask design will have on the safety of the athlete. As athletes have increased their capacity for speed, size, and strength, so too has the head injury risk increased in American football. To align with the increase in head impact injury in American football, the protective head impact community must expand its capacity to evaluate protective equipment systems. This dissertation focuses specifically on one helmet system component: the football facemask. This dissertation was completed in three steps to evaluate the mechanical characteristics of football facemasks: 1.) a review of literature regarding existing methods used to evaluate protective headgear in American football; 2.) an evaluation of the industry standard for evaluating the impact performance of a helmet system made up of a football facemask, an outer shell, and internal padding; and 3.) an isolated evaluation of the structural stiffness of existing football facemasks designs. The results demonstrated that the existing methods used to evaluate football facemask performance lack the sensitivity necessary to differentiate the performance of various facemask designs. The contribution of this dissertation to the field is a novel method, including a patented apparatus and protocol, to characterize the structural stiffness of football facemasks to set up future work examining the relationship between the stiffness and impact performance.

DEDICATION

To my father, who taught me humor, and to my mother, who covered everything else.

ACKNOWLEDGMENTS

Carrying out research is like raising a child: it takes a village. This dissertation was no exception. I'd like to acknowledge several groups of people without whom these words could not have been written:

Thank you to Dr. DesJardins and Dr. Batt, who continued to believe in me long after I stopped believing in myself. Your perseverance and patience with me quite literally pulled this thing out of the gutter.

Thank you to the CHIPMUNKs, Nick, Steve, Tim, Ally, Noah, and Tessa, for somehow matching my chaotic schedule to aid in data collection, sorting, and analysis while politely laughing at my hilarious jokes. You truly were mentored undergrads needing knowledge.

Thank you to Jay Elmore and Green Gridiron for supplying the industry perspective that served as the impetus for this project. Thank you also for supplying over 1000 facemasks over the course of this project. Without your insight and push to address the needs of multiple facemask market stakeholders, this project never would have reached the scope it reached.

Thank you to the Clemson University football equipment staff, Abe Reed and Nick Yarid, for supplying additional industry perspectives and additional used facemasks.

Thank you to the staff in Newman Hall, Bob, Tanner, Michael, Pat, Dr. Darby, and Franklin, for opening up doors, installing equipment, and setting up schedules throughout this project.

TABLE OF CONTENTS

Page

Table of Contents (Continued)

CHAPTERS Page

Table of Contents (Continued)

CHAPTERS Page

LIST OF TABLES

LIST OF FIGURES

List of Figures (Continued)

Figure Page

List of Figures (Continued)

Figure Page

List of Figures (Continued)

Figure Page

List of Figures (Continued)

Figure Page

List of Figures (Continued)

Figure Page

CHAPTER ONE

INTRODUCTION

Over the past two decades, despite a national conversation that has heightened the awareness of concussion risk in American football, the sport's popularity has continued to rise. From 2008 to 2012, participation in American football at all levels has increased from 1.8 million to 4.2 million players.[1,2] From 2008-2013, college football experienced an average annual increase of 2% in athlete participation, reaching over 70,000 players in 2013.[3] As football popularity increased, so, too, has the physical capacity of its players. Over the last 70 years, the average football player's weight has increased as much as 15% for certain positions.[4] From 1987 to 2000, the average football player's speed and strength also increased.[5] With these increases in player size and performance, on-field collisions have the potential to place players at a higher risk for injury, thus concern for player safety has increased as well.

The motivation for this Ph.D. dissertation is to provide football equipment managers, coaches, parents, athletes, and relevant industry personnel with an understanding of the implication a chosen football facemask design will have on the safety of the athlete. This dissertation was completed in three steps to evaluate the mechanical characteristics of football facemasks: 1.) a review of literature regarding existing methods used to evaluate protective headgear in American football; 2.) an evaluation of the industry standard for evaluating the impact performance of a helmet system based on the football facemask; 3.) an

isolated evaluation of the structural stiffness of existing football facemasks designs; and 4.) a multi-method evaluation of the relationship between facemask structural stiffness and impact performance. With the information gathered in this dissertation, consumers can make evidence-based decisions regarding their selected facemasks. Manufacturers can use this dissertation as a foundation for future facemask designs and iterations.

The remainder of the introduction section summarizes the current state of football headgear evaluation methods, with a specific focus on laboratory simulations of football head impacts, followed by a series of motivating factors that provide the inspiration for the remainder of the dissertation. Non-laboratory simulation methods, such as finite element analysis or on-field impact exposure research are also available, but were not the focus of the current study.

1.1 Review of Literature Concerning Protective Headgear Evaluation

The literature review section is broken down into 3 sections: 1.) background on head impact trauma and protective headgear, 2.) an overview of common methods used to evaluate full helmet systems, and 3.) a summary of methods used to evaluate helmet system components. Once a firm foundation in existing literature is presented, the motivations for the remainder of the dissertation should become clear.

1.1.1 Head Impact Trauma and Protective Headgear Background

The head injury mechanism that occurs upon head impact has been well-documented. The spectrum of injuries that occur as a result of head impact trauma ranges from mild to severe traumatic brain injuries,[6] and can be described by the abbreviated injury scale presented in Figure 1. Upon impact, three brain responses occur: 1.) at the site of the impact (coup site), a positive pressure gradient (compressive stress) occurs; 2.) at the site opposite of the impact (contrecoup), a negative pressure gradient occurs; and 3.) a shear stress occurs between the skull and the surface of the brain.[7] Head impacts cause the head to experience both linear and rotational acceleration. Linear acceleration is commonly theorized to result in focal injuries related to the pressure gradients that form at both the coup and contrecoup locations.[8] Rotational acceleration

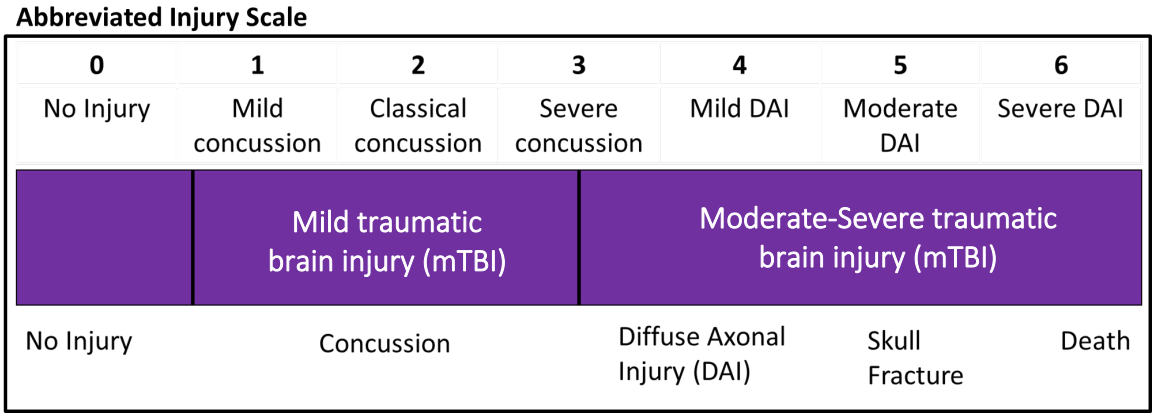

Figure 1.1: The abbreviated injury scale summarizes the spectrum of possible injuries that result from head trauma.

differences in the brain and skull response has been postulated to result in shear strain at the skull-brain interface, resulting in a more severe traumatic brain injury, such as diffuse axonal injury,[7,8] which can lead to subdural hematoma and possible death.[9]

An example of a mild traumatic brain injury is a concussion, which is defined as a temporary impairment of brain function resulting from a mechanical stimulus.[10] The Center for Disease Control estimates the yearly number of sport-related concussions to be between 1.6 and 3.8 million in the United States.[6] Between 5% and 6% of all high school and college football players are expected to experience at least one concussion each year [12]. The incidence rate for concussions ranges between 0.5 and 1 concussion per 1000 athlete exposures for college and high school football players [12]. In the NFL, from 2011 to 2014, concussions resulting from practices increased by 35% [13]. Even in the absence of acute incidences of mild traumatic brain injury or concussion, the effect of accumulated head impacts has been shown to change brain chemistry and function [14–18]. In addition to brain inhibition resulting from accumulated subconcussive impacts, evidence has also been discovered that connects repeated head impacts and head injuries to long term changes in brain structure and function [19–22].

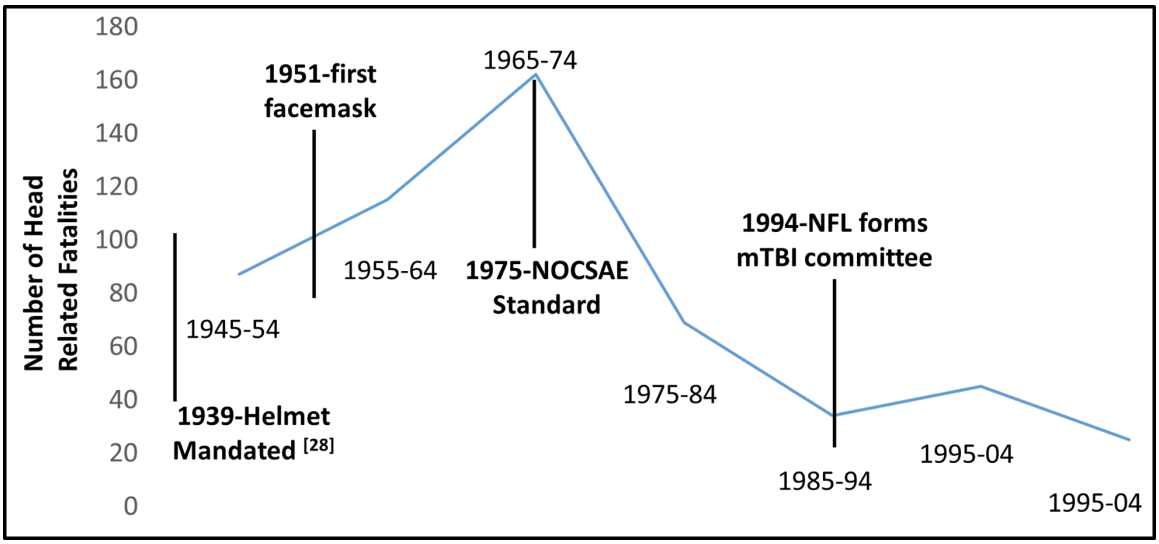

Figure 1.2: The total number of fatalities that occurred because of head impacts sustained during American football practice or competition. Data to generate this graph was presented by Mueller, et al.

Since its inception, playing American football has resulted in mild, moderate, and severe traumatic brain injuries. The number of head impact related fatalities that occurred because of playing American football each decade is presented in Figure 2. Even after use of protective headgear was mandated in 1939,[23] head impact related fatalities continued to rise[1] until the introduction of a standard that codified the minimum requirements for the protective capacity of a helmet system.[24] In response to this standard, developed by the National Operating Committee on Standards for Athletic Equipment (NOCSAE), and in an effort to combat head injury severity, protective equipment has evolved with the needs of the sport.

The implementation of the first NOCSAE standard that outlined required testing methods for protective headgear introduced a codified linear drop method

for headgear evaluation. Linear drop tests require the helmeted headform to fall from a specific height in order to generate a desired impact velocity. The headform is usually guided by a set of twin wires, as prescribed by standards set by NOCSAE, or by a monorail system, which is used more frequently for research. Linear drops have also been performed without a guidance system at all [25], but unguided drop methods are not common and thus not evaluated in this review.

NOCSAE was formed in 1969 to address on-field fatalities resulting from head impact trauma in football competition [24]. In 1973, NOCSAE released the first standard for certifying a football helmet's ability to reduce the risk of severe traumatic brain injury and skull fracture. At this time, helmets relied on the use of internal lining made of foam padding, pneumatic padding, suspension webbing, or a combination of padding systems to protect the head upon impact.[23] Over the next few decades, mechanical testing using both quasi-static and dynamic loading methods demonstrated the superiority of padded lining compared to web-based suspension systems.[26,27] During this time, the methods available to evaluate protective headgear evolved with the focus moving away from eliminating severe traumatic brain injury to the reduction of mild traumatic brain injuries.

1.1.2 Full Helmet System Evaluation Methods

Full helmet systems are commonly evaluated using a procedure to reconstruct a football head impact in a laboratory. The purpose of a laboratory

reconstruction of a football head impact is not to study impact conditions that might occur during on-field impacts, but to provide a controlled environment with less variability so that these events can be studied [28–31]. The goal of laboratory reconstructions is similar regardless of reconstruction method, but the mechanism for impact generation can differ significantly. Similar reviews have summarized biometric data related to brain injury [32,33], but none have evaluated the history of laboratory reconstruction methods used to further understand the current state of the field. This review will detail and discuss the four most common methods used to evaluate full helmet systems: linear drop, pendulum,

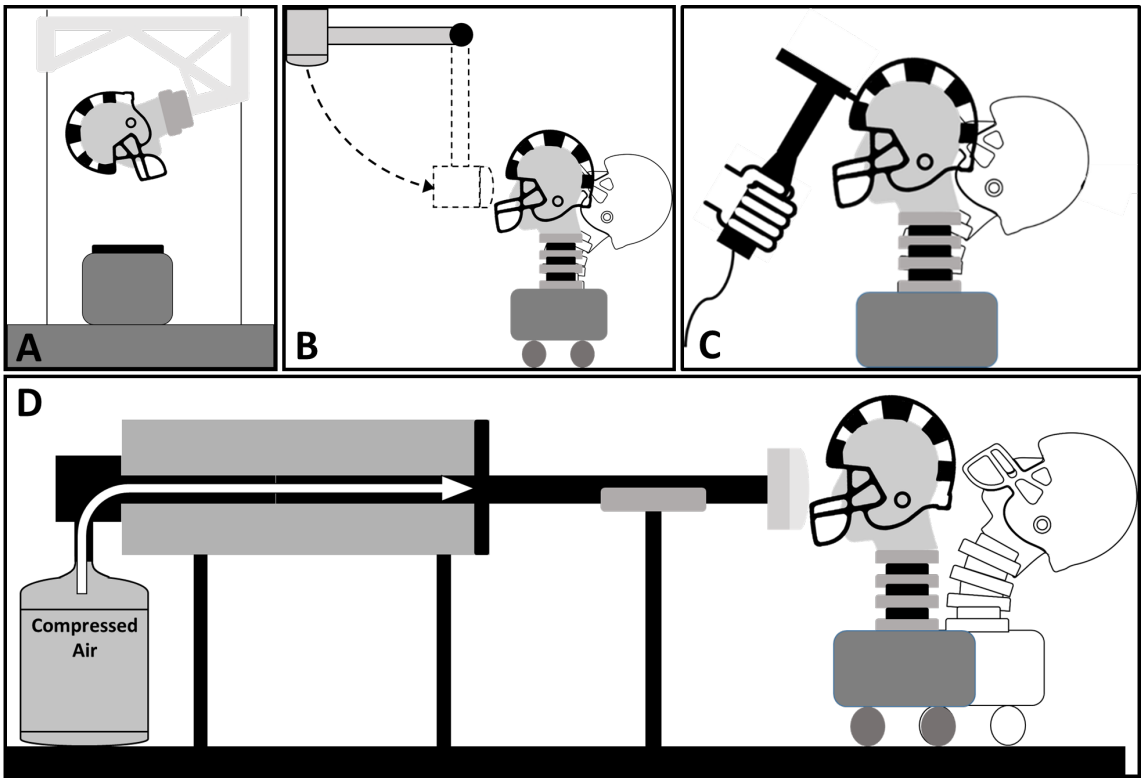

Figure 1.3: An overview of the existing methods used to evaluate full helmet systems: Linear Drop method (A), Pendulum method (B), Impulse Hammer method (C), and the Pneumatic Ram method (D).

impulse hammer, and pneumatic ram. Each method is represented in Figure 3. Each head impact reconstruction method section will be broken down into an evolution of that method section and a discussion of that method's limitations section. An evaluation of the history of laboratory reconstructions reveals the evolution of research focus in head impact trauma for football specific head impacts. The evolution of methods used to characterize head impacts starts with the linear drop method, which utilizes gravity to generate impacts.

1.1.2.1 Linear Drop Methods

1.1.2.1.1 Evolution of Linear Drop Method

Linear drop tests require the helmeted headform to fall from a specific height in order to generate a desired impact velocity. The headform is usually guided by a set of twin wires, or by a monorail system, which is used more frequently for research. In 1973, NOCSAE released the first standard for certifying a football helmet's ability to reduce the risk of severe traumatic brain injury and skull fracture. In the NOCSAE drop test system, a helmeted humanoid headform is attached to a magnesium drop carriage with the absence of a neck replica. Soon after the release of the NOCSAE standard for football helmet performance, Calvano and Berger sought to answer the question, "what liberties may test developers take in selecting test conditions or in choosing output parameters?" [34]. Calvano and Berger observed how impact reconstructions differed depending on four inputs: impact velocity, the impact location, the type of impact surface used (soft vs hard polyurethane), and the type of headform used

(metal vs humanoid). An increase in impact velocity by 0.5 m/s was accompanied by an increase in impact severity by about 20%. The impact location also affected the impact severity, but the hardness of the impacted material did not have a significant difference on impact response. Calvano and Berger found that the difference between the metal and humanoid headforms is that, for impacts to the rear of the headform, humanoid headform impacts are accompanied by bending in the neck region, which is thought to result from a misalignment between the headform center of gravity and the impact location [34]. The misalignment in center of gravity resulted in reduced headform response to impact. However, as the NOCSAE twin guide wire test became more popular, the use of a metallic headform was rarely used in laboratory reconstructions. A more recent analysis of humanoid headforms shows that the Hybrid III (HIII) headform may experience more concentrated impact loads resulting from impacts to the rear of the helmet when compared to the NOCSAE humanoid headform [35], which is similar to the humanoid headform used by Calvano and Berger [34]. These studies show that for laboratory reconstructions, the headform material and geometry, the impact velocity, and the impact location all will have an effect on the measured impact response.

Early validation testing of the NOCSAE linear drop test method explained that a neck replica for impact testing is not necessary for impacts resulting from NOCSAE drop tests because NOCSAE drop test impacts cause headform accelerations in the transverse plane [24]. More recent work has shown that the

presence of a neckform or humanoid torso has no effect on the linear acceleration of an impacted headform [36]. Cadaver-based experimentation and *in vivo* impact video analysis has shown that for transverse impacts of a short duration (t<15 ms), the head responds independently from the body, as the neck response time has been shown to range between 50-60 ms [34].

While the linear acceleration response of a headform may not be dependent on a neckform or torso response, there is evidence that a headform's angular acceleration is affected by the presence of a neckform [37–40], and some groups have included both neckforms and torsos in their testing systems for linear drop tests [41,42]. To perform impacts with a neckform attached to the helmeted headform, a monorail linear drop tower is commonly used. This system is often used with a HIII neckform and headform in order to generate a translational and rotational response [37,41,43,44]. Newman, et al. found that lateral impacts, which are commonly experienced by a struck player, resulted in limited neck coupling effects on linear head acceleration but significant effects on rotational acceleration [37]. However, this finding has not stopped researchers from using linear drop methods to quantify rotational impact response [45]. The findings of Newman, et al. mean that in order to recreate the rotational response of a head in a laboratory reconstruction, the simulated struck player must include a neckform of similar stiffness to the *in vivo* struck player's neck during impact. Mathematical simulations also showed negligible effects of the torso for simulated struck player impacts [37]. Taking this information into consideration, a

simulated struck player should be moving and include at least a biofidelic neckform, but not necessarily a torso.

The monorail guided linear drop system allows the research team to measure the load applied to the neckform. Force transducers placed at the interface between the headform and neckform measure neckform compression forces resulting from impact [41,43,44] to represent impact loading supported by the neck. The monorail system has been used to evaluate novel helmet designs [41,42], recreate severe on-field impacts resulting in concussions to study the biomechanics involved in on-field impacts [44,46,47], and to validate methods used to reconstruct football head impacts [34,37,48].

1.1.2.1.2 Limitations and Discussion of Linear Drop Method

One limitation of the linear drop method involves impacts to the faceguard. NOCSAE requires newly manufactured and recertified faceguards to be tested with a linear drop method according to NOCSAE Standard ND087 [49]. However, linear drop methods are not commonly used to perform research on helmets with faceguards attached [39]. Faceguard geometry moves the impact location from above the brow on the helmet down towards the front of the headform face. This change in impact location increases helmet rotation with respect to the headform, as well as the load applied to the chin strap [50], which is difficult to quantify and control and has an effect on the acceleration experienced by the headform by changing the normal contact force applied to the headform. Thus, to characterize the impact performance of a helmet with a faceguard, the impact location must

be more controlled than the twin wire linear drop test allows. One potential way to improve impact location consistency while continuing to leverage gravity to propel the helmeted headform towards impact is to guide the impact with a monorail system rather than twin wires.

The linear drop method has been cited has having a poor ability to reproduce consistent impact results for any given drop condition. Viano et al. used the linear drop method when recreating the impact conditions observed during football impacts from on-field video. Viano used the impact location and velocity from video as inputs into the laboratory impact reconstruction, and reported that each on-field impact required between six and ten drop tests in order to create an impact that simulated the on-field impact [42]. However, fatigue testing performed by Cournoyer, et al., has shown that impact to impact variability across 100 impacts is reduced enough to conclude that an increase in impact severity occurs after 90 impacts [51]. The twin-wire system has limited out-of-plane constraints and impacts can create significant lateral movement, noise, and vibration, which challenge the ability of this test method to generate repeatable impact simulations.

Rotational response during impact has been identified as an important metric in the literature, [52,53] and the twin wire guided linear drop system has been criticized as enabling only a limited rotational response. Hernandez et al. analyzed the NOCSAE linear drop test's ability to recreate on-field impact accelerations and found that the NOCSAE linear drop test results in inadequate

rotational acceleration and velocity response of the headform [38]. Hernandez et al. points out that on field impacts are described by six degrees of freedom: three degrees of freedom describe the location of the impact on the helmet according to a three axis frame of reference, and another three degrees of freedom describe the impact direction vector. However, the linear drop tower only allows for three degrees of freedom: two degrees of freedom describe the rotational ability of the headform within the sagittal and horizontal planes and one degree of freedom describes the drop height [38]. Based on the analysis by Hernandez et al., more accurate impact reconstructions occur by increasing the degrees of freedom for the system to improve the rotational behavior of the impacted head form. Hernandez et al. suggest that the degrees of freedom be increased by including the ability to not only adjust impact location, such as front, back, side, top, etc, but also to adjust the impact direction, allowing for both centric and non-centric/oblique impacts. Currently, the twin guide wire system only simulates centric impacts, which means the impact direction vector intersects the headform center of gravity.

1.1.2.1.3 Summary of Linear Drop Method

Regardless of a twin-wire or a monorail system, a linear drop method relies on the force of gravity to generate a simulated head impact. Monorail systems are used in order to replicate a rotational neck response, and allows for more control over the impact location on a helmeted headform. Both a monorail and twin-wire system exposes the simulated head impact to low amount of

degrees of freedom, less than that experienced in an on-field head impact. Also, variation in impact response is high for the linear drop method, especially for a twin-wire system. Impact variation is amplified when the impact location includes the facemask. In conclusion, using a Linear Drop method may not provide the sensitivity needed to evaluate facemasks as components of the full helmet system. This point will be evaluated further in body of this dissertation.

1.1.2.2 Pendulum Method

1.1.2.2.1 Evolution of the Pendulum Method

The primary motive for the use of a pendulum system in football-specific head impact laboratory reconstructions was to generate a rotational response to the impacted headform. In addition to being seen as a more realistic way to simulate on-field impacts, it has also been used to validate the accuracy of angular acceleration measured by a 3x2x2x2 array of linear accelerometers [36]. Newman et al. used a pendulum set up to evaluate the HIII headform and neckform frequency response as a potential source of noise in video reconstructions [37]. This pendulum system features a weighted hammer impactor surface covered with a layer of polycarbonate meant to mimic helmet to helmet collisions. Newman et al. showed that pendulum laboratory impact reconstruction conditions vary depending on the purpose of its use.

Additional development and validation of the pendulum system resulted from a series of studies performed by Pellman et al., who evaluated a pendulum system's ability to replicate on-field impacts [43]. In the original testing set up, a

helmeted headform placed upon a neckform remained stationary and was struck by a swinging, weighted pendulum. However, future evolution of the pendulum system placed the helmeted head and neckform onto a sliding table to allow linear motion after impact. This motion reduced the bending load placed on the neckform, which was too high when the neckform was held stationary after impact compared to video analysis or monorail-guided laboratory reconstructions [43]. To match energy transfer resulting from pendulum impacts to impacts observed in video of on-field impacts, a pendulum speed of 6.9 m/s was used to represent the average collision speed between two players, 9.5 m/s. The difference in pendulum impactor speed and the speed of an impacting player results from the larger pendulum mass than the effective mass of the striking player, which would result in higher momentum transfer in pendulum impacts for equal impact velocities [43].

The pendulum system has also been used to quantify the impact response of the HIII head and neckform when impacted at different locations and with different energies. Bartsch et al. used a 3.6 kg steel impactor to strike a bare HIII headform attached to a stationary neckform. Impact energies were chosen in order to prevent the neckform from over bending and ranged from 27 J to 89 J. The results of this study suggest that future researchers take care when using the HIII neckform, which is built out of several rubber blocks that compress differently depending on the impact location [40]. Bartsch et al. also showed the ease with which the pendulum system can impact different locations in different

directions. The latter point is especially important, as impacts occurring in different directions are much more difficult in linear drop test systems.

Pellman et al. compared the measured parameters (impact velocity, peak acceleration, change in velocity and severity index) generated by the pendulum to those generated by the monorail-guided drop system. For impacts of average impact velocity, the pendulum system impact severity index differed from that of the monorail impacts by between ±12.5%, depending on the impact location. Impacts at lower velocity showed similar trends [43]. These results indicate that, for impacts of the same impact velocity, impacts generated by the pendulum system result in both less severe and more severe impacts than impacts generated using the linear drop method. This shows that it is difficult to compare impact results between monorail impacts and pendulum impacts, as the consequence for using either reconstruction technique differs depending on impact location.

1.1.2.2.2 Limitations and Discussion of Pendulum Method

One cited limitation of the pendulum system is the inability to match all impact velocities, locations, and directions associated with *in vivo* head impacts, requiring impact locations to be sorted into quadrants rather than defined as specific points [43,54]. This limitation, however, was also present in the linear drop test methodology. One limitation specific to the pendulum system is a restricted impact velocity range based on pendulum geometry. A pendulum system requires the pendulum to drop from 4.6 m to reach the required impact velocity for the most severe impacts seen in professional football (9.5 m/s), if gravity is

the only force applied to the pendulum swinging mass [43]. This requires a great deal of laboratory space to perform, and some pendulum arms cannot be dropped from 4.6 m due to laboratory ceiling height limitations. Thus, to recreate severe impact velocities, additional forces must be applied to the swinging arm of the pendulum by bungee cords or torsion springs. However, bungee cords or torsion springs introduce variability into the system, which increases the difficulty in recreating consistent impact severity [43]. If impact velocity cannot be reached, then the impact's momentum transfer can be increased by increasing the impactor mass, which was seen by Pellman et al., increasing the impactor mass to 28 kg [43].

Another limitation of the pendulum method was revealed when Bartsch et al. attempted to compare leather football helmets to modern, plastic shell football helmets [55]. Bartsch et al. used a headform equipped with a hard shell helmet as the impactor on the end of the pendulum while the stationary impacted headform was equipped with both leather and hardshell helmets. The pendulum system was used in this impact study in order to control horizontal impact conditions and reduce variability while maintaining impact energy transfer similar to that found in linear drop laboratory reconstructions [55]. Bartsch et al. found that leather helmets outperformed modern helmets [55]. However, these findings were refuted by Rowson, et al., who pointed to the use of two helmets in the impact as an inaccurate way to compare leather helmets to modern, hard shell helmets [56]. Rowson et al. claimed that the impacting hard shell "baseline" helmet introduced

additional compliance to the leather helmet impacts and absorbed much of the impact energy, inferring that the test system proposed by Bartsch was more effective in measuring the impact performance of the baseline hard shell helmet [56]. Rowson et al. also pointed to the low impact velocities used by Bartsch as a possible reason why leather helmets outperformed modern helmets, since low impact velocity may not be enough to properly recreate the impact response of the headform within a leather helmet [56].

An impact between two helmeted headforms means that impact energy will be attenuated by both helmets. In this situation, one helmeted headform should represent the striking player, and the other should represent the struck player. When comparing different helmet designs, the striking player model headform must be equipped with a baseline helmet design or with a standard nylon or polycarbonate capped non-compliant material in order to ensure impact energy attenuation will be consistent across all impact tests. However, absolute helmet impact performance will not be measured, as some of the impact energy will be attenuated by the striking player model's helmet. For a pendulum system, the impactor surface must absorb a low amount of energy in order to ensure that energy absorption involved in the impact is a direct result of the performance of the helmet being studied. This can be done by using a layer of polyurethane foam between a metal impactor body and an ultra-high molecular weight polyethylene cap [43]. A nylon cap, meant to represent the outer shell of a football

helmet, has also been used [31]. In conclusion, care must be taken to use an impactor that will not absorb energy upon impact.

1.1.2.2.3 Summary of the Pendulum Method

To summarize, the pendulum method can improve the generated rotational response of the helmeted headform compared to the linear drop method, but high velocity impacts are difficult to produce. In addition, the limitation of using two helmeted headforms in a simulated head impact has led to the development of a hemispherical impactor cap. However, the use of an impactor cap complicates impacts to the facemask, as the hemispherical impactor commonly causes the entire helmet system to shift with respect to the headform, similarly to impacts generated with a Linear Drop Method. Thus, a method is necessary to generate high velocities and still allows for a rotational response of the impacted headform that can be reliably used to evaluate the helmet system with a facemask. The pneumatic ram linear impactor avoids some of the limitations of the pendulum system.

1.1.2.3 Impulse Hammer Method

1.1.2.3.1 Evolution of Impulse Hammer Method

To date, only one research group has demonstrated the use of an impulse hammer to generate controlled impacts to a helmeted headform [57]. The biggest difference between the impulse hammer impacts and impacts generated by any of the other methods presented above is that the input from an impulse hammer impact is measured in force, not velocity. The impulse hammer delivers a blow at

a measurable force, and the impact response acceleration is correlated to that impact force. Continuing the work of Beckwith et al., [28] Cummiskey et al. used the impulse hammer to validate several impact sensors used for head impact in sports.

1.1.2.3.2 Limitations and Discussion of Impulse Hammer Method

One limitation of the impulse hammer is that there is a low effective weight associated with the impact, which reduces the amount of momentum transferred for a given impact velocity [57]. However, when the impact force is known for a series of impacts with measured impact accelerations, a correlation between impact force and accelerations may result in a transfer function that will relate input to output, a relationship that has not been shown in any laboratory reconstruction method to date.

Another limitation of the impulse hammer is its current dependence on human input to generate an impact. Each swing of the hammer requires a hand to generate the impact force. However, a system could be developed that controls the hammer input for each impact. Also, since impact force is measured by the hammer, changes in input can be easily correlated to differences in acceleration response, making the impulse hammer ideal in generating a high volume of impacts quickly, if not always easily repeatable.

Measuring the frequency response of an impacted system does not require, however, an impulse hammer. Gwin et al. has compared the frequency response of impacts generated by the pneumatic ram linear impactor, the twin

guide wire and players on the field [39]. Specifically, Gwin et al. observed the factors that affect the damping ratio and natural period of oscillation for each of the three impact sources. The damping ratio is related to the helmet materials used as well as the impactor surface. For the linear impactor, the impactor surface affecting the damping ratio is the HIII neckform. For the twin guide wire impacts, the damping ratio is determined by the impacted surface, which is an elastic material of low compliance. For on-field impacts, the damping ratio is related to the musculature of the neck and shoulder. The natural period of oscillation is related to the mass of the headform or head as well as the stiffness of the neckform or neck. For the pneumatic ram linear impactor, the damping ratio and natural period of oscillation are 1.6x and 2x higher, respectively, than on-field values [39]. This quantifies the differences in stiffness between the human neck and the HIII neckform commonly used in laboratory impact reconstructions, exposing the neckform used as a limitation of this laboratory reconstruction technique in replicating on-field impact responses. However, this is not necessarily unique to impacts using the pneumatic ram impactor, and may be more closely related to the biofidelic neckform used in laboratory reconstruction. Further research is needed to develop a neckform that responds more appropriately to football specific impacts.

1.1.2.3.3 Summary of Impulse Hammer Method

Further research is needed using the impulse hammer to determine the effectiveness of an input:output frequency transfer function as an evaluation of a

full helmet system. However, the use of the impulse hammer method eliminates the ability to generate a high severity head impact, or an energy transfer similar to that of an on-field head impact. One potential method that could still measure the input:output frequency transfer function is the Pneumatic Ram/Lineaer Impactor Method.

1.1.2.4 Pneumatic Ram/Linear Impactor Method

1.1.2.4.1 Evolution of Pneumatic Ram/Linear Impactor Method

Soon after the pendulum system made its debut in football helmet testing, development began on the pneumatic ram linear impactor. In response to increasing demands for an impactor system that elicits appropriate rotational responses, the National Football League sponsored the design of a pneumatic ram linear impactor that was later transferred to NOCSAE [43]. Featuring a pressure system that propels an impacting arm towards a stationary headform, the linear impactor is capable of repeatedly generating high impact velocities with a relatively small experimental footprint and has an ability to strike specific locations on the headform. The initial impact mass was 12.0 +/- 0.1 kg, impact velocities spanned from 6-12 m/s, and the impactor material was a polyurethane foam. Other impactors have been composed of vinyl nitrile foam enclosed by a nylon cap [30,58]. Non-traditional linear impactor systems have also been used to quantify impact force [59], but these methods are not as common as the NOCSAE developed pneumatic ram system. Despite differences in linear impactor materials used across different research groups, a few trends have been shown

in comparisons between linear impactor methods and other laboratory reconstruction methods.

Initial comparisons to monorail-guided linear drop impacts showed that, at high velocity, the severity index for the impacts generated by the pneumatic ram linear impactor differed from linear drop impacts by between 7.9 and 44.0% [43]. Unlike the pendulum system, which unpredictably differed from linear drop impacts, the pneumatic ram linear impactor consistently produces higher severity impacts, based both on severity index and impact energy, than the linear drop system. In a direct comparison between the pneumatic ram linear impactor and the twin wire guided linear drop system, Gwin et al. showed that to generate a similar severity index as an impact produced by a 1.52 m drop (about 5.4 m/s) with a twin guide wire system a linear impactor must generate an impact velocity of 9 m/s. The energy associated with the twin guide wire drop is between 60 and 88 J, depending on the headform size, and the energy associated with the linear impactor impact is 539 J [39].

The difference in energy required between twin guide wire impacts and those generated by a pneumatic ram linear impactor can be explained by the difference in movement after impact that the headform experiences between the two described impact methods. In the twin guide wire system, the headform velocity is brought to zero, resulting in a high change in velocity and a short impact duration. In the linear impactor system, the headform and neckform slide down a sliding table after impact, dispersing impact energy and increasing the

impact duration [39]. At such high impact velocities generated by the pneumatic ram linear impactor, restricting the motion of the head and neckform after impact would put the neckform at risk of permanent damage.

The linear impactor method has been used to compare helmets from different eras. Viano et al. showed that certain helmet styles from 2010 actually performed worse (resulted in higher head impact rotational accelerations) than the 1990s baseline helmet design for impacts to the front of the helmet. Also, for low velocity impacts (3.6 m/s), impacts to the side of the 2010 helmets resulted in higher peak linear head accelerations than helmets from the 1970s or 1980s [60]. Similar testing comparing 2010 helmets to 1990s helmets also shows some 2010 helmet styles performing worse than 1990s helmet styles, possibly due to issues with the chinstrap becoming unlatched during testing [61]. In addition, NFL-sponsored research performed by Biokinetics, summarized the rotational impact response of 17 helmet models used by 99% of NFL players to recommend different helmet models to equipment managers, coaches, and players [62].

The major benefit to using the linear impactor method to reconstruct head impacts is the freedom to strike specific locations at specific angles. Similar to the work of Bartsch et al. on the pendulum system, Walsh et al. observed the kinematic response of the HIII headform to impacts at different locations and in different directions generated by the pneumatic ram linear impactor [30]. This study shows that it is possible to strike the impacted headform at three different impact angles at locations ranging from the front to the back of the headform. Using an

impact velocity associated with a linear drop of 1.5 m (5.5 m/s), Walsh et al. found that centric impacts result in higher linear acceleration, while non-centric impacts that strike at an angle result in higher rotational accelerations. This study shows that the linear impactor easily generates impacts at various impact locations and directions, an increase in degrees of freedom compared to linear drop tests. Post et al. was also able to impact a helmet at several different locations and angles, this time to understand what types of impacts result in the highest acceleration response experienced by the headform [29]. Post et al. not only impacted the helmeted headform at different angles in planes parallel to the transverse plane, but also impacted at different elevation angles in the sagittal plane. This is similar to the way Beckwith et al., Jadischke et al., and Siegmund et al. have used the pneumatic ram linear impactor in order to validate a sensor system used to quantify on-field head impacts [28,63–65], and how Viano et al. used the pneumatic ram to study the effect helmet weight has on neck loading upon impact [54].

1.1.2.4.2 Limitations and Discussion of Pneumatic Ram/Linear Impactor Method

Similarly to the linear drop method and the pendulum methods, one limitation of the pneumatic linear impactor concerns impacts to the faceguard. One common issue that occurs at high velocity impacts is impactor penetration within the faceguard [39,50]. This penetration causes the helmet to rotate with relation to the headform, which reduces the energy transferred to the headform and increases the variability of the headform response to the impact. Similar to

the findings of Gwin et al.[39], Beckwith et al. reported that, for impacts to the faceguard, the helmet will rotate down and counter clockwise until the impactor has settled inside the faceguard opening. This helmet movement occurs approximately 5 ms before head acceleration begins. Not only do impacts to the faceguard affect headform response, but faceguard impacts also require low impact velocities (lower than 3.3 m/s) in order to prevent faceguard damage [66,67].

In addition to difficulty with faceguard impacts, the pneumatic ram linear impactor has also resulted in a high number of helmet component "issues," defined as results that invalidate the impact by Viano et al. [61]. These issues include chin straps becoming unbuckled or breaking, jaw pads escaping from within the helmet, faceguard attachment failures, etc. Viano et al. showed that impacts using the pneumatic ram linear impactor resulted in 22 issues for the four modern helmets tested, and as much as 16 issues for the 92 impacts to a baseline helmet model from the 1990s [61]. This shows that the linear impactor results in issues that require repeated tests, which slows down research time and increases the financial burden of testing.

1.1.2.5 Conclusions

A review of methods used to evaluate the impact performance of full helmet systems has revealed a few trends, summarized in Table 1. First, regardless of the method used to simulate head impacts, test-to-test reliability has been demonstrated to be poor. This poor test-to-test reliability may be the result of the difficulty in ensuring that each component of the helmet system

performs similarly for each test. To improve test-to-test reliability when evaluating protective equipment, it may be more suitable, especially early in the design process, to evaluate individual components prior to evaluating full helmet systems with regards to impact performance. Evaluating individual components of football helmets may improve the understanding of how incremental adaptations to existing technology will contribute to the safety of athletes. Individual component evaluation has been performed at the research level on the external shell material, internal padding materials, chin strap, and facemask.s

Table 1.1: An overview of methods commonly used to evaluate the impact performance of full football helmet systems.

	Linear Drop	Pendulum	Impulse Hammer	Pneumatic Ram
Test-Retest Reliability	Low	Moderate	Moderate	Low
Degrees of Freedom	1 (Twin Wire) 2 (Monorail)	2	1	2
Energy Transfer	Moderate	Low	Low	High
Max Impact Severity	High	Low	Very Low	Very High

1.1.3 Evaluation Methods for Helmet System Components

Presently, football helmet systems are the combination of internal padding, commonly the combination of vinyl nitrile, ethylene vinyl acetate, and/or expanded polypropylene foam; an external shell made of polycarbonate or composite material; a chin strap, which can be either hard shell or soft shell and commonly attaches to the external shell of the helmet at four locations; and a facemask, which is constructed out of welded bars of carbon steel, hollowed stainless steel, titanium, or proprietary alloys.[68,69] The evolution of the helmet system is commonly the result of incremental improvements to individual helmet

system components.[41,50,70–80] Previous research has evaluated the performance of the internal padding,[72,75–77,80,81] the external helmet shell,[41,70,73,74,79] the chin strap,[50,78] and the facemask,[82–91] however, the methodology and goals for the research concerning each component of the helmet system have varied greatly.

The primary focus for research on the internal padding used in helmet systems is an evaluation of the energy absorption of the padding system. MacAlister et al. has used a NOCSAE linear drop tower combined with a hydraulic material test system to evaluate energy absorbed by common helmet padding materials after repeated impacts.[81] Commonly, internal padding materials are first characterized using a similar type material testing apparatus that applied a quasi-static load at a controlled rate.[72,75,76] Material testing is performed in an effort to quantify energy absorption potential in terms of the stiffness coefficient (Young's Modulus) of the materials prior to integration into the full helmet system. The material properties of the internal liner foams may then be used as inputs for a computational model, as shown by Honarmandi et al.[76] Johnston et al., for instance, developed and validated a novel internal liner material through computational modelling without the need for traditional, laboratory-based material characterization.[77] Regardless of the method, internal padding is commonly validated through controlled material testing prior to helmet system integration and head impact simulation testing.

Once the material is validated, internal liner materials are commonly tested within the full helmet system. Krzeminski et al. used a monorail-based

drop tower (see section 1.1.2) to evaluate the impact performance of a helmet system compared to product claims.[80] Other authors have used the twin-guided drop tower[72,77,81] or a linear, pneumatic ram testing unit[77] to evaluate liner material. The industry standard for the evaluation of football helmet liner materials is to identify the material properties (through the Young's Modulus) of the material to inform the selection of or the computational modelling of the material, then apply that material to an existing or novel helmet system to evaluate further using a dynamic system.

Similar to internal liner padding, the research on external shells has been focused on both material behavior as well as structural performance as part of a full helmet system. For instance, Krzeminksi et al. has used small polycarbonate samples (a blend of bisphenolA polycarbonate and polyethylene terephthalate) to demonstrate the effect weather exposure has on existing external helmet shell material[70]. Krzeminksi et al. also used a similar procedure to evaluate the effect repeat impacts have on external helmet shell material performance.[73] Different from internal lining, however, is a research focus not only on material behavior of external shells, but also of completely novel structural designs of the external shell component. Dressler et al. introduced the Pro-Neck-Tor (PNT) system that allows the external shell to rotate with respect to the internal pads.[41] The PNT system, applied to existing helmet systems, was evaluated with a linear drop tower (monorail) system in order to evaluate the impact performance of the PNT addition. Not only are structural differences potential improvements to helmet

systems, but other research groups have attempted to evaluate external shell covers.[79,92] Zuckerman, et al. used a novel method to select materials for an external shell cover prior to evaluating full helmet system performance using a linear pneumatic ram unit.[79] By dropping a medicine ball on different material samples and measuring the resulting force applied to the ground beneath the material sample, Zuckerman et al. identified an appropriate material differently than common methods used to select internal liner padding materials. However, whether applying a load from a specific height like Zuckerman et al. or applying a load at a controlled rate such as MacAlister et al., the material is still selected based on a parameter related to the Young's Modulus of the material. In the case of Zuckerman, et al., the force that propagates through the material is related to the Young's modulus based on Hooke's Law, in which

$$F=kx \qquad \text{Equation 1}$$

where F=force, k = spring constant (which is analogous to Young's Modulus), and x=the vertical compressive deflection of the material. In the case of MacAlister et al., Young's Modulus is measured directly based on the ratio of applied load to resulting deflection:

$$k=F/d \qquad \text{Equation 2}$$

where k=Young's Modulus, F=applied load, and d=vertical deflection of the material. In each case, the understanding of the material stiffness is important in the eventual selection of the material.

The chin strap of the helmet system has evolved from a soft cloth attached to the helmet shell in two locations to either a hard or soft chin cup attached to the helmet shell in four locations. Traditionally, chin straps have attached to the external shell using a buckle, but more recently, novel chin strap attachments such as the ratchet system of the Riddell SpeedFlex or the locking mechanism of the Wegener Lock devices have been introduced. Regardless of the method used to attach the chin strap to the external shell, research on the chin strap's contributions to the full helmet system has been limited. Both Rowson et al. and Craig have used a pneumatic linear impactor to demonstrate the load experienced by the mandible through the chin strap.[50,78] However, neither of these methods have been revisited to demonstrate the effect novel attachment methods have affected force transmission to the jaw through the chin strap. Additionally, Craig demonstrated the difficulty in reliably evaluating helmet systems using the pneumatic ram system for impacts to the facemask region, thus demonstrating the difficulty in reliably evaluating the impact performance of the full helmet system based on any one component.

A bulk of the research on the football facemask has been on the ease of facemask removal after the athlete has sustained a spine or neck injury.[85–90] While an important characteristic of a facemask is ease of removal, the focus of this dissertation is the protective capacity against an impact of headgear components, primarily the facemask. The effect the facemask has on the full helmet system has been analyzed in two capacities. First, the performance of a

helmet system when impacted using a twin-wire guided drop tower was observed by Rush et al.[83,84] The results from this experimentation, however, were inconclusive. In order to remove the noisy contributions of the twin-wire guided drop tower to the impact performance of protective headgear, Johnson et al. evaluated facemask contributions to athlete safety through computational modelling. Johnson et al. determined that the optimal facemask has the maximum ratio of vertical bars to horizontal bars, and postulated that the reason for this finding is that vertical bars will reduce the stiffness of the facemask.[82] The stiffness theory for facemask performance by Johnson et al. could potentially be supported by Ramirez et al., who found that an increase in Young's modulus of viscoelastic material reduces the density of the material, which had a beneficial effect on the impact performance of the helmet system.[72] To justify this comparison, further research is needed with regards to the relationship between the facemask stiffness and its impact performance.

1.1.4 Football Facemask Nomenclature

One difficulty in evaluating football facemasks is the idiosyncrasies and inconsistencies in facemask nomenclature across facemask manufacturers. Thus in order to establish proper methods to evaluate facemask performance, it is important to establish general facemask naming principles. The three primary helmet and facemask manufacturers used in the research presented in this dissertation are Riddell, Schutt, and Xenith. Each of the three manufacturers use

different naming conventions for facemasks, but many of the facemask geometries for these masks are similar. For example, Riddell's naming convention uses letters and numbers to describe the appropriate helmet for the mask, the location and number of horizontal bars, but gives specific letters to describe the presence of specific vertical bars. For Riddell, the first 1-3 letters or numbers indicates the helmet the facemask fits. The letter S indicates the Speed helmet, the letters SF indicate the SpeedFlex helmet, the letter G indicates the Revolution helmet, and the numbers 360 indicates the 360 helmet. If the facemask style name starts with a Z, the facemask will fit a Riddell VSR-4 helmet.

The second number indicates whether the mask is a "short" (2) or "long" (3) facemask. The letter following a 2 or a 3 either indicates the presence (E) or absence (B) of an "eye guard" (E). Following this letter is either a D to indicate a double top bar (reinforced forehead bar), or is left blank to indicate a single top bar. The letters SW indicates a single horizontal bar ("single wire") that traverses the space in front of the nose. The letter C stands for "closed" and indicates a smaller eye opening in the mask. For some helmet styles, the letter U indicates a "U-bar" at the top of the mask between the two forehead clip locations. The letters CU at the beginning of the facemask name indicates the mask is a custom style. The letter BD stands for "Bull Dog" and indicates an "upside down u" bar across the jaw and nose locations that represents the underbite of a bulldog. BD facemask bars are more common for Schutt styles, however.

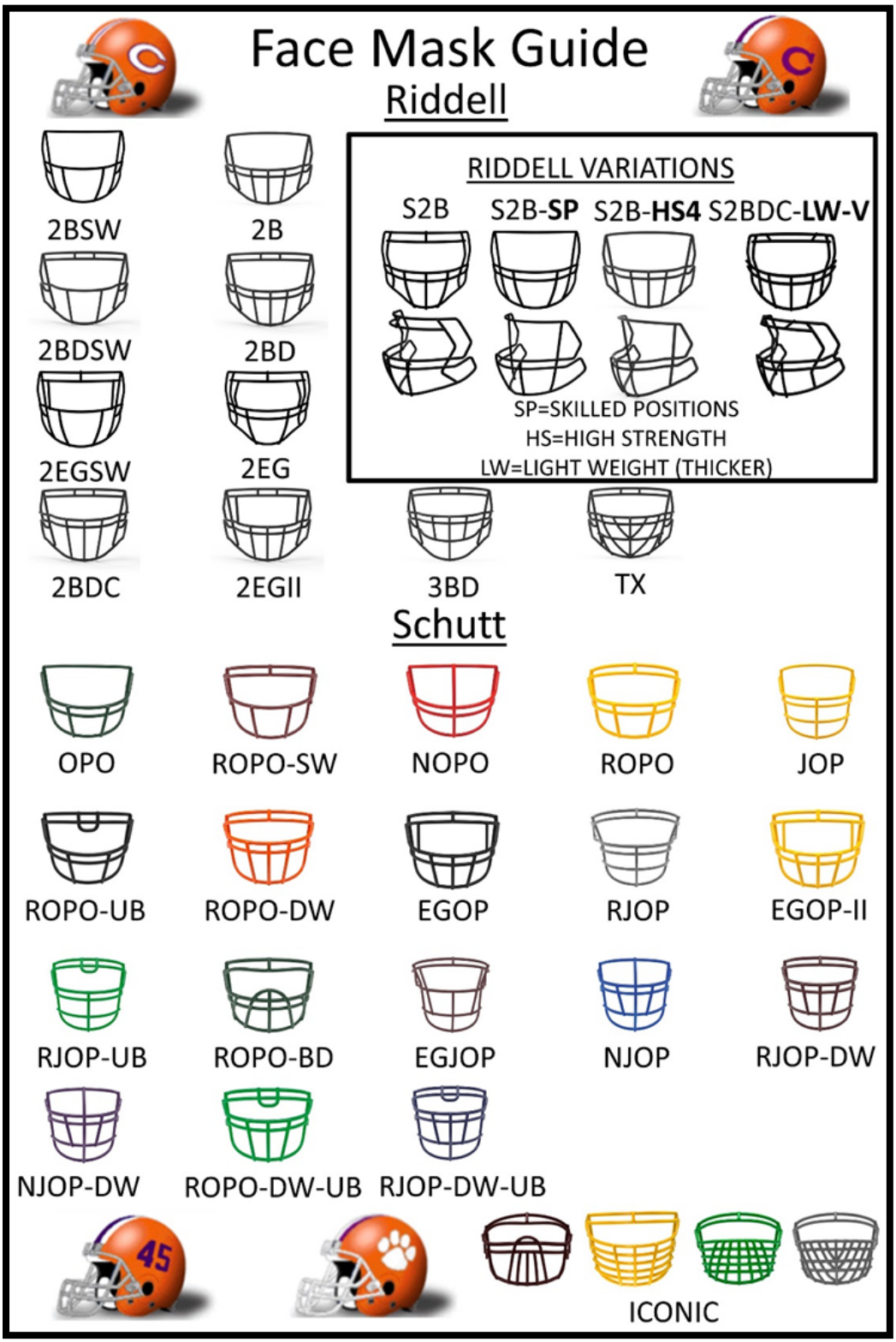

Figure 1.4: Common facemask design nomenclature across the two most common facemask manufacturers (Riddell and Schutt).

Riddell facemasks also use letter codes to indicate the material used to create the facemask. The letters LW or LW-V indicate the mask is made of a light weight material, which also means the bars are hollow. The letters HS4 indicate the "high strength" material is used to make the facemask, and these masks will be the lightest possible version of a Riddell facemask. No additional letters indicates the mask is made of traditional carbon steel bars. Common Riddell facemask names are summarized in Figure 1.4.

Schutt naming conventions are focused more specifically on the areas of protection the facemask provides. Similar to the Riddell Facemask naming convention, the first section of Schutt facemask style names indicates the helmet the facemask will fit. The letter V indicates the facemask fits a Vengeance helmet, Z10 indicates the Z10 helmet, and F7 indicates the F7 helmet. The lack of a beginning series of letters indicates the facemask belongs to the "Super Pro" family of facemasks that will fit the Schutt XP, Schutt Air XP Pro, Schut Air XP Pro VTD, Schutt Air XP Pro Q10, and the Schutt Air XP Pro Q11. The facemask that provides the least protection is the OPO facemask, which stands for Oral Protection Only, and only has horizontal bars in front of the nose and jaw. For Schutt facemasks, the letter R stands for "reinforced" which indicates an additional horizontal bar across the brow/forehead in an effort to extend the lifespan of the facemask, since a single brow/forehead bar commonly experiences permanent deformation. Schutt facemasks with an "R" are similar to Riddell facemasks with a "D" to indicate the double horizontal bar. Similar to

Riddell facemasks, “SW” indicates a single horizontal bar (“single wire”) across the nose part of the facemask. The letters “N” and “J” indicate “nose” and “jaw” protection, respectively. Nose protection indicates a long vertical bar across the eye opening of the facemask from the brow to the lowest point of the mask. Jaw protection indicates an extended facemask, similar to a Riddell facemask with a 3B in the name. Also, similarly to Riddell facemasks, the letters “UB,” “EG,” and “BD” stand for “upper bar,” “eye guard,” and “bull dog, respectively, which have the same meaning regarding facemask bar placement as Riddell facemasks. Schutt facemasks are either carbon steel or titanium. Facemasks with a “T” are made of titanium, otherwise, Schutt facemasks are made of carbon steel.

Xenith offers much less styles of facemasks, but also offer each style in a titanium or carbon steel material. Xenith has a series of facemasks called the “Pro Series” which are named after and resemble common images from American pop culture. The Pro Series includes “Prime,” “Prowl,” “Pursuit,” “Pride,” “Predator,” “Precept,” “Portal,” and “Prism.” None of the Xenith Pro Series masks were used in the research presented in this dissertation. More traditional facemask styles from Xenith make up the “Classic Series.” Facemasks in the Xenith Classic Series either start with XRS, XRN, or XLN. XRN masks are similar to Riddell facemasks with a C, which indicates a smaller eye opening (“closed” type facemask). XLN masks are similar to 3BD Riddell facemasks and “J” Schutt facemasks in that they extend down to protect the jaw area. After the first three letters, Xenith Classic masks either have a 22, 12, or 21. The first

number indicates the number of bars at the brow/forehead location of the helmet. Thus, Xenith facemasks with a 12 in the title are similar to Riddell facemasks without a D, or Schutt facemasks without an R. As of 2019, Xenith does not sell new facemasks with a 12, but these facemasks are still in circulation. The second number indicates the number of horiztonal bars that traverse the nose location of the facemask. Xenith facemasks with a 21 are similar to Riddell and Schutt facemasks that include “SW” and indicates a single horizontal bar (“single wire”) across the bottom of the eye opening of the facemask. Finally, Xenith masks with an “S” at the end are similar to Riddell and Schutt facemasks with an “EG” in the title, indicating the presence of two “eye guard” vertical bars at the periphery of the eye opening.

With the exception of specialty and custom facemasks, there are similarities between the facemask geometry, also known as bar placement. Facemask materials are commonly proprietary for Riddell (HS4, LW), but are either carbon steel or titanium for Schutt and Xenith. Throughout the course of this dissertation, facemask styles will be sorted based on their geometry, material, and helmet style in an effort to understand the effectiveness and sensitivity of facemask evaluation methods in differentiating facemask performance. When necessary, facemasks of similar geometries across different manufacturers will be grouped together.

1.2 Issues to Address

After a review of relevant literature, it was postulated that full helmet system evaluation methods are difficult to replicate, result in damage to the tested protective equipment, and the impact performance results for the same helmet are difficult to compare across different testing methods. What was unclear, however, is the relevance of these full helmet system evaluation limitations on the efficacy of using full helmet system evaluation methods to identify the contribution of a change in an individual component to the performance of the entire system. For instance, if a manufacturer develops a novel design for a clip that attaches a facemask to the outer shell, will testing the full helmet system with and without the new facemask attachment clip demonstrate a performance change of the entire system that can be attributed to the change in clip? This question served as a focal point throughout the work presented in this dissertation.

Another potential gap identified in the review of relevant literature concerns the performance of the facemask. On field impact exposure research has demonstrated that 30-40% of a season's worth of football head impacts occur to the front quadrant of the helmet system. [93–100]. Impacts to the front of the helmet system have also been shown to result in high rotational accelerations [98,101]. This impact exposure research demonstrates the need to identify and quantify variables that can describe facemask performance in an effort to understand the role the facemask plays in the impact performance of football

helmet systems. However, as stated previously, facemask performance research has either been through computer simulation, which provides an important underlying theory but not irrefutable conclusions,[82] or through full helmet system analysis, the results of which were simply inconclusive.[83] However, research concerning other components of the helmet system, such as the internal padding or the external shell, focus first on the material selected prior to implementing the novel design into the full helmet system. Thus, another focus of the work presented in this dissertation was an attempt to determine the relationship between structural properties of a facemask and the impact performance of the facemask through a series of methods similar to those used commonly to evaluate internal padding and external shell systems.

1.3 Specific Aims

Once the focus of facemask characterization was identified, three specific aims of the work presented in this dissertation became clear:

SPECIFIC AIM I: Use methods available and dictated through existing industry standards to quantify the role the facemask plays in the full helmet system.

SPECIFIC AIM II: Create and validate a novel testing apparatus that measures the structural stiffness of existing and future facemask designs.

SPECIFIC AIM III: Relate the structural stiffness of football facemasks to the impact performance of the football facemasks as individual helmet system components and within the full helmet system.

After accomplishing all three specific aims, the limitations of existing methods for facemask evaluation became clear, which introduced the necessity for the implementation of a structural stiffness test for future facemask designs. The goal for this dissertation is the dissemination of a unique realization that the evaluation of football facemasks can be non-destructive, easily repeatable, and effective in determining differences in facemasks based on structure and material.

CHAPTER TWO

EFFORTS TO USE EXISTING EXPERIMENTAL METHODS TO EVALUATE FACEMASKS

The goal of this chapter is to summarize the evaluation of full helmet system performance based on the facemask used using existing test methods. This goal was achieved by using a twin-wire guided linear drop tower as described by the National Operating Committee for the Standards of Athletic Equipment (NOCSAE). An overview of the standard use of the NOCSAE drop tower, including calibration methods, installation requirements, and testing procedures, is included in Appendix A. The results of this chapter demonstrate that the NOCSAE drop tower is ineffective in differentiating impact performance based on the facemask alone.

Two different experimental designs were used to evaluate the capacity of the NOCSAE drop tower to characterize the effect a facemask has on the performance of the helmet system. One experimental design summarized the performance of reconditioned facemasks across 7 different helmet models using the NOCSAE drop tower. The goal of this experimental design was to determine whether the NOCSAE drop tower was effective in differentiating performance based on facemask geometry, helmet attachment, or facemask material. The second experimental design was used to determine the effect a facemask has on the helmet system performance by impacting the helmet system with and without a facemask. The goal of this experimental design was to determine the

effectiveness of the NOCSAE drop tower in exposing a helmet system to repeat impact damage and then quantifying the effect of that damage.

2.1 Background on Reconditioned Facemasks

The impetus for the work performed in this chapter was brought by a facemask reconditioning service provider, Green Gridiron, located in Greenville, SC, USA. Facemask reconditioning is a process in which the thermoplastic polyethene powder coating of the facemask is completely removed and replaced by new coating. Prior to re-entering the playing field, a sample of reconditioned facemasks must be certified according to the standard outlined in the NOCSAE Document 087 Section 9: "Recertification Procedure For Metal Faceguards NOCSAE."[49] According to ND087, the sample of reconditioned facemasks must experience one impact at 4.23 m/s (which results from about a 3

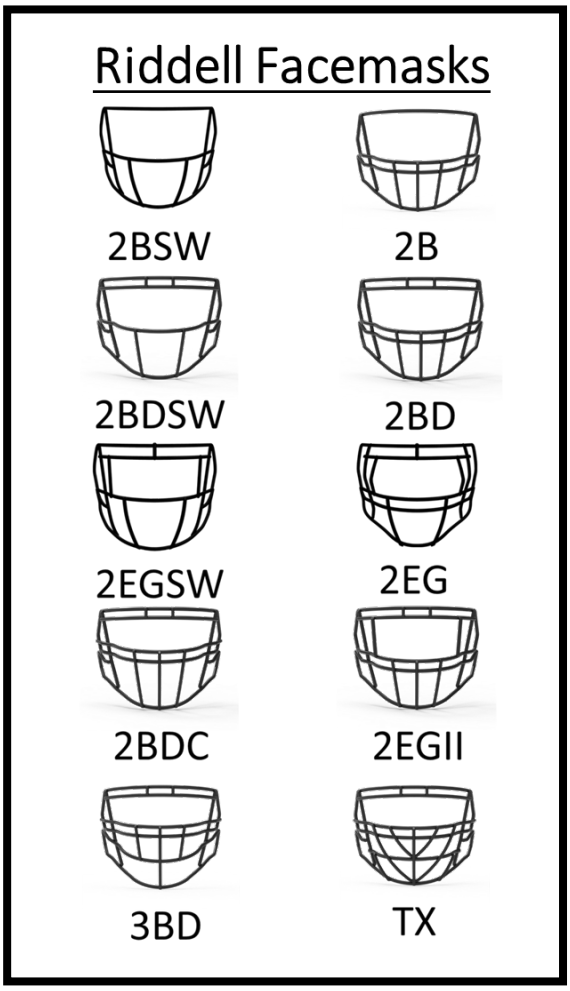

Figure 2.1: A sample of existing facemask structures available by the protective equipment manufacturer Riddell.

foot drop) without allowing the nose of the biofidelic headform to contact any part of the impacting surface or full helmet system, including the facemask. In addition, each of the reconditioned facemasks must withstand an impact at 5.47 m/s (which results from about a 5 foot drop) while mitigating the impact severity of the headform below a specific threshold. However, it was unclear at this time whether the use of the NOCSAE drop tower was effective in differentiating impacts of the same inputs based on different facemasks designs.

When a facemask is added to a full helmet system, the rigidity of the facemask increases the stiffness of the entire helmet system. This is especially important since recent advances in helmet system design have focused on increasing the flexibility of the entire helmet system. By increasing the flexibility of the helmet system, the helmet deflection upon impact will increase, thus increasing the duration of the head impact, which subsequently decreases the resulting head acceleration. Thus, it is expected that the addition of a football facemask will, by decreasing the helmet system flexibility, increase the head acceleration, which could potentially increase injury risk across the head injury spectrum (see Figure 1.1).

A spectrum of facemask styles made by facemask manufacturer Riddell is presented in Figure 2.1. The work presented in this chapter was the first attempt to allow facemask consumers the opportunity to identify which facemask style in Figure 2.1 has the best likelihood of reducing the impact severity experienced on the field. This work was done in two steps: 1.) collect and analyze a sample of

reconditioned masks of various styles and measure the resulting helmet impact performance; and 2.) identify the difference in helmet system performance in the presence and in the absence of a football facemask. If the NOCSAE drop tower can be used to evaluate the difference in helmet system response to impacts of different severities, then the database of facemask-specific contributions to the helmet system performance can be built using the NOCSAE drop tower. However, if the NOCSAE drop tower is found to be insufficient in sensitivity to differences in facemask design, then it should be necessary to generate alternative methods to evaluate football facemasks beyond those used to simply certify athletic equipment. It is the hypothesis of this section that the NOCSAE drop tower will generate data sensitive enough to 1.) differentiate across facemask styles, specifically related to facemask geometry (bar placement) and structural material; and 2.) measure repeatable differences in the performance of a football helmet with and without a facemask. To evaluate the difference in helmet system performance in the presence and absence of a facemask, a repeat impact test was performed. To evaluate the impact results of helmet systems with various facemask designs, the NOCSAE twin-wire guided drop tower method was used.

2.2 Materials and Methods

2.2.1 Facemask Performance on the NOCSAE Drop Tower

To determine the effect a specific facemask style has on the impact performance of the entire helmet system, the NOCSAE Twin-Wire guided drop

tower was used. Over two years, reconditioned facemasks were visually inspected for permanent deformations greater than 3/8 inches (9.52 mm). Any reconditioned masks that passed visual inspection were attached to the appropriate helmet and evaluated following the protocol for reconditioned facemasks outlined in NOCSAE Document 087[102] and in Appendix A. Briefly, the helmet system, including the facemask, was placed on a Medium NOCSAE headform. The helmeted headform was raised and subsequently dropped from three and five feet. For impacts from three feet, a facemask was evaluated based on whether the headform's nose contacted any part of the facemask, helmet, or impact surface. Nose contact was identified by placing a thin layer of white cream on the tip of the NOCSAE headform nose, and visually and tactilely inspecting the inside of the facemask, the pads located at both the jaws and the brow of the helmet, the inside of the chin strap, and the impactor pad. If any white lotion was found through visual or tactile inspection, the impact was flagged for facemask rejection. For impacts from five feet, the impact severity was defined with Gadd's Severity Index (Figure 2.2) and the peak acceleration (in g's). Acceleration-based metrics were measured with a triaxial accelerometer (PCB Piezotronics, Depew, NY).

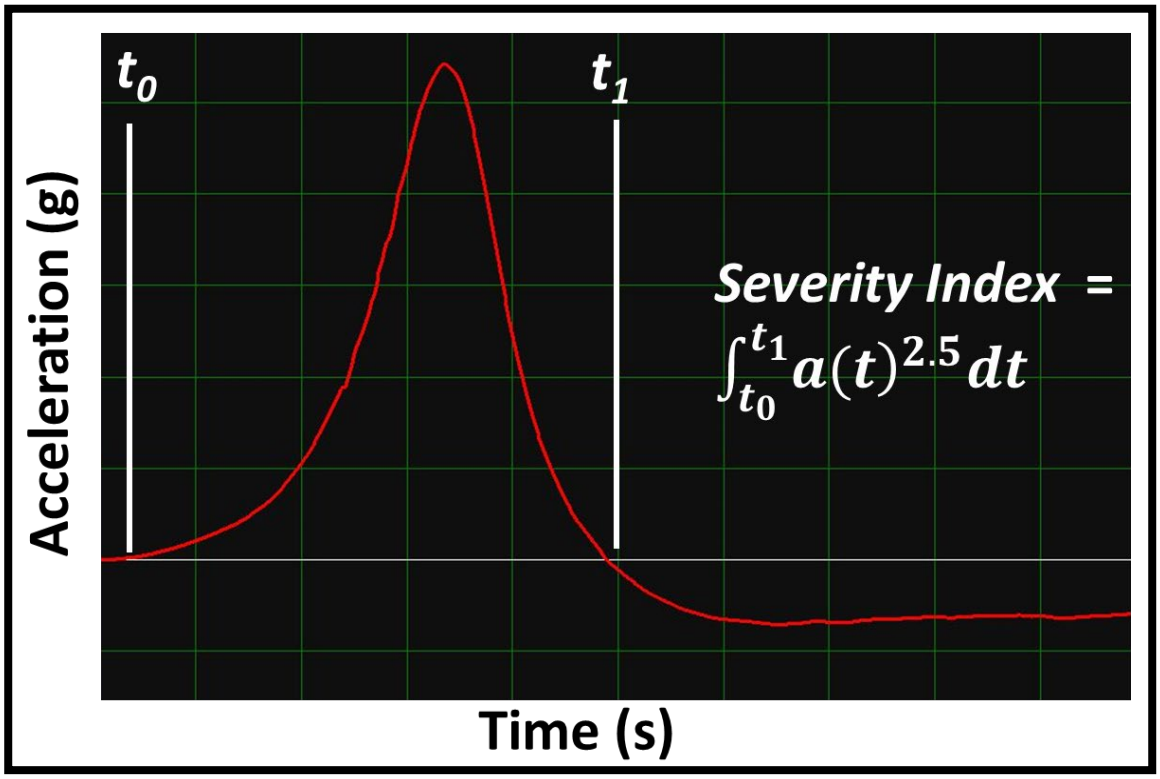

Figure 2.2: An acceleration-time chart of a shock impulse. The severity index is calculated as the area under the acceleration-time curve during the duration of the impact, raised to a scaling factor associated with severe traumatic brain injury in humans.

Reconditioned facemasks (n=1087) were evaluated using the above protocol. Facemask impacts were rejected and removed from the final analysis for the following reasons: 1.) impact velocity occurred outside the accepted velocity window for three and five foot impacts; 2.) impacts resulted in the failure of the chin strap, which was defined as the de-buckling of any one of the four buckle locations between the chin strap and the helmet shell; or 3.) impacts performed caused the failure of any component of the helmet system, such as the clip attaching the facemask to the helmet shell, the internal pads dislodging

from the helmet shell, the fracture of any location on the helmet shell, or the failure of any quick release bolt affixing the facemask clip to the helmet shell. Each incidence of impact rejection was recorded, and the data from these impacts were eliminated from analysis.

The capacity for the NOCSAE drop tower to differentiate helmet system performance based on facemask style used was evaluated based on the presence of nose contact upon impact following a three foot drop, and the acceleration-based severity of an impact following a five foot drop. Facemasks that fit a Riddell Revolution, Riddell Speed, Riddell 360, Schutt XP, Schutt DNA, Schutt Vengeance, Xenith Epic, and Xenith X1 were used (Figure 2.3). The facemasks used range in brand-specific nomenclature, but include masks that feature a two and three horizontal bar style, nose guards, carbon steel and lightweight material, custom “specialized” styles, linemen masks, skill position masks, quarterback masks, and specialist masks.

Facemasks were affixed to the outside of the helmet shell according to manufacturer instruction. Facemasks that fit the Riddell Revolution, Schutt XP, Schutt DNA, Schutt Vengeance, Xenith Epic, and Xenith X1 required the use of manufacturer-specific plastic clips, metal screws, and t-nuts. These facemasks were attached to the external side of the helmet shell in four locations, two of which on the jaw portion of the helmet, and the other two above the brow of the helmet. Facemasks that fit the Riddell Speed and Riddell 360 used a manufacturer-specific mechanism, called “quick release” clips, to attach to the

helmet shell, also in the same four locations as the previous collection of masks for the Riddell Revolution, Schutt XP, Schutt DNA, Schutt Vengeance, Xenith Epic, and Xenith X1 helmets.

Once facemasks were attached, helmets were placed on a NOCSAE headform, size medium. Helmets were fit to the NOCSAE headform according to manufacturer directions for each helmet style. Care was taken to ensure chin strap placement was consistent for each evaluation. Soft cup chin straps were attached to the helmet shell in four locations using Noggin Loc attachment mechanisms. These attachment mechanisms were used in place of the manufacturer-default buckles to ensure that chin straps consistently remained attached to the helmet shell throughout each impact. Each Chin Strap was placed over the chin of the NOCSAE headform, and the location of the Noggin Loc attachment was marked with a permanent marker in order to ensure this location was consistent across all impacts for each helmet.

For Schutt helmets, jaw pads were permanently attached to the interior of the helmet shell using a screw and a t nut. This was done to limit the incidence rate of rejected data resulting from impacts in which jaw pads detached from the inside of the helmet shell. This was only performed for Schutt helmets because other helmet manufacturers did not provide this option for attaching jaw pads to the helmet shell.

Statistical analysis was performed using SPSS and JMP statistical software packages. Facemask performance was measured binomially for 3 foot

impacts, in which a dummy variable was established to indicate the presence of nose contact. Three foot drops were analyzed to identify trends in helmet facemask combinations likely to result in facemask rejection based on NOCSAE standard ND087. For five foot impacts, severity index and linear acceleration, measured in g's, were used to indicate facemask performance within a helmet system. Differences across facemask performance after five foot impacts were determined through a comparison across all pairs using Tukey's Highest Significant Difference. Facemask performance differences during three foot impacts was determined using a binomial analysis on the nominal data set. After analyzing the complete data set, a separate analysis of mask styles for which over 15 masks were tested was performed to increase the power of the analysis.

2.2.2 Helmet System Overall Impact Performance with and without a Facemask

To determine the impact performance effect of football helmet systems with and without a facemask, the NOCSAE drop tower was used. Impact performance was measured in two ways, both of which relied on the use of a triaxial accelerometer (PCB Piezotronics, Depew, NY): severity index, which has arbitrary units, and peak linear acceleration, measured in g's. Severity index is calculated using the relationship in Figure 5, and has been commonly used as a metric for head impact severity in laboratory impact simulation research.[103,104] The helmeted headform, without a facemask, was raised and subsequently dropped from three feet ten times, then was raised and dropped from five feet ten

times. Then, the facemask was placed on the outer shell of the helmet, and the helmeted headform was raised and dropped ten times from the three foot height, followed by the five foot height. Following each impact, the headform and helmet system was examined for any individual component failure. Component failures included broken facemask clips, failed chin strap buckles, disconnected jaw pads within the helmet shell, and permanent damage or cracking of the helmet shell. For each impact, the impact severity was defined with Gadd's Severity Index and the peak acceleration (in g's). Acceleration-based metrics were measured with a triaxial accelerometer. Before and after the entirety of the testing, the width of the facemask was measured using a set of calipers in order to calculate the permanent horizontal deformation (spreading) that occurred for each facemask.

The facemasks and helmet systems used are summarized in Figure 2.3. The Riddell Revolution helmet was tested with a traditional carbon steel G2B facemask. The Riddell 360 helmet was tested with the carbon steel 360-2BD facemask. The Riddell Speed helmet was tested with the carbon steel S2BD and the lightweight, hollow tube version of the S2BD facemask. The Xenith Epic helmet was tested with the XRS-12-S facemask, and the Zuti PreciZion facemask, a "no-weld" facemask manufactured by a third-party vendor (Zuti Facemasks). The impact location for each combination of helmet system facemask was based on the "Front" location in the NOCSAE standard ND-087, but was adjusted in order to safely examine the helmet impact performance

without the facemask, but make the facemask impacts comparable to the impacts without a facemask.

The impact performance for each impact was measured and charted for each helmet and helmet-facemask combination. Both the fatiguing effect resulting from consecutive impacts and the bulk impact performance of all impacts were observed. Impact severity of each subsequent impact was normalized to the impact severity of the initial impact sustained by each helmet or helmet-facemask combination. A linear regression analysis was performed on the results of the simulated head impacts to elucidate the effect that consecutive impacts had on the impact performance of helmet and helmet-facemask combinations. Coefficients of determination (R^2) less than 0.2 were considered not statistically relevant. A two-tailed ANOVA test was performed to determine whether a difference occurred between impacts occurring to a helmet or a helmet-facemask combination, followed by a Tukey's HSD post hoc test to determine where the differences occurred.

The relationship between severity index and peak linear acceleration was identified in section 2.2.1 to be highly correlated, thus statistical analysis was performed exclusively on the severity index for each impact combination. For helmet styles with one facemask style (Riddell Revolution and Riddel 360), standard t-test was performed to identify a difference between the helmet with and without a facemask. For helmet styles that were used to evaluate more than one facemask style (Riddell Speed and Xenith Epic), two tailed analysis of

variance (ANOVA) was performed for both the three foot and five foot drop data sets. If significant difference was determined, then Tukey's HSD test was used to pick out the helmet-facemask combinations that were statistically different. Difference in performance was then presented as a percent difference in severity index from the helmet without a facemask.

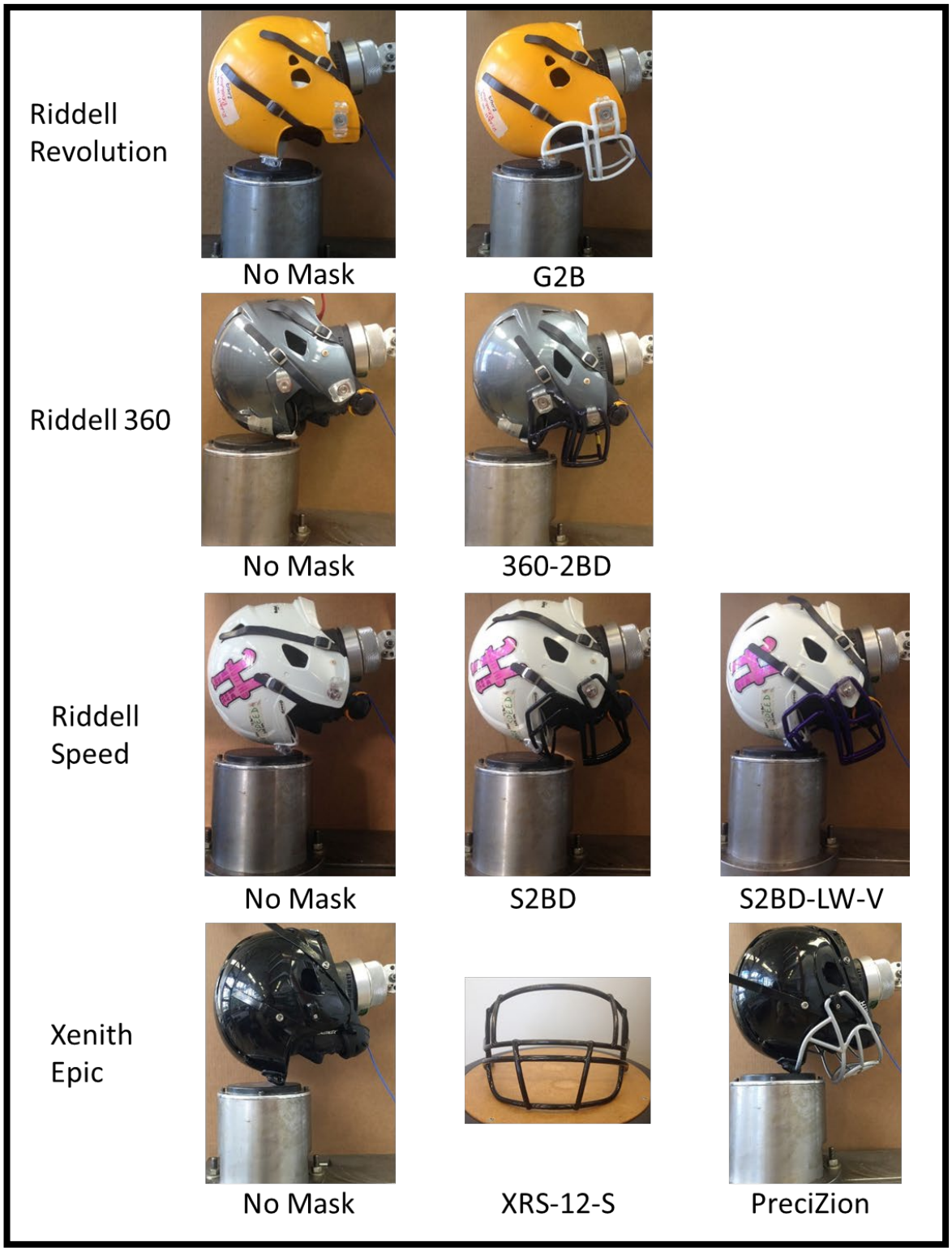

Figure 2.3: The facemask styles and appropriate helmets used to evaluate the effect the facemask has on the impact performance of the full helmet system.

2.3 Results

2.3.1 Facemask Performance on the NOCSAE Drop Tower

Of the original 1087 facemasks impacted using the NOCSAE drop tower, 97 were excluded because impacts to these masks occurred outside acceptable range of impact velocities for a 5 foot drop, and an additional 15 masks were eliminated from further analysis because impacts to those mask occurred outside acceptable velocity range for 3 foot drops, meaning that 975 facemasks were available for further analysis. The complete list of facemasks used in the final analysis are summarized in Table 2.1. Further analysis was performed on mask styles in which more than 15 individual masks were evaluated, as indicated by a yellow highlight. 22 facemask styles that fit the Schutt XP (n=7 styles), Riddell DNA (n=4 styles), Riddell Revolution (n=6 styles), Riddell Speed (n=3 styles), and Xenith X1 (n=2 styles) had 15 or more mask styles available for evaluation.

2.3.1.1 Nose Contact after 3 ft Drops

Of the 975 valid impacts, impacts to 97 facemasks (9.86%) were rejected because these impacts resulted in nose contact with either a component of the helmet system, including the facemask, or the impactor pad. Different facemask styles (n=37 styles) experienced NOCSAE drop tower failure during three foot drops that resulted in nose contact. The complete list of facemasks that experienced nose contact during the 3 foot drop is compiled in Table 2.1.

Table 2.1: A summary of facemask and helmet styles used for NOCSAE drop tower evaluations.

Schutt XP	
Mask Style	**n**
NOPO	32
ROPO-DW	29
NJOP	28
RJOP-DW	23
ROPO-UB-DW	19
Z2BN	16
ROPO	15
EGJOP	13
ROPO-UB	12
ZLT	10
NJOP-DW	9
ZLTDU	9
Z3BD	8
RJOP-UB-DW	7
RJOP-UB	7
Z2B	7
RJOP	6
JOP-DW	6
Z3B	6
Z3B 1ST GEN	6
EGOP-II	5
Z2BD	4
JOP	3
Z2EG	3
OPO	2
SUPER PRO EGOP-II	2
Z2BDU	2
EGOP	1
CU-Z2BSW	1
OPO-DW	1
RJOP-UP-DW	1
ROPO-LW	1
Z2N	1
Z3BDU	1
Total	**296**
% of Total Masks	**30%**

Schutt Vengeance	
Mask Style	**n**
RJOP-UB-DW	1
RJOP	1
ROPO	1
Total	**3**
% of Total Masks	**0.3%**

Riddell DNA	
Mask Style	**n**
DNA-ROPO-DW	23
DNA-EGOP	22
DNA-RJOP-UB-DW	18
DNA-RJOP-DW	16
DNA-RJOP	14
DNA-ROPO	14
DNA-EGOP-II	12
DNA-EGJOP	11
DNA-ROPO-UB-DW	6
DNA-BD-ROPO	5
DNA-EGJOP-II	3
DNA ROPO	2
DNA ROPO-DW-LONG	2
DNA-AFL-EGJOP	2
DNA-AFL-EGOP	2
DNA-EGOP	1
DNA RJOP-DW	1
DNA ROPO-DW	1
DNA-RJOP-DW-XL	1
DNA-RJOP-UB	1
DNA-ROPO-DW-LONG	1
DNA-ROPO-UB	1
Total	**159**
% of Total Masks	**16%**

Riddell Speed	
Mask Style	**n**
S2BDC-SP	29
S2EG-LW-V	29
S3BD-SP	20
S2EG-II-SP	11
S2BD-LW-V	9
S2BD-SP	7
S3BD	6
S2EG	5
S3BD-LW-V	5
S2BDC	4
S2BDC-LW-V	4
S2BDUC	3
S2B	2
S2BD	2
S3BDC	2
S3BDC-LW-V	2
S2BD-HT-LW	1
S2BD-II-SP	1
S2BD-LW	1
S2BDC-HT	1
S2BDC-HT-LW	1
S2EG-II	1
S2EG-SW-SP	1
S3BDC-SP	1
Total	**90**
% of Total Masks	**9%**

Riddell Revolution	
Mask Style	**n**
G3BD	46
G2EG	45
G2BD	44
G3EG	27
G2BDC	26
G2B	15
G2BDUC	7
G3BDU	6
ROPO	5
G2EG-LW	5
RJOP-DW	4
G2BN	4
G2BC	3
G2BD-1ST GEN	3
G2BDU	3
G3BD-1ST GEN	3
G3BDC	3
G3EG-1ST GEN	3
G3B-1ST GEN	2
G3BN	2
ROPO-DW	1
RJOP-UB-DW	1
EGOP-II	1
G2B-LW	1
G2BD4	1
G2BDC-1ST GEN	1
G2BUC	1
G2EG-1ST GEN	1
REVO SHORT	1
Total	**265**
% of Total Masks	**27%**

Riddell 360	
Mask Style	**n**
360-3BD-LW	7
360-2BD-LW	4
CU-360-2B-SW	3
360-2EG-SW-SP	1
360-3EG-LW	1
Total	**16**
% of Total Masks	**2%**

Xenith X1	
Mask Style	**n**
XRS-22	18
XLN-22	17
XRS-22-S	9
XRN-22	6
XRS-21-S	6
XLN-22-XL	4
XRN-22-S	2
XRN-XL	1
XRS-21	1
Total	**64**
% of Total Masks	**7%**

Xenith Epic	
Mask Style	**n**
XLN-22	9
XRS-22-S	5
XRS-22	3
XRN-22	3
XRS-21-S	3
XRS-12-S	1
Total	**24**
% of Total Masks	**2%**

Table 2.2: A summary of facemask and helmet styles used for NOCSAE drop tower rejections (3 foot drop).

Schutt XP	
Mask Style	**n**
NJOP	13
NOPO	6
Z2BN	6
ROPO	5
ZLT	5
RJOP-DW	4
EGJOP	4
ROPO-UB	4
Z3B 1ST GEN	4
ZLTDU	3
Z2B	3
ROPO-DW	2
Z3BD	2
RJOP-UB	2
ROPO-UB-DW	1
RJOP-UB-DW	1
RJOP	1
EGOP-II	1
Z3B	1
OPO	1
Total	**69**
% of Rejected Masks	**72%**
% of Total Masks	**7%**

Riddell Revolution	
Mask Style	**n**
G3BD	4
G2EG	3
ROPO-DW	1
ROPO	1
G2B	1
Total	**10**
% of Rejected Masks	**10%**
% of Total Masks	**1%**

Riddell DNA	
Mask Style	**n**
DNA-RJOP-DW	3
DNA-RJOP	3
DNA-ROPO-DW	1
DNA-ROPO	1
DNA-EGJOP	1
DNA-ROPO-UB-DW	1
DNA-EGJOP-II	1
Total	**11**
% of Rejected Masks	**11%**
% of Total Masks	**1%**

Riddell Speed	
Mask Style	**n**
S2EG-LW-V	1
Total	**1**
% of Rejected Masks	**1%**
% of Total Masks	**0.1%**

Riddell 360	
Mask Style	**n**
CU-360-2B-SW	1
Total	**1**
% of Rejected Masks	**1%**
% of Total Masks	**0.1%**

Xenith X1	
Mask Style	**n**
XRS-22	1
Total	**1**
% of Rejected Masks	**1%**
% of Total Masks	**0.1%**

Xenith Epic	
Mask Style	**n**
XLN-22	2
Total	**2**
% of Rejected Masks	**2%**
% of Total Masks	**0.2%**

Of all the facemasks that were rejected, 72% (n=69) were facemasks that fit the XP helmet. An effort was made to identify potential reasons for the high incidence rate of facemask rejections due to nose contact occurring to facemasks using the Schutt XP helmet. Five different Schutt XP helmets were used during the course of all 1087 facemasks evaluations. Incidence of facemask rejections for each specific Schutt XP helmet used (labelled XP 1, XP 2, XP 3, XP 4, and XP 5) is summarized in Table 2.3.

Table 2.3: A summary of Schutt XP helmets used for NOCSAE drop tower rejections (3 foot drop).

Helmet Code	Nose Contact	n	Percent of Helmet Facemasks	Percent of Total XP Facemasks
XP 2	Y	15	18%	5%
	N	68	82%	23%
XP 3	Y	12	11%	4%
	N	102	89%	35%
XP 4	Y	15	31%	5%
	N	34	69%	12%
XP 5	Y	27	56%	9%
	N	21	44%	7%
Total	**Y**	**69**		**23%**
	N	**225**		**77%**
	Total	**294**		

The data collected using the XP 1 helmet was filtered out of this analysis (n=2 masks) because this helmet experienced catastrophic failure prior to its removal from the testing protocol. As a result, 294 facemasks were evaluated using four versions of the Schutt XP helmet. For the XP 2, XP 3, and XP 4

helmets, 12-15 facemasks were rejected due to nose contact (n=42 total rejected masks, 20% of facemasks tested on helmets XP 2, 3, and 4). However, over half of the facemasks evaluated with the XP 5 helmet were rejected based on nose contact resulting from the three foot drop. This indicates that the result of facemask evaluation using the NOCSAE drop tower is influenced by the specific helmet used for analysis.

In addition to the specific helmet used, one facemask category resulted in a higher incidence rate of rejection than other facemask styles. The three facemask styles that experienced the highest rejection incidence rate were the NJOP (n=13 rejections), NOPO (n=6 rejections), and Z2BN (n=6 rejections). These three facemask styles represented 36% of the total number of masks rejected based on nose contact. As indicated by the “N” in their facemask style name, these three facemasks all feature a “nose guard” bar that spans the vertical space between the brow of the facemask and the horizontal bar at the base of the ocular opening of the facemask.

Of all the mask styles that feature a “nose guard” bar (n=13 styles, n=138 total masks, Table 2.4), 27% of facemasks were rejected. For all the mask styles do not feature a “nose guard” bar (n=949 total masks), only 10% were rejected based on nose contact. As it stands to reason, there is a higher incidence rate of facemask rejection based on nose contact when the facemask features a bar with greater contact area in front of the nose, such as a “nose guard” bar. The odds ratio of a facemask with a nose bar resulting in a failed 3 foot drop due to

nose contact is 3.03 (95% CI: 1.87-4.92), indicating that it is roughly 3 times as likely for a facemask with a nose bar to fail the 3 foot evaluation than a facemask with a completely open eye window.

Table 2.4: A summary of all facemask styles that feature a vertical nose bar.

NOPO	32
NJOP	28
XLN-22	26
Z2BN	17
NJOP-DW	10
XRN-22	9
G2BN	5
XLN-22-XL	4
G3BN	2
XRN-22-S	2
NJOP-XL	1
XRN-XL	1
Z2N	1
All	138

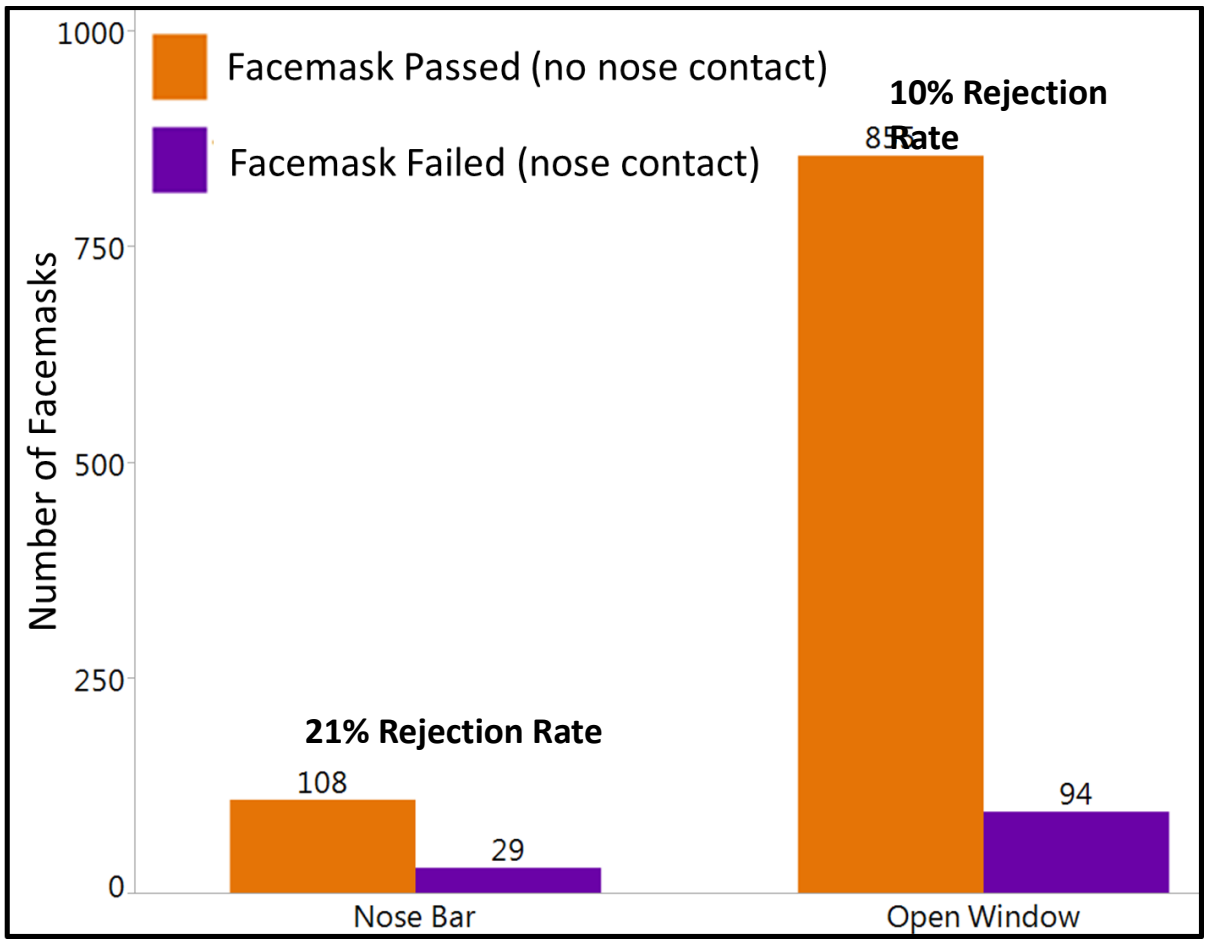

Figure 2.4: The frequency of facemask rejection based on the presence of a nose bar.

As indicated in Figure 2.4, according to the NOCSAE drop tower evaluation method for rejecting facemasks, there is a greater likelihood of facemask rejection due to nose contact for facemasks that have a nose bar than those that do not have a nose bar. For comparison, these facemasks were used further to understand the effect nose contact has on impact severity of five foot impacts. These facemasks were also used to understand the effect the nose bar has on the impact severity of five foot drops.

2.3.1.2 Impact Severity of 5 foot Drops

In order for a facemask to be rejected after the 5 foot impact, the impact must result in a Severity index greater than 1200. Peak linear acceleration was also collected for each 5 foot impact. The distribution of severity index values, measured in arbitrary units (au) resulting from 5 foot impacts using the NOCSAE Drop Tower is presented in Figure 2.5. For the 975 qualified facemask impacts, the mean severity index was 292 au (95% CI: 283-301 au), and the median severity index was 258 au. Based on the purple line in Figure 2.5A, the resulting severity index values was not normally distributed, but was instead skewed left. 97.5% of the severity index values collected were below 657 au. None of the facemasks were rejected based on exceeding a severity index of 1200 au during a 5 foot impact. One impact came within 12% of the exclusion threshold, a facemask that measured 1057 au in severity index.

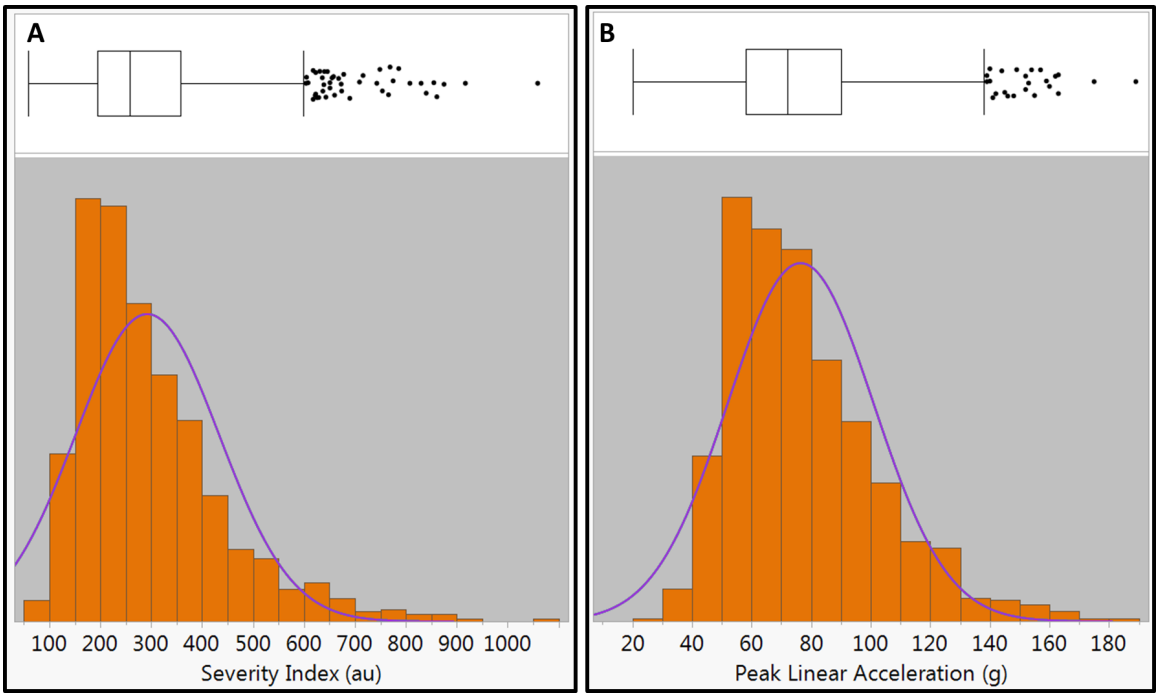

Figure 2.5: A histogram for A.) severity index and B.) peak linear acceleration resulting from all 5 foot drops.

The distribution of peak linear acceleration, measured in g units, is presented in Figure 2.5B. While there is no facemask rejection criteria associated with peak linear acceleration, this metric is commonly used in headwear evaluation protocols, both on fields and in laboratories, so linear acceleration is included here. The mean peak linear acceleration from 5 foot drops was 76 g (95% CI: 75-80 g), and the median peak linear acceleration was 72 g. Similar to severity index, the distribution of peak linear acceleration was not normal, but slightly skewed to the left.

The relationship of severity index and peak linear acceleration is presented in Figure 2.6. The relationship between severity index and peak linear acceleration (r^2=0.831) demonstrates that severity index and peak linear

acceleration is positively correlated to a high degree. For each increase of 1 g of peak linear acceleration, it is expected that the severity index of that impact will increase by 5.2 au. Because of the strong correlation between severity index and peak linear acceleration for NOCSAE drop tower impacts, severity index was used exclusively for the analysis of the capacity of the NOCSAE drop tower to differentiate impact performance across a variety of facemask styles.

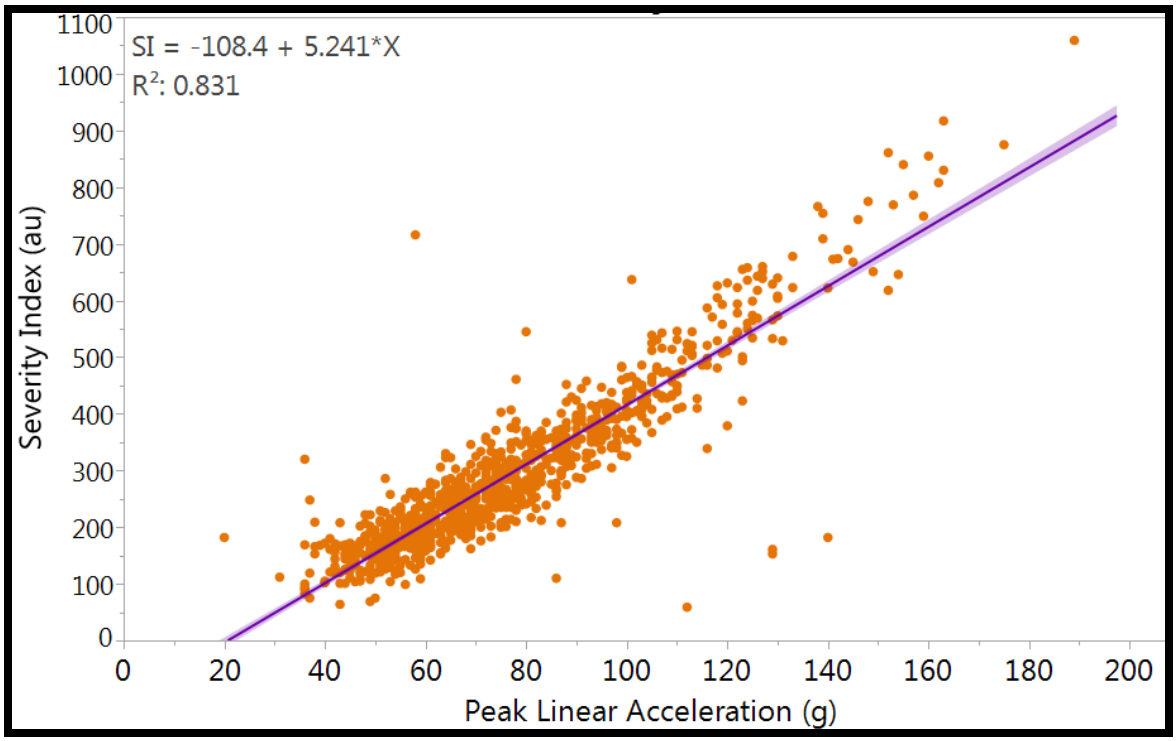

Figure 2.6: The linear relationship between severity index and peak linear acceleration for 5 foot drops.

To analyze the capacity for the NOCSAE Drop Tower to adequately differentiate facemask performance based on the specific style of mask used, the data set was filtered to include only facemask styles that had more than n=20

masks evaluated using the NOCSAE Drop Tower. The filtered data set included impacts of 495 facemasks, representing three facemask and helmet manufacturers (Riddell, n=245 facemasks; Schutt, n=179 facemasks; and Xenith, x=49 facemasks), and two different facemask materials (carbon steel, n=466 facemasks; lightweight tubes, n=29 facemasks). The average severity index measured for each of the facemask styles is presented in Figure 2.7, with error bars that span the standard deviation above and below the mean severity index.

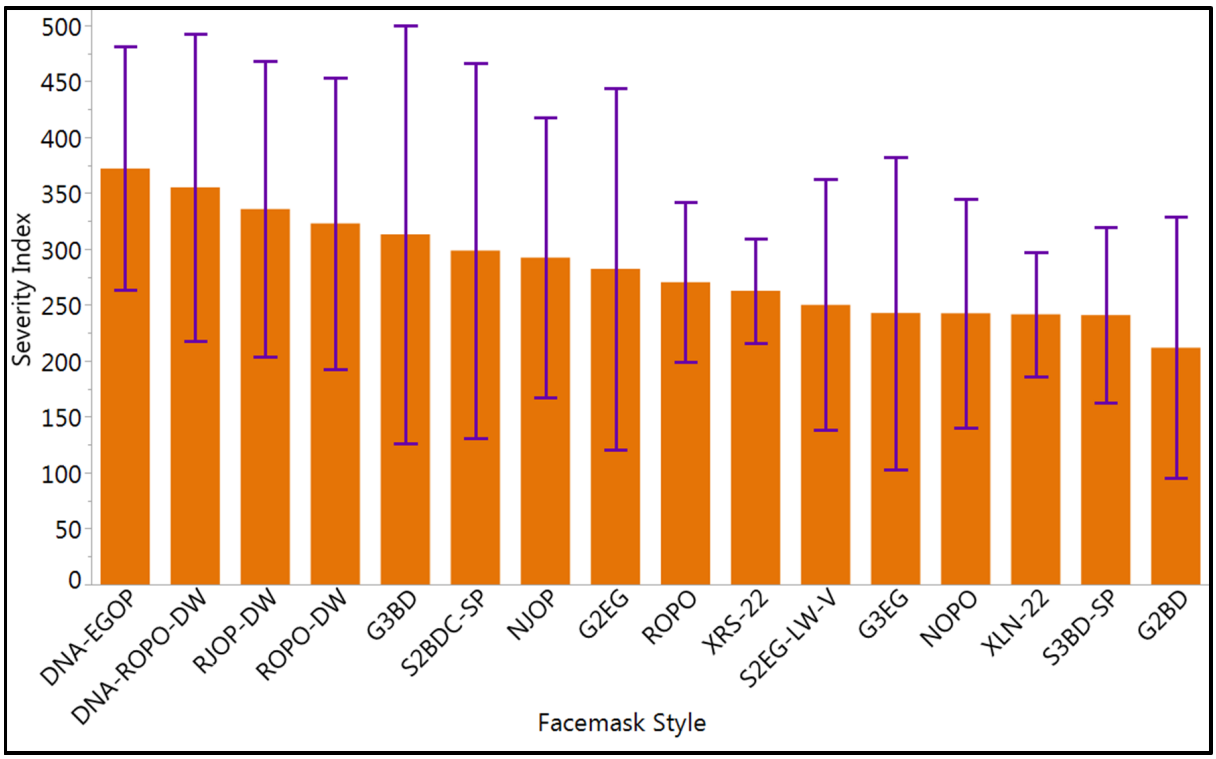

Figure 2.7: The impact response of a helmet system based on the facemask style used in the helmet system in terms of severity index experienced by the instrumented headform.

2.3.2 Helmet System Overall Impact Performance with and without a Facemask

The impact performances, measured by the severity index, of each helmet and facemask combination for the 3 foot drops are summarized in Figure 2.8.

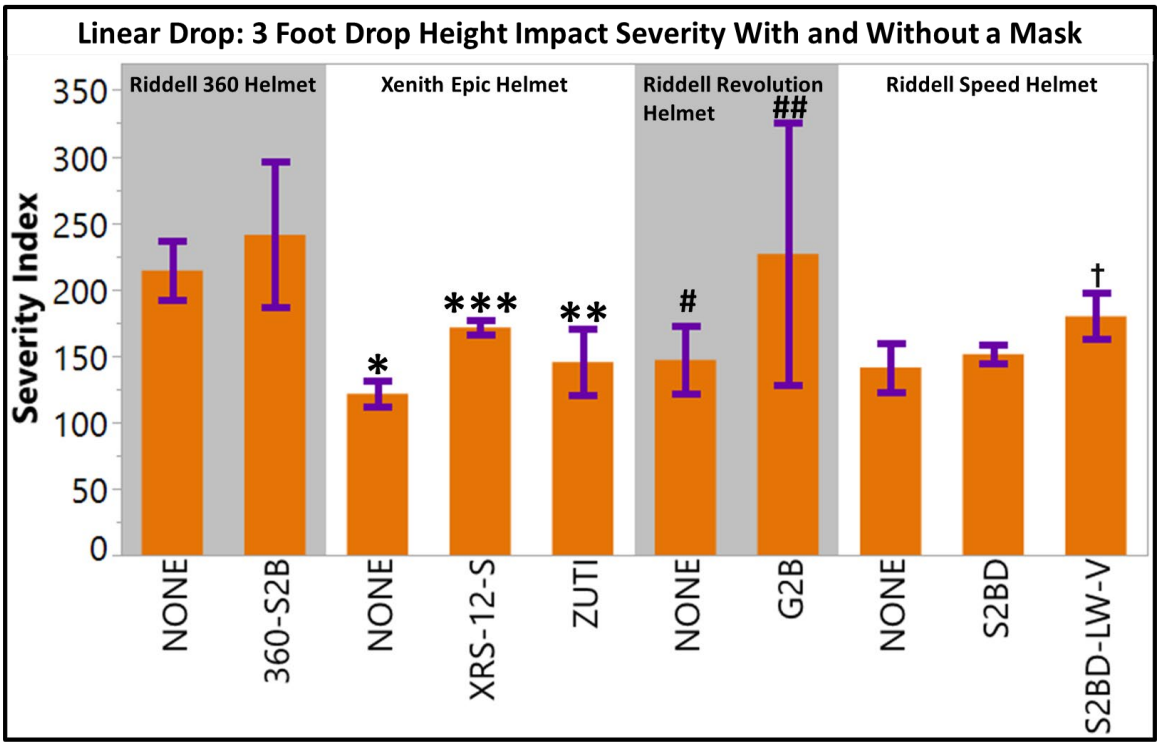

Figure 2.8: The severity index for 3 foot drop impacts to helmet systems with and without a facemask.

The specific averages and standard deviations of the helmet system impact performances are summarized in Table 2.5 for the 3 foot drops. The peak linear acceleration, measured in g, is summarized in Figure 2.9. Because the relationship between helmet system performances when using peak linear acceleration as an indicator of performance is similar to using severity index, statistical analyses were performed using severity index. Further exploration of

the relationship between severity index and peak linear acceleration is performed in section 2.3.1.

Table 2.5: A summary of impact severity with and without a facemask for all four helmet systems for 3 foot drops.

Helmet	Mask	Severity Index		Peak Lin Accel (g)	
		Mean	Std Dev	Mean	Std Dev
360	NONE	214	22	90	9.1
	360-S2B	241	55	99	11
EPIC	NONE	122	9.7	50	3.1
	XRS-12-S	171	5.6	66	1.8
	ZUTI	145	25	56	11
REV	NONE	147	25	59	12
	G2B	227	98	75	18
SPEED	NONE	141	18	58	8.4
	S2BD	151	7.5	57	1.7
	S2BD-LW-V	180	17	70	3.5

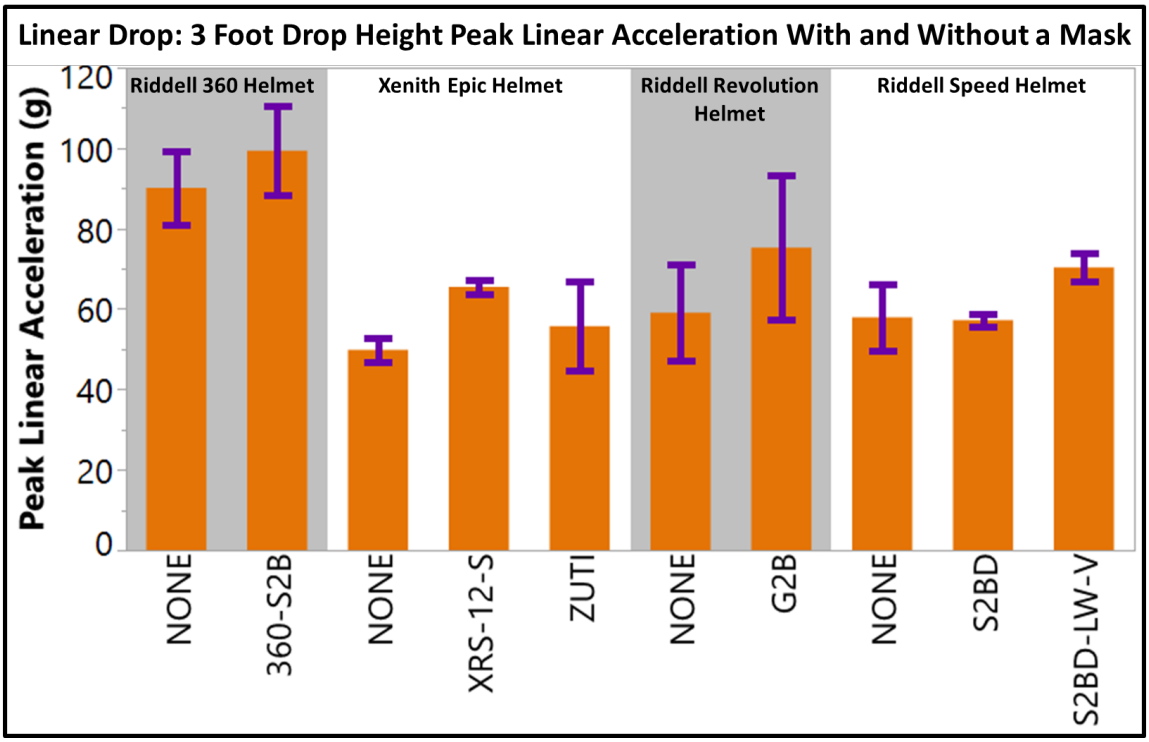

Figure 2.9: The linear acceleration for 3 foot drop impacts to helmet systems with and without a facemask.

As indicated by the error bars, indicating the standard deviation of each helmet system performance, as well as the standard deviations reported in Table 2.5, each sample group has differing variances. As a result, Welch's ANOVA was performed to identify differences in the data, within each helmet group. Each helmet group was analyzed individually, since the purpose of this line of experimentation was to indicate the effect a facemask has on a helmet's performance compared to the absence of a facemask on the helmet system. The results of the Tukey's HSD test is indicated in Figure 2.9 by different symbols for each helmet group, which indicates a statistically identified difference in mean impact performance.

For the Riddell 360 helmet, the presence of a facemask did not have a significant effect on the repeat impact performance of the helmet system. However, for the Riddell Speed, the Riddell Revolution, and the Xenith Epic, the presence of a facemask increased the impact severity applied to the headform compared to the headform impact using a helmet without a facemask. For the Xenith Epic, the Zuti facemask increased the impact severity by 19%, and the XRS-12-S facemask increased the impact severity by 40% compared to a helmet without a facemask. For the Riddell Revolution, the G2B facemask increased the impact severity by 54%. For the Riddell Speed, the S2BD facemask did not have a significant effect on the repeat impact performance of the helmet system, but the S2BD-LW-V facemask increased the impact severity by 28%. For all cases in which the facemask had a significant effect on the impact performance of the

helmet system, the presence of the facemask increased the impact severity experienced by the headform, measured by both the severity index and the peak linear acceleration. In most cases, with the exception of the Riddell Speed using the S2BD facemask and the Xenith Epic with the XRS-12-S facemask, the presence of a facemask increased the variance (and, thus, the standard deviation) of the performance of the helmet system.

The impact severity experienced by the NOCSAE headform undergoing an impact with the NOCSAE Linear Drop Tower with each helmet and facemask combination from a 5 foot drop is summarized in Figure 2.10.

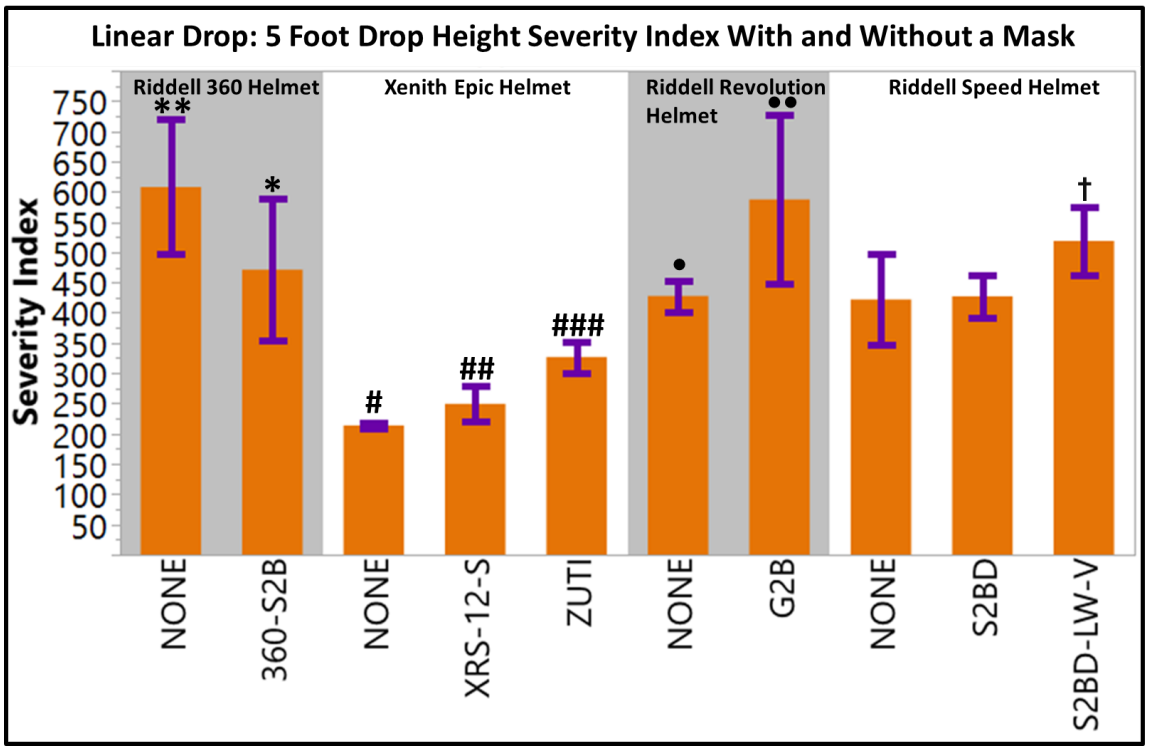

Figure 2.10: The severity index for 5 foot drop impacts to helmet systems with and without a facemask.

The specific averages and standard deviations of the helmet system impact performances are summarized in Table 2.6 for the 5 foot drops. The peak linear acceleration, measured in g, is summarized in Figure 2.11. Similar to the 3 foot drops, the relationship between helmet system performances when using peak linear acceleration as an indicator of impact performance mirrors the impact performance when severity index is used as an impact performance indicator. Thus, statistical analyses were performed using severity index. Further exploration of the relationship between severity index and peak linear acceleration is performed in section 2.3.1.

Table 2.6: A summary of impact severity with and without a facemask for all four helmet systems for 5 foot drops.

Helmet	Mask	Severity Index		Peak Lin Accel (g)	
		Mean	Std Dev	Mean	Std Dev
360	NONE	608	111	131	11
	360-S2B	471	117	117	15
EPIC	NONE	214	4.3	70	0.8
	XRS-12-S	249	29	76	11
	ZUTI	327	26	88	6.7
REV	NONE	428	26	109	8.6
	G2B	587	139	133	14
SPEED	NONE	422	75	108	18
	S2BD	427	35	106	5.7
	S2BD-LW-V	519	57	122	8.8

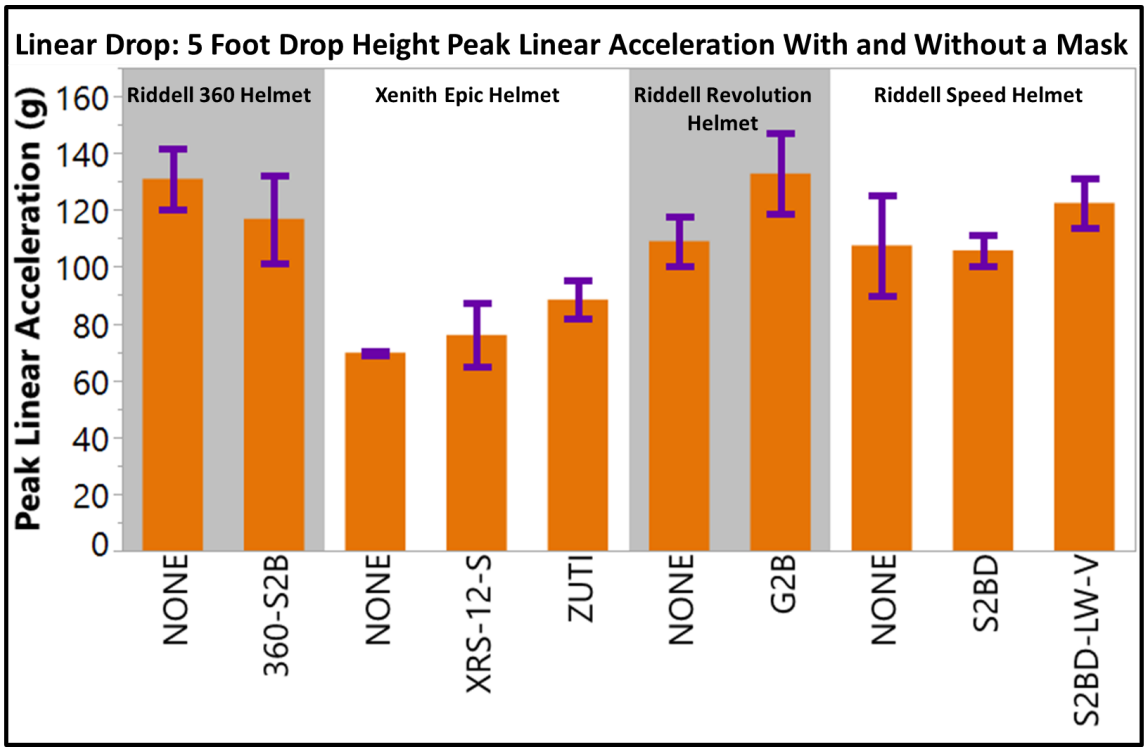

Figure 2.11: The peak linear acceleration for 5 foot drop impacts to helmet systems with and without a facemask.

As indicated by the error bars, indicating the standard deviation of each helmet system performance, as well as the standard deviations reported in Table 2.6, each sample group has differing variances. As a result, Welch's ANOVA was performed in order to identify differences in the data, within each helmet group. Each helmet group was analyzed individually, since the purpose of this line of experimentation was to indicate the effect a facemask has on a helmet's performance compared to the absence of a facemask on the helmet system. The results of the Tukey's HSD test are indicated in Figure 2.10 by symbols for each helmet group, which indicates a statistically identified difference in mean impact performance.

For each of the helmet groups, the presence of a facemask had a significant effect on the repeat impact performance of the helmet system. The Riddell 360 helmet system was the only helmet system in which the average impact severity was more severe without a facemask than with a facemask, by 23%. For the Xenith Epic, the repeat impact performance for all three helmet and facemask combinations were different, the XRS-12-S facemask increasing average impact severity by 16%, and the Zuti facemask increasing average impact severity by 53% compared to the helmet without a facemask. For the Riddell Revolution helmet, the G2B facemask increased the average impact severity of the helmet system by 37%, and increased the variance of the helmet system repeat impact performance by 435%. For the Riddell Speed, the S2BD facemask had no significant effect on the repeat impact performance of the helmet system, but the S2BD-LW-V facemask, made from the lightweight hollow tube bars, increased the average impact severity by 23%. In all cases except the Riddell 360-S2B and Riddell Speed S2BD systems, the presence of the facemask increased the variance of the repeat impact performance of the helmet system.

The severity index and peak linear acceleration results for each impact to the Riddell Revolution helmet are presented in Figure 2.12 in order to show the effect of repeated impacts on helmet system performance with and without a facemask. With each additional impact, the severity index and the linear acceleration for both three foot and 5 foot drops increased when the G2B

facemask was used. However, when no facemask was used, each consecutive impact resulted in a lower headform acceleration and resulting severity index.

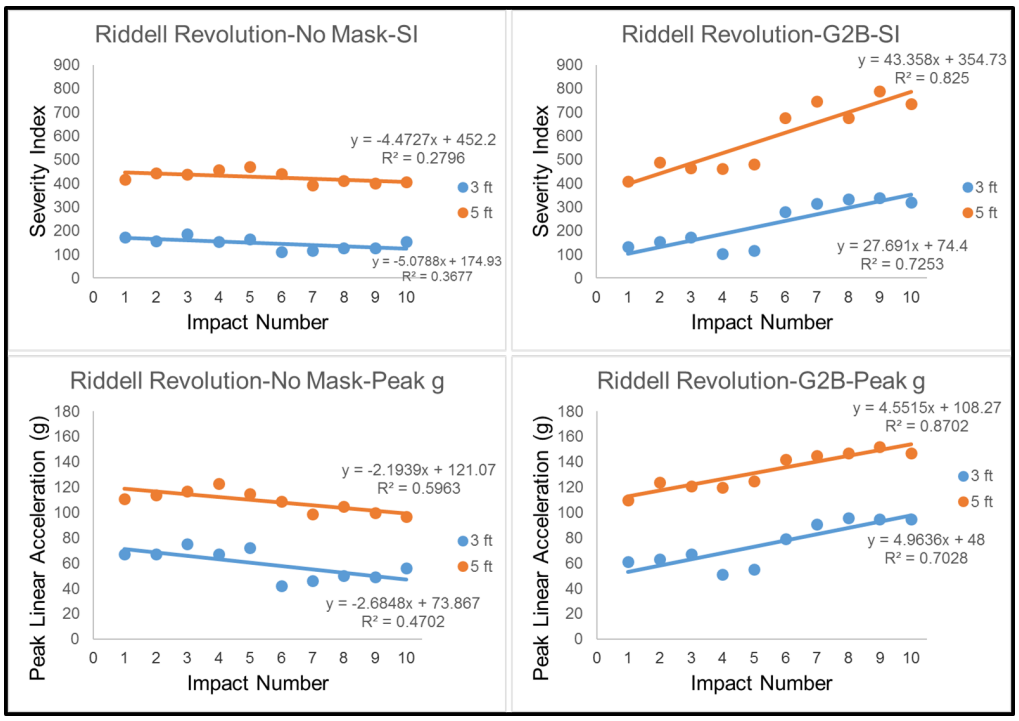

Figure 2.12: The severity index and peak linear acceleration for each of the ten impacts to the Riddell Revolution, with and without a facemask.

The severity index and peak linear acceleration results for each impact of the Riddell 360 helmet are presented in Figure 2.13. For both the 3 foot and 5 foot drops, repeated impacts to the 360 helmet with a 2BD facemask did not have a statistically relevant (r^2<0.2) relationship to previously accumulated impacts. For the 360 helmet without a facemask, subsequent impacts did not have a statistically relevant effect on headform linear acceleration upon impact for either the 3 foot or 5 foot drops. For the 3 foot drops, the severity index of impacts increased with each impact, but only by an average of 5 arbitrary severity index units per drop, which is less than 1% of the severity index threshold associated with head injury.[103]

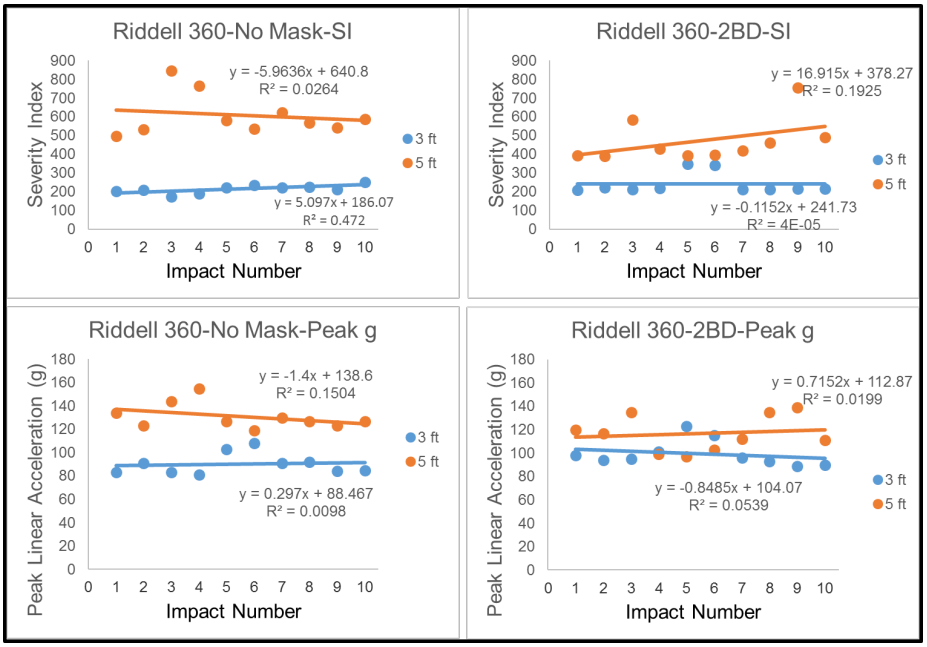

Figure 2.13: The severity index and peak linear acceleration for each of the ten impacts to the Riddell 360, with and without a facemask.

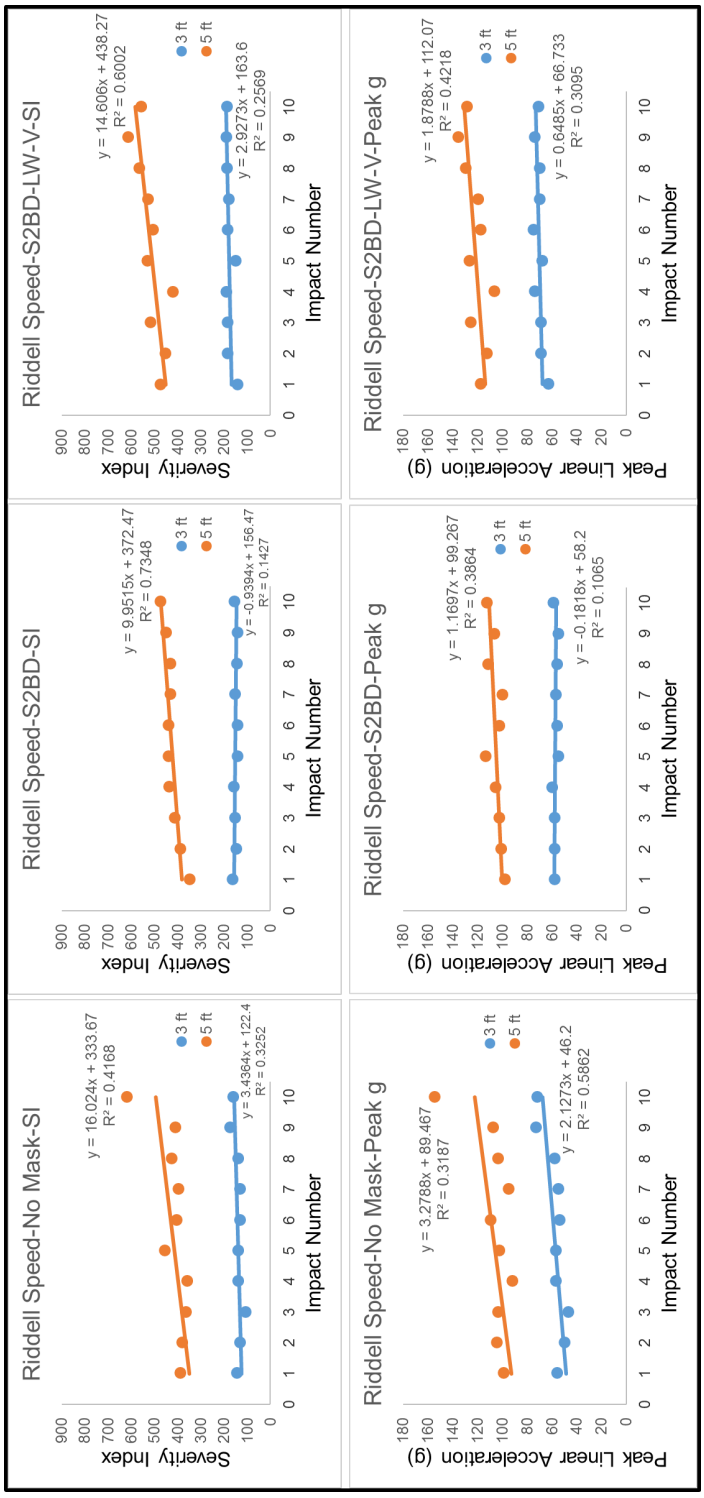

Figure 2.14: The severity index and peak linear acceleration for each of the ten impacts to the Riddell Speed, with a carbon steel and a lightweight hollow tube facemask, and without a facemask.

The severity index and peak linear acceleration results for each impact of the Riddell Speed helmet are presented in Figure 2.14. Two different facemask materials were evaluated using the Riddell Speed helmet. For the 3 foot drop, neither of the two the with-facemask, nor the without-facemask helmet system experienced a significant change in impact severity index or linear acceleration between subsequent impacts. For the 5 foot drops, both of the facemasks and the without facemask helmet system experienced an average increase in both severity index and peak acceleration with each subsequent impact. The helmet system without a facemask experienced the greatest change in severity index with each subsequent impact (16 units), followed by the S2BD-LW-V facemask (14 units), then by the carbon steel S2BD facemask (10 units).

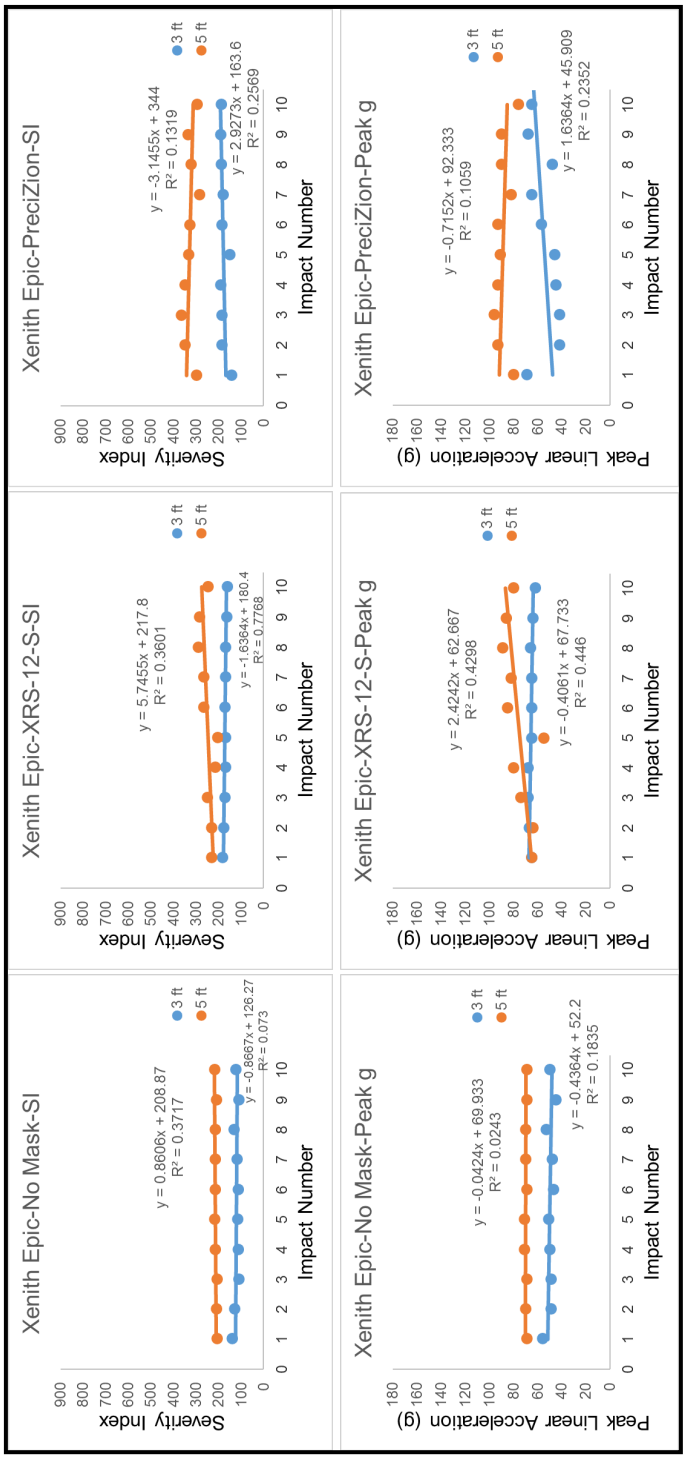

Figure 2.15: The severity index and peak linear acceleration for each of the ten impacts to the Xenith Epic, with a traditional facemask, a single piece facemask, and no facemask.

The severity index and peak linear acceleration results for each impact of the Xenith Epic helmet are presented in Figure 2.16. For the 3 foot drop, the helmet systems that experienced a non-negligible relationship between severity index and impact number was the Epic helmet with the Zuti PreciZion facemask. However, while the impact severity was non-negligibly correlated with impact number, the effect of the impact number on the impact severity was low (1% increase in impact severity for each subsequent impact). The linear acceleration measured for each impact had a non-negligible correlation to impact number for the XRS-12-S facemask and the Zuti PreciZion facemask helmet systems. The effect of the impact number on linear acceleration of the impact was an increase of 4% per subsequent impact for the PreciZion facemask helmet system, and 1% per subsequent impact for the XRS-12-S helmet system.

For the 5 foot drops, the non-facemask helmet system and the XRS-12-S helmet system had non-negligible correlations between the severity index of an impact and the impact number. For the non-facemask helmet system, the severity index increased by <1% for each subsequent impact. For the XRS-12-S helmet system, the severity increased by 3% for each subsequent impact. Also for the 5 foot drops, the linear acceleration of each impact non-negatively correlated to the impact number for the XRS-12-S helmet system. For the XRS-12-S helmet system, the linear acceleration increased by an average of 4% for each subsequent impact.

The total amount of spreading, normalized by the original facemask width, that occurred to each facemask after all 20 impacts (10 impacts from a 3 foot drop, and 10 impacts from a 5 foot drop) is presented in Figure 2.16.

The largest spreading occurred to the XRS-12-S (10.7%) and G2B (9.2%) facemasks. The spreading that occurred to the remaining four facemask styles was between 4% and 6%. The effect of spreading on facemask performance is evaluated further in Chapter 3. However, comparing Figure 2.15 and Figure 2.16

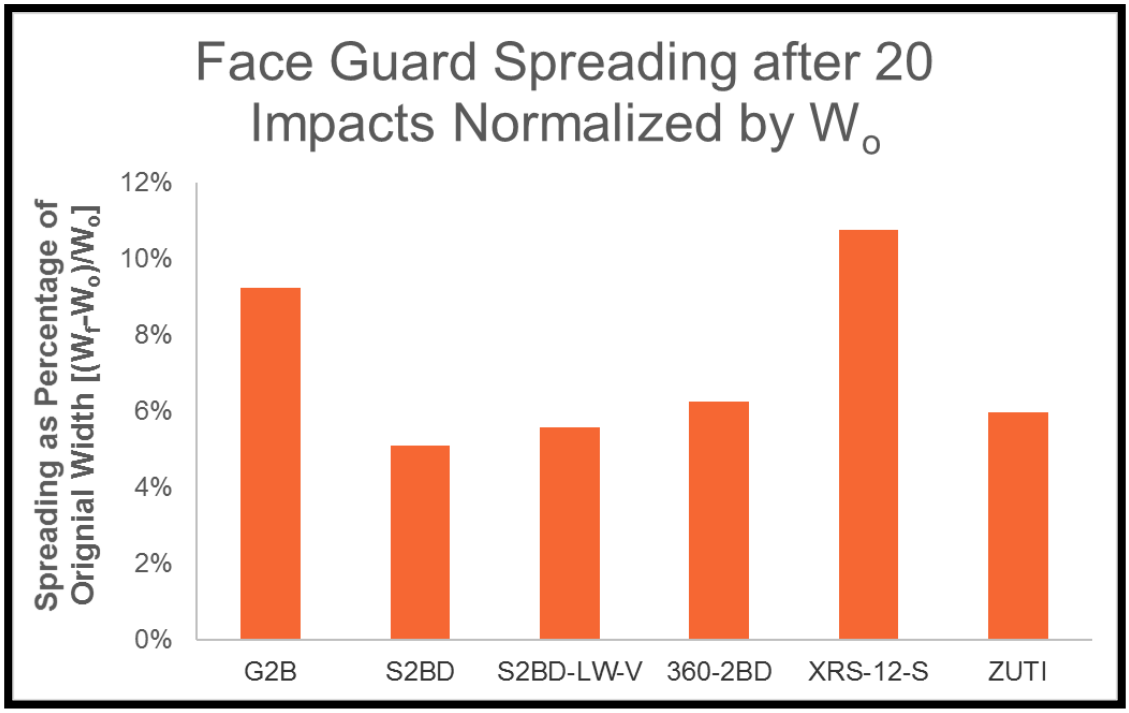

Figure 2.16: The amount of spreading that occurred to each facemask after 20 impacts, 10 from 3 feet and 10 from 5 feet, presented as a percent change in facemask width from the original facemask width (Wo).

demonstrates a variable effect of spreading on facemask performance.

For instance, using the Epic helmet, the SI and peak acceleration both increased and decreased with each subsequent impact in both the mask and no mask scenario, seemingly in a random pattern, regardless of spreading progression. The Zuti mask and the XRS-12-S mask experienced a difference in spreading by 5%, but when dropped from 3 feet, only the Zuti mask experienced an increase in peak acceleration with each subsequent impact. When dropped from 5 feet, the XRS-12-S mask experienced an increase in both SI and peak acceleration spreading severity increased. Thus, spreading does not seem to influence the impact performance of the facemask when the facemask is tested with the NOCSAE drop tower.

2.4 Discussion

2.4.1 Facemask Performance on the NOCSAE Drop Tower

The purpose of this chapter is to evaluate the potential expansion of the appropriate use of the NOCSAE drop tower. This expansion would include the use of the NOCSAE drop tower to differentiate the performance of existing and novel facemask designs in an effort to recommend the potential safety ramifications of facemask selection. To determine the effectiveness of the NOCSAE drop tower to evaluate facemask performance beyond its intended use as a general safety standard, two experiments were performed. The first experiment was designed to explore the use of the drop tower to differentiate

impact performance based on individual facemask designs. The second experiment was designed to explore the performance of a helmet system with and without a facemask, in an effort to understand the contribution of an increase in stiffness of the helmet system with the addition of a facemask.

The results of the first experimental designed help to explain several limitations of the NOCSAE drop tower in demonstrating differences in the impact performance of individual facemask designs. In order to serve as a reliable facemask impact performance testing method, the NOCSAE drop tower must generate reliable input stimuli, specifically related to the impact velocity. Of the 1087 facemasks impacted in this experimental process, 112 (10.3%) impacts were removed from further evaluation based on an impact velocity outside the acceptable threshold set forth by NOCSAE standards ((NOCSAE087). Losing impact data that results in permanent damage to 10.3% of the impacted facemasks can cost between $2,500 and $4,500 worth of facemasks lost to improper testing each year. While user error accounts for the majority of impacts that result in impact velocities outside acceptable thresholds, future facemask design evaluation methods must reduce the potential loss due to improper test parameters.

After rejecting facemasks due to improper impact conditions, further evaluations based on facemask design were limited. Facemasks can be evaluated using the standard NOCSAE drop tower in two different manners depending on the drop height used to generate the impact. Following a 3 foot

drop height, facemasks are visually inspected for indicators of internal facemask impacts to any part of the headform. If the facemask was responsible exclusively, or even indirectly, for an impact with the headform, one would expect that facemask-specific indicators, such as mask material or the location or volume of bars used in the facemask design, would be present in the results. However, 72% of all facemasks rejected based on the 3 foot drop height criteria occurred to the same helmet design, and one helmet within the design (Schutt XP 5) resulted in the rejection of 56% of all facemasks evaluated with this helmet. These results indicate that the helmet used for impact was more responsible for facemask rejection than facemask design.

The only design criteria that seemingly points toward the facemask as potentially responsible for impact to the headform is the presence of a vertical nose bar traversing the space tangential to the center of the headform (specifically hovering over the path connecting the chin, nose, and forehead). Almost 20% of all facemasks rejected after the 3 foot drop featured a “nose guard” vertical bar that connected the bottom of the mask to the top directly in the middle of the facemask. However, more nuanced design criteria such as facemask material, additional vertical and horizontal bar placement, and connection methods between the facemask and the outer shell of the helmet do not seem to generate a pattern of rejection based on the 3 foot drop.

A broader potential reason for the lack of apparent pattern in helmet system rejection based on the 3 foot drop is the use of a discrete, binary rejection

method. The “yes/no” response to a 3 foot drop does not allow for a strong correlation between design criteria of a facemask and the performance of that facemask. Thus, an evaluation method that allows for a continuous variable to measure the impact performance of a facemask is necessary for a future evaluation method. The 5 foot drop component of the NOCSAE drop tower does include a continuous variable, the severity index, as a metric that drives helmet system rejection or acceptance.

Following a 5 foot drop height, the severity index and peak linear acceleration of the headform upon impact is calculated. Based on the histogram of all 975 qualified 5 foot impacts, both the severity index and peak linear acceleration are not normally distributed, both data sets skew to the left as a result of roughly 25 high severity impact outliers. The severity index is a function of both linear acceleration and impact duration, which is likely why over 80% of all variance in an impact severity index is explained by the peak linear acceleration of the impact. Thus, little information is added by collecting both an impact’s severity index and peak linear acceleration. A more generalizable and interpretable piece of information collected alongside the peak linear acceleration of an impact would be the impact duration. Future assessment tools that evaluate impact performance of protective helmet systems should aim to include impact duration.

As a continuous variable, even one that is not normally distributed, severity index should provide more nuanced insight into the performance of a

helmet system than a discrete, binary variable. However, the variance within a facemask design, as outlined in Figure 2.7 and quantified in Figure D8 (Appendix D) indicates that the facemask attached to the helmet system creates a noisy environment that makes characterizing the facemask based on design criteria impossible. A statistically significant difference between facemask designs using severity index resulting from 5 foot drops using the NOCSAE drop tower was not present. Thus, future facemask characterization systems must reduce the noise to the system, potentially by isolating the facemask from the helmet system, to inform future facemask design.

To the knowledge of the authors present, this is the first instance in which NOCSAE drop tower data collected using NOCSAE 087 protocols and over 1000 impacts has been characterized and described in this manner. As a result of this distinct analysis, it can be postulated that the NOCSAE 087 protocols are not effective in validating potentially novel design criteria against standard facemask design. This theory is expanded upon in the following section that explores the results of impact testing a helmet system with and without a facemask and compares these results to previously reported data across multiple laboratories.

2.4.2 Helmet System Overall Impact Performance with and without a Facemask

Another way to understand the effect a facemask has on the impact performance of a helmet system is to evaluate the performance of a helmet system with and without a facemask. The theory tested in this section is that a

facemask will have a repeatable increase in the impact severity of a helmet system when using a NOCSAE twin-wire drop tower. The increase in impact severity with a facemask should be the result of an increase in the rigidity (stiffness) of the entire helmet system upon application of a facemask. The secondary proposition is that if a helmet system consistently performs with higher impact severity metrics (severity index and peak linear acceleration) with a facemask attached, then design differences in the facemask should be measurable based on the same impact generation system (NOCSAE drop tower).

According to the data presented in Section 2.3.2, impacts to the front of the headform performed at low velocity (3 foot drop height) only generated a difference in impact severity for two out of the four helmet systems (the Xenith Epic and the Riddell Revolution). Both of these helmet systems experienced an increase in severity index when a facemask was added to the helmet system. However, the variance in impact severity measured with severity index for the Riddell Revolution helmet increased by a factor of four when a facemask was added to the system. This increase in variance likely inflates the perceived increase in severity index when a facemask was added to the Riddell Revolution, making low velocity impact results comparing a helmet system's performance with and without a facemask inconclusive.

For high velocity impacts (5 foot drop), the relationship between helmet system performance with and without a facemask was muddied further. For

instance, the severity index of the Riddell 360 helmet decreased by roughly 25% on average when a facemask was attached to the helmet outer shell, but impact severity increased for all three other helmet systems when a facemask was attached. The lack of a consistent effect the facemask has on the performance of a helmet system makes using the NOCSAE drop tower difficult in making facemask design comparisons based on the impact severity mitigation performance between novel designs and market standards.

In a similar study to the one presented presently, Rush et al. documented a series of impacts of varying impact locations and severities to helmet systems with and without facemasks.[83] The results of this study were inconclusive, as the relationship between impact location, severity, and presence of a facemask was unclear. For medium impact velocity impacts (4.88 m/s), the difference between severity index with and without a facemask was not pronounced and little statistical significance was found across helmet and facemask designs. For high impact velocity (5.46 m/s), the conclusiveness of the effect of a facemask on a helmet system's protective capacity was more difficult to establish. For instance, impacts to the front of the helmet system, that would require contact to the facemask, resulted in increased severity index with a facemask for the 360 helmet, but a decrease in severity index for the X2 helmet. Taking a more general approach, the authors claim a 113% increase to the mean peak acceleration at the center of gravity of the headform when the facemask was included in the helmet system across all helmet styles and impact locations.

However, this general conclusion loses its appeal when the data is broken down by impact velocity, impact location, and helmet system used.

Based on the results of previously published data as well as data presented in this document, it is clear that the NOCSAE drop tower is ineffective in comparing facemask designs based on their contributions to the impact mitigation performance of the helmet system upon single impacts. However, it was theorized that facemask performance could be evaluated based upon repeated impacts instead of single impacts. This theory was tested using the NOCSAE drop tower to study the change in performance of a helmet system with and without a facemask resulting from multiple impacts. Similar to the single impact results, there was not conclusive evidence that the presence of a facemask increases or decreases the effectiveness in impact severity mitigation of the helmet system after multiple impacts. According to the data across four different helmet styles, the subsequent impact performance after ten impacts would either remain consistent with the first impact or increase/decrease in severity at the same rate with or without a facemask.

One final effort was made to evaluate facemask designs by comparing the permanent spreading of each facemask that resulted from 20 impacts (10 high velocity impacts (5 foot drops) and 10 low velocity drops (3 foot drops). The permanent spreading ranged between 4% and 11% of the facemask's original dimensions. As presented previously, it is inconclusive whether permanent spreading has a consistent effect on overall impact performance of a facemask.

Even though the NOCSAE drop tower was shown to be effective in establishing the permanent spreading experienced by a facemask, the amount of noise introduced to each impact made it impossible to use the NOCSAE drop tower to evaluate a novel facemask design against commercially available products.

Based on the results using the NOCSAE drop tower to evaluate the role a facemask has on the helmet system performance, a novel methodology is necessary in order to expose the effect design criteria (bar material, bar placement, mass, etc) of a facemask has on its capacity to mitigate head impact trauma. This novel methodology must generate a repeatable stimulus to the facemask and use continuous metrics that differentiate the performance of the mask based on specific design criteria. Ideally, the novel methodology should not generate permanent damage to the facemask in order to allow the use of tested facemasks on the field and reduce evaluation waste. The design criteria of a novel method to evaluate the performance of facemask design is the subject of Chapter 3 of this document.

CHAPTER THREE

A QUASISTATIC METHOD TO MEASURE FACEMASK STRUCTURAL STIFFNESS

3.1 Background

As evidenced in Chapter 2, existing methods used to evaluate football facemasks are not sensitive enough to differences in facemask material or structure to be effective in evaluating novel facemask designs. In addition, existing methods used to evaluate facemasks as part of a full helmet system expose the facemask to impact severity that permanently destroy the facemask beyond safe re-use. Finally, the variance in linear drop results for impacts generated with the same inputs make it impossible to effectively evaluate football facemask performance with the NOCSAE drop tower. To save financial and temporal costs in the development phase of novel helmet component designs, it is necessary to evaluate the performance of individual component prior to integrating new components into existing helmet systems.

Prior literature has reported the difficulty in identifying the effect that a facemask has on the impact performance of the full helmet system when using a NOCSAE drop tower [83,105]. This is possibly due to the fact that the NOCSAE method, outlined by the NOCSAE Standard for faceguard impact performance,[49] characterizes the performance of full helmet systems, making it difficult to isolate facemask performance from the performance of the full helmet, especially for facemasks used for different helmet styles. Current facemask reconditioners are required to use the NOCSAE drop tower technique to certify that their

reconditioning methods have not significantly altered the performance of the facemask. However, the NOCSAE methodology is not able to isolate the performance of the mask from the full helmet system, making this regulatory requirement of limited use to the reconditioner and the users of these masks.

Therefore, a need exists for more discrete methods to characterize and measure facemask performance, such that a more robust understanding of how a facemask's design, use, and interactions with other components influence the performance of football helmet system. One theory concerning football facemask effect on head impact injury is that a mask with less structural stiffness will result in a reduction in brain deformation and thus brain injury risk [82]. However, there is currently no information concerning existing football facemask stiffness. The purpose of this chapter is to present a non-destructive, helmetless method that can be used to characterize football facemasks based on structural stiffness. Following the development of testing method, reliability testing was performed to ensure this method repeatedly generates the same output stiffness in response to the same combination of experimental inputs. Finally, validity testing was performed to 1.) demonstrate that this stiffness test is non-destructive according to NOCSAE standards, and 2.) that facemask stiffness is effective as a measurement of differences between facemask styles. A larger goal of this work was to develop a novel facemask stiffness test could be used for the non-destructive evaluation of facemasks by reconditioners, and by facemask

manufacturers to differentiate the potential impact performance of novel facemask designs.

3.2 Materials and Methods

For the purposes of developing a testing methodology, the facemask was positioned in a manner to represent the arch structure of the mask when attached to a helmet. Each side of the facemask was secured to a platform at the two locations used to attach the facemask to the helmet shell, as shown in Figure 3.2A. The sagittal plane orientation of each mask could be angled to allow for different directions of loading at locations such as the forehead, nose or chin. These contact locations were determined based on the locations of the facemask

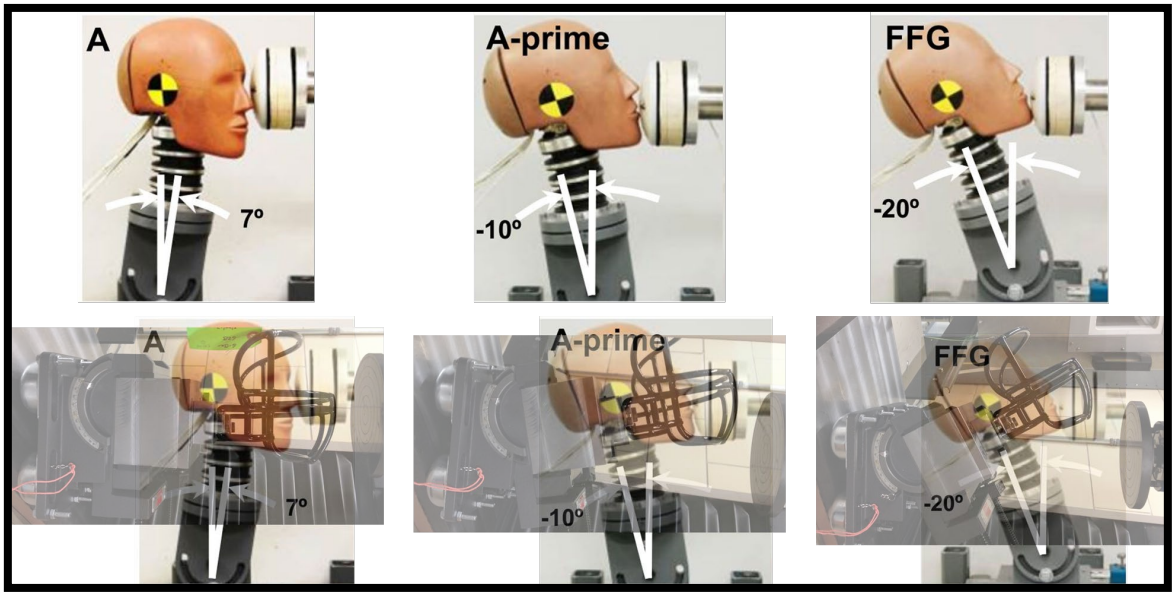

Figure 3.1: The top row, A, A-prime, and FFG, are impact locations that have been shown by Craig (2007) to frequently result in injury. The bottom row overlays a facemask on top of the figures from the top row in order to demonstrate where on the facemask the stiffness testing apparatus should apply a load to represent similar type contact orientations to those related to injury.

identified as frequently impacted and resulting in injury.[50] The corresponding impact location between these nose, mouth, and chin locations can be seen in Figure 3.1. When loaded, the facemask arch was allowed to spread, allowing the facemask to be modelled as a spring. The attachment platforms were each composed of an angle vice (Zoro, Buffalo Grove, IL) to allow for variation in the loading location for each mask (Figure 3.2B). Each angle vice was supported by four ball bearings (Hudson Bearings, LLC, Columbus, OH) that are rated for 250 lb loads, each to allow for low-friction lateral movement of the facemask when loaded. These ball bearings ensured two degrees of freedom of translation, and one degree of freedom of rotation. The testing fixture also featured three different support blocks depending on the facemask used, as summarized in Figure 3.2C. From the possible pool of over 100 modern facemask styles, 20 facemask styles were chosen that spanned a representative spectrum of existing facemask structures and materials. All facemasks chosen could fit a Large size helmet. Table 3.1 summarizes the facemasks used and test performed for the purpose of this work. Facemasks that include “LW” in the name were constructed with hollow steel tubes. Facemasks that include “HS4” in the name were constructed with a proprietary “high strength” alloy by Riddell. All other facemasks were constructed with solid carbon steel bars. Each facemask was secured onto a testing fixture seen in Figure 3.2.

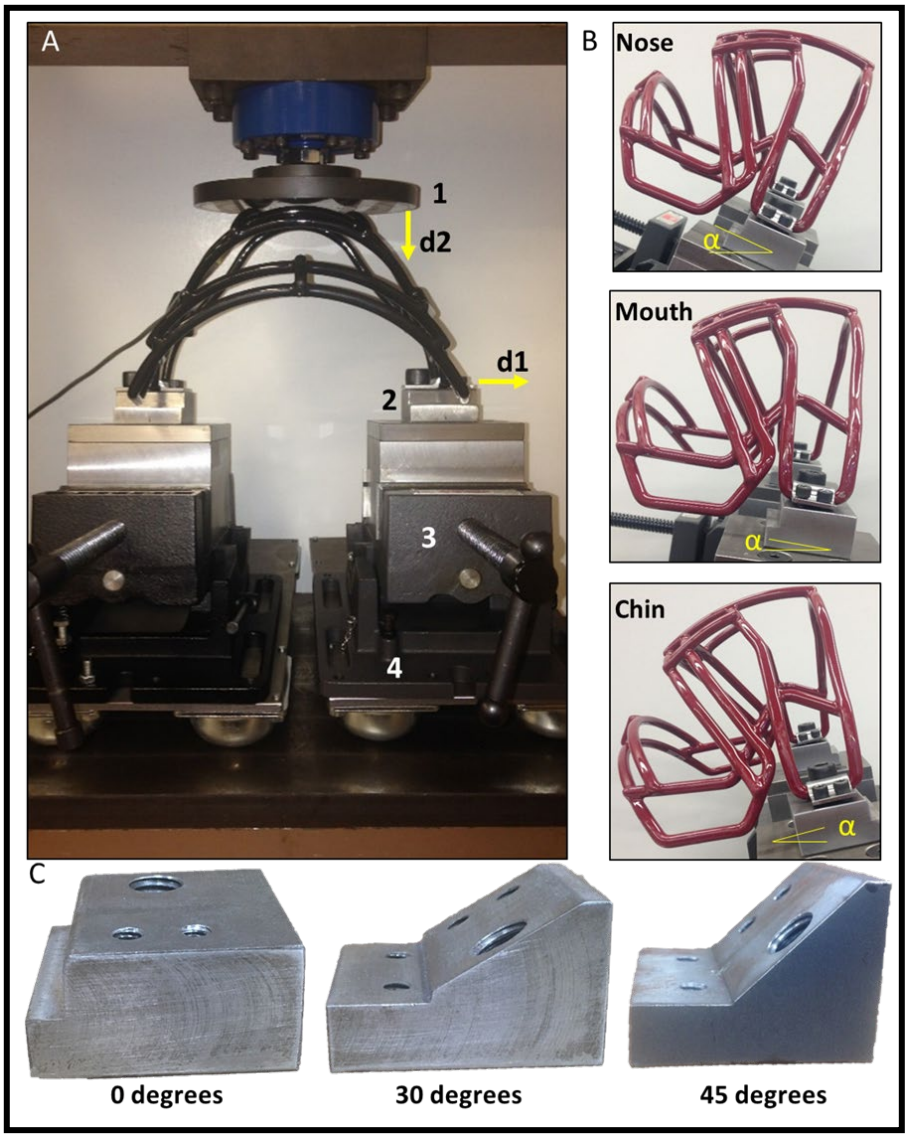

Figure 3.2: The facemask stiffness testing rig used to orient facemask in proper position during stiffness testing (A). The contact platen (1) applies an input deflection to the facemask, which is attached to the testing fixture support block (2). The contact location between the facemask and the platen is adjusted using the vice clamp (3), which is supported by four ball bearings (4). Deformation of the facemask is defined as either horizontal (d1) or vertical (d2). The facemask is attached to one of three support blocks (C) depending on the helmet associated with the specific facemask style. Masks are adjusted so the platen contacts the mask at three different locations (B), representing contacts aimed at the nose, mouth, or chin. Alpha represents the angle vice angle, and the mask used in (B) is the S3BD.

Table 3.1: A summary of facemask styles used for stiffness test validation.

Facemask Manufacturer	Helmet	Facemask Style	Average Mass (±SD) (g)	Average Pre-test Width (±SD) (mm)	Test Performed	Contact Location	Mask Sample Size	Test Per Mask	Age
Riddell	Revolution	G2B	467	232	Reliability	Nose	1	10	Used
			490 (1.41)	228 (2.83)	Non-destructive	Nose	3	6*	New
		G3BD	548 (4.04)	217 (4.51)	Non-destructive	Nose	3	6*	New
	360	360-2BD-SW-SP	388 (6.51)	237 (0.578)	Construct Validity	Nose	3	1	New
						Mouth	3	1	New
						Chin	3	1	New
		360-2EG-LW	446 (1.83)	237 (0.816)	Construct Validity	Nose	6	1	New
						Mouth		1	New
						Chin		1	New
		360-2BDC-LW	441 (1.53)	237 (0.577)	Construct Validity	Nose	3	1	New
						Mouth		1	New
						Chin		1	New
		360-2BD-LW	432 (2.53)	241 (9.26)	Construct Validity	Nose	6	1	New
						Mouth		1	New
						Chin		1	New
	Speed	S2BD	539 (1.14)	228 (1.79)	Construct Validity	Nose	5	1	New
						Mouth		1	New
						Chin		1	New
		S2BD-LW	435 (N/A)	252 (N/A)	Reliability	Nose	1	10	Used
		S2EG	557 (1.58)	228 (0.548)	Construct Validity	Nose	5	1	New
						Mouth		1	New
						Chin		1	New
		S3BD	626 (1.64)	228 (1.79)	Construct Validity	Nose	5	1	New
						Mouth		1	New
						Chin		1	New
					Non-destructive	Nose	3	6*	New
		S2BD-HS4	364 (1.00)	235 (3.61)	Non-destructive	Nose	3	6*	New
		S3BD-HS4	416 (3.21)	237 (1.00)	Non-destructive	Nose	3	6*	New
	Speed Flex	SF-2BD-SW	325 (4.16)	210 (1.53)	Construct Validity	Nose	3	1	New
						Mouth		1	New
						Chin		1	New
		SF-2BD	377 (1.00)	215 (0.577)	Construct Validity	Nose	3	1	New
						Mouth		1	New
						Chin		1	New
		SF-3BD	424 (0.00)	212 (1.41)	Construct Validity	Nose	3	1	New
						Mouth		1	New
						Chin		1	New
		SF-2BDC-TX-LW	449 (1.00)	213 (2.65)	Construct Validity	Nose	3	1	New
						Mouth		1	New
						Chin		1	New
Schutt	XP	RJOP-SW	408 (0.577)	241 (3.21)	Non-destructive	Nose	3	6*	New
		RJOP-DW	623 (5.51)	240 (4.36)	Non-destructive	Nose	3	6*	New
		NJOP	537	242	Reliability	Nose	1	20	Used

*each mask of this style was tested at six different input deflections: 5 mm, 10 mm, 15 mm, 20 mm, 25 mm, and 30 mm

3.2.1 Stiffness Measurement Procedure

The overview of the stiffness measurement process is shown in Figure 3.2. Each mask was secured onto the support blocks (Figure 3.2B) using six bolts to maintain facemask orientation during the stiffness test. An electromechanical Universal Testing System (Satec T10000, Instron, Norwood, MA) was used to apply an input point deflection to each facemask. A 44 kN load

cell (Interface 1210SP-10k, Scottsdale, AZ) was used to measure the force applied to the facemask. Each facemask was pre-loaded with 100 N of force before data was collected in order to ensure the facemask was in proper position with respect to the testing fixture when data was collected. The mask was compressed using a flat, circular disk platen with a diameter of 15.2 cm. The platen applied a deflection to the facemask at 100 mm/min, a similar rate used for helmet pad material characterization [75]. Each deflection input was applied

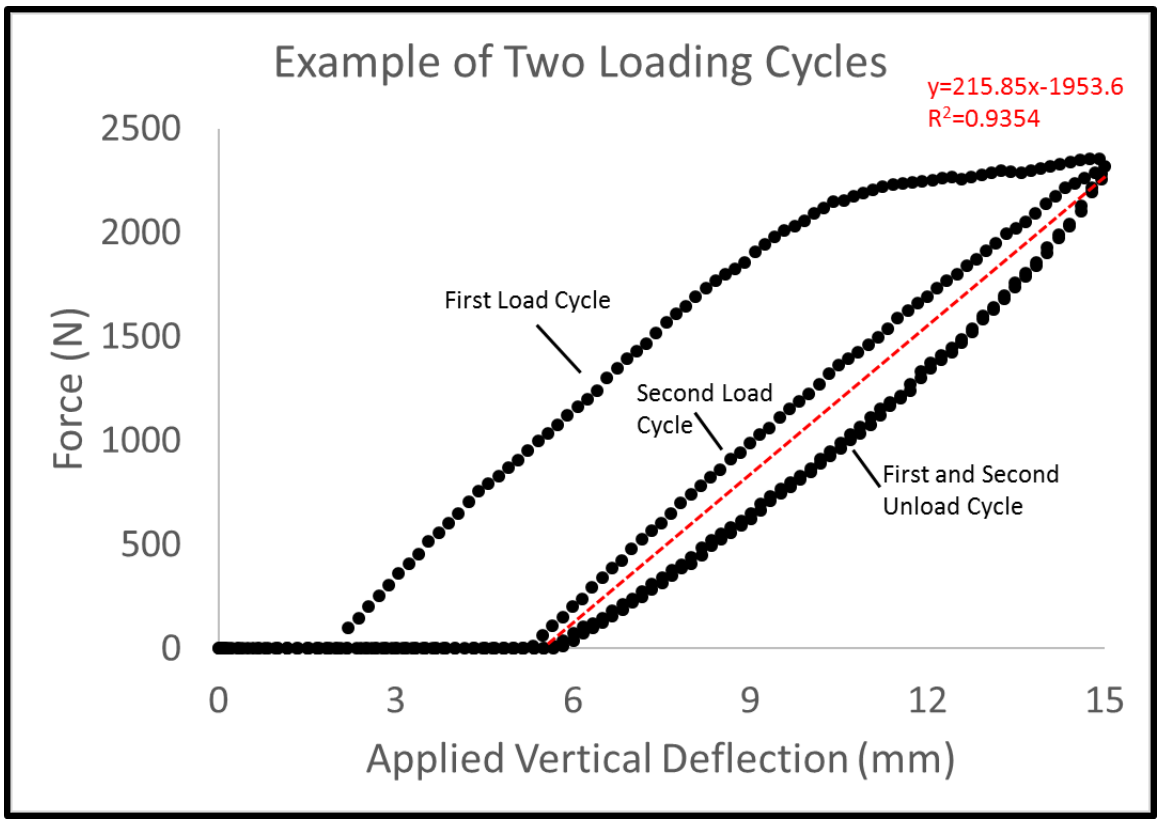

Figure 3.3: The force-deflection curve for two loading and unloading cycles performed on one facemask. When calculating the stiffness of the mask, the slope of the dashed red line is taken. In this case, the slope of the red dashed line, and thus the stiffness of the facemask, is 215.85 N/mm.

twice, and data from the second deflection cycle was used for stiffness calculation. One example of the two loading and unloading cycles represented as a force-deflection curve is presented in Figure 3.3. When developing the protocol to measure structural stiffness of facemasks, up to five loading cycles were applied (data not shown). Consistently, the first loading cycle resulted in larger stiffness, regardless of facemask style, and the subsequent cycles resulted in consistent stiffness readings. Thus, the stiffness was calculated using data collected from the second loading cycle. Deflection and applied force was collected with Bluehill Software (Instron, Norwood, MA) at a sampling rate of 20 Hz. Force and deflection data was plotted, and a linear regression line was fit to each force-deflection data set. The slope of this linear regression line was used as the measurement for facemask stiffness.

3.2.2 Non-Destructive Test Validation

The deflection applied to facemasks to measure stiffness must be small enough to allow continued use of the facemask according to NOCSAE standards,[49] but large enough to result in stiffness measurements that are different across facemask styles and materials. The first step in establishing a facemask stiffness test procedure was to identify an input deflection that would not result in extensive permanent facemask deformation. To do this, a set of new facemasks (Table 3.1) were tested at input deflections of 5 mm, 10 mm, 15 mm, 20 mm, 25 mm and 30 mm. Input deflection was defined as the distance travelled

by the impacting platen, and was user-controlled. The facemasks used to determine the appropriate applied input deflection were G2BD, G3BD, S3BD, S2BD-HS4, S3BD-HS4 (Riddell, BRG Sports, Elyria, OH) and RJOP-SW and RJOP-DW (Schutt Sports, Litchfield, IL). Three masks of each style were used. Each facemask was attached to the testing fixture using either 0 degree or 45 degree support blocks (Figure 3.2B), depending on the shape of the facemask attachment bar. All facemasks were compressed at a location meant to represent "nose impacts" (Figure 3.2C). Three masks were used for each style. Extensive permanent damage to a facemask was considered permanent deflection in the horizontal or vertical direction greater than 3.175 mm (1/8 in) [49]. An indication of horizontal and vertical deflection directions are shown with yellow arrows in Figure 3.2A. To measure permanent horizontal deflection, the facemask width was measured before and after each load test with a set of calipers. To measure vertical deflection, the Universal Testing System was used to measure the difference from the starting contact point, and the contact point at the end of the load test. Permanent deformation results of the non-destructive input threshold test are shown in Figure 3.4.

The second criteria for validation of the appropriate input deflection for a facemask stiffness test is that the input deflection is large enough to measure significant differences in stiffness across a variety of facemask styles. Six facemasks, representing masks that correspond to three different helmets, were used to demonstrate the relationship of facemask stiffness and input deflection.

Three masks of each style were tested at each input deflection. The facemask stiffness that resulted from each input deflection for each of the six facemasks is shown in Figure 3.5.

3.2.3 Stiffness Test Reliability

The reliability assessment of the proposed stiffness test was performed by repeating the stiffness measurement process outlined in section 3.2.2 on a single mask style, and calculating its coefficient of variance. One previously used and reconditioned mask of three different styles were used for the reliability testing: G2B and S2BD-LW (Riddell, BRG Sports, Elyria, OH) and NJOP (Schutt Sports, Litchfield, IL). The stiffness testing was performed at the “nose” location (Figure 1C) 11 times for the S2BD-LW mask, 10 times for the G2B mask, and 21 times for the NJOP mask. The stiffness measured for each style is represented in Figure 3.6 as a box and whisker plot. The box represents the interquartile range of stiffness for each mask style, and the whiskers represent 1.5x the 3rd and first quartile, respectively. The coefficient of variance for each mask style subgroup was also calculated by dividing the standard deviation by the subgroup mean and is reported in Figure 3.6. The repeatability coefficient for each mask stiffness was measured and is recorded in Table 3.2.[106]

3.2.4 Facemask Stiffness Test Construct Validation

To demonstrate that the method could be used to non-destructively quantify differences between facemask styles, the permanent deflections found in section 3.2.2 were assessed, and differences in facemask stiffness were compared. The facemasks used to demonstrate stiffness differences across facemask styles were 360-S2BD-SW-SP, 360-2ED-LW, 360-2BDC-LW, 360-2BD-LW, S2BD, S2EG, S3BD, SF-2BD-SW, SF-2BD, SF-3BD, SF-2BDC-TX-LW (Riddell, BRG Sports, Elryia, OH). Three masks of each style were used and their stiffness measurements were taken using the process outlined in section 3.2.1. Stiffness for each mask were measured at three different impact locations (Figure 3.2C): “nose”, “mouth” and “chin.” To identify if facemask stiffness differs across facemask styles, the difference in stiffness of each style of facemask tested was analyzed using a one-way ANOVA test (alpha=0.05), followed by a Tukey’s Least Significant Difference Test to determine which facemasks differed in stiffness significantly. The effect impact location has on stiffness is shown in Figure 3.7, and the spectrum of facemask stiffness at the nose location is shown in Figure 3.8.

3.3 Results

3.3.1 Non-destructive Test Validation

The horizontal and vertical deformation that occurred after stiffness testing at 5, 10, 15, 20, 25, and 30 mm input deflection is shown in Figure 3.4. For all

input deflections, facemasks experienced more permanent horizontal deformation (spreading) than permanent vertical deformation. Permanent horizontal deformation is also more variable than permanent vertical deformation for all input deflections. The black bar in Figure 3.4 indicates 3.2 mm (1/8 in), the amount of permanent deformation that is acceptable for a used facemask by standards established by NOCSAE. An applied vertical deflection of 5 mm results in permanent deformation less than the threshold that dictates rejected facemasks (Figure 3.4).

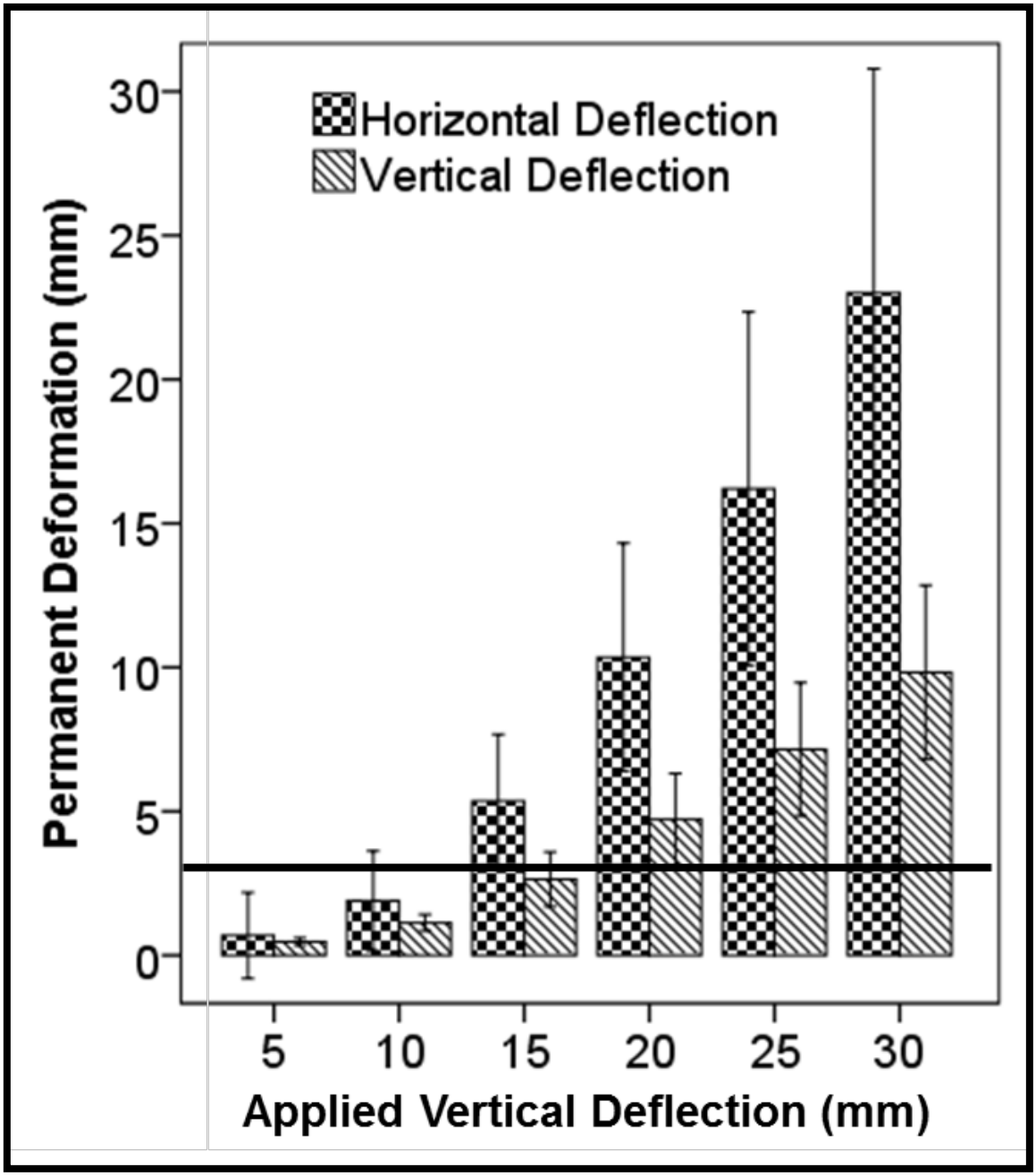

Figure 3.4: The horizontal (checkered) and vertical (hatched) permanent deformation that occurred at different levels of input vertical deflection of the facemask. The threshold for acceptable permanent deformation in any location on the facemask is 1/8 in (3.2 mm), as indicated by the black bar. Error bars represent 1 standard deviation.

The ability to differentiate facemask stiffness across facemask styles at 5, 10, 15, 20, 25, and 30 mm of input deflection is summarized in Figure 3.5. The error bars in Figure 3.5 represent one standard deviation from the mean. For masks that fit the Riddell Revolution, the Schutt XP, and the Riddell Speed, the difference between the stiffness of the two types of mask is similar. This near parallel line behavior indicates that input deflections from 5 mm to 30 mm is sufficient in demonstrating stiffness differences that exist across facemask styles. Since 5 mm of input deflection results in permanent deflection less than the NOCSAE threshold for accepting used facemasks, and since an input deflection of 5 mm is effective in demonstrating stiffness difference across facemask styles, 5 mm input deflections was used for the remainder of the stiffness testing presented in this article.

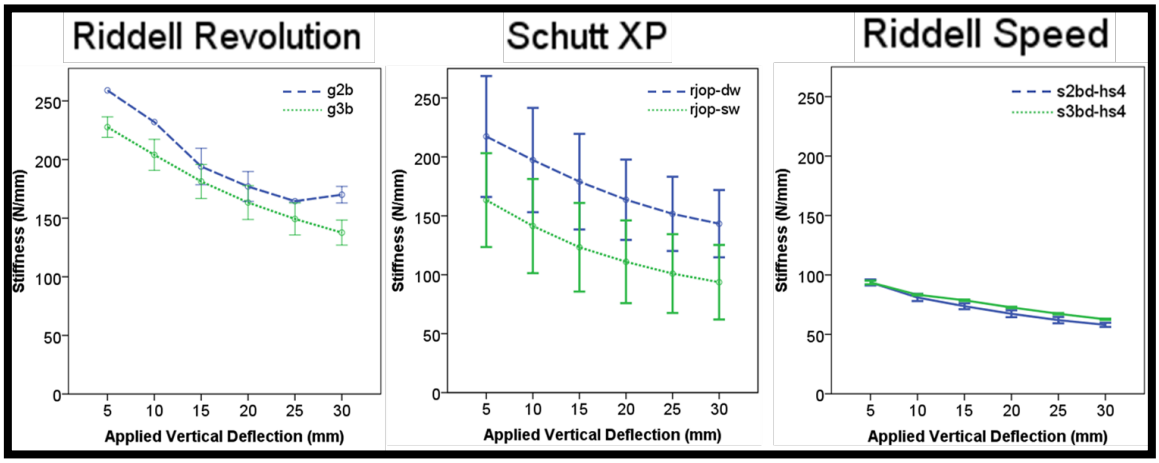

Figure 3.5: The relationship between the applied deflection to the facemask and the stiffness measured for six different facemask styles. The relationship of stiffness between two masks used for the same helmet is similar across a range of input deflections. Error bars represent 1 standard deviation.

3.3.2 Stiffness Test Reliability

Figure 3.6 is a box and whisker plot for each of the three masks used to determine the reliability of the stiffness test. The S2BD-LW and G2B masks were tested 11 and 10 times, respectively and the NJOP mask was tested 21 times. The range of coefficients of variance were 1.1% to 3.3%. The box and whisker plots show the interquartile range for the stiffness measured on each mask. The

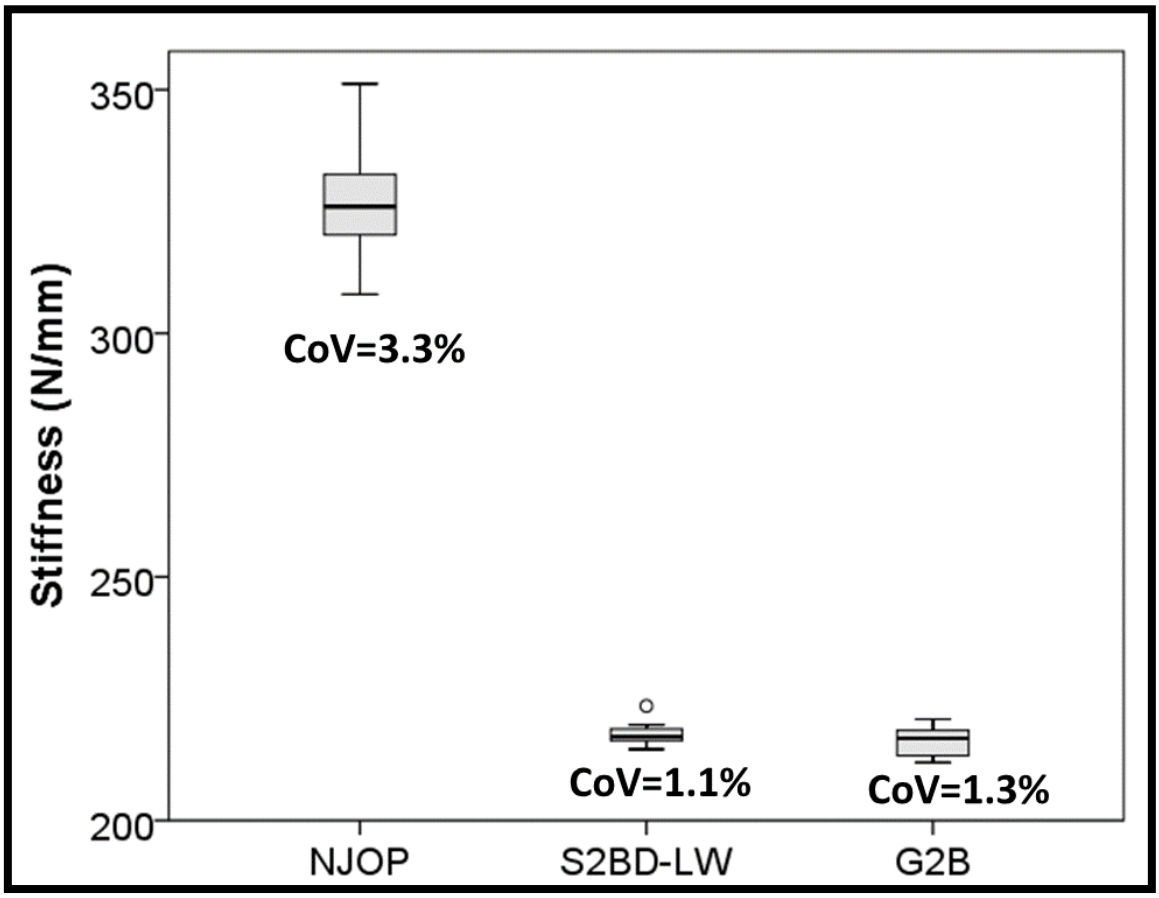

Figure 3.6: The reliability of the stiffness test was demonstrated by repeating the stiffness measurement process on three styles of facemasks. The coefficient of variation was calculated by dividing the mean of stiffness measured for each mask by the standard deviation of the stiffness for each mask. In each box and whisker plot, the box represents the interquartile range, and the whiskers represent 1.5x the first and third quartile. The middle black bar in each box represents the median.

interquartile range for the S2BD-LW, G2B, and NJOP masks were 2.6 N/mm, 5.85 N/mm, and 13.5 N/mm, respectively. The 95% confidence intervals for the S2BD-LW, G2B, and NJOP masks were 216-219 N/mm, 214-219 N/mm, and 322-332 N/mm, respectively. Table 3.2 summarizes the descriptive statistics for the reliability test. The repeatability coefficients for the tested facemasks indicate that any measured change in stiffness across facemask styles more than 6.6 N/mm can be considered significant.[106]

Table 3.2: The reliability test results, including smallest significant difference measured for each mask style as the repeatability coefficient.

Mask Style	Mean Stiffness (N/mm)	Sample Size (n)	Standard Deviation	Std Error of Mean	Repeatability Coefficient
G2B	216	10	3.11	0.983	2.72
NJOP	327	21	10.9	2.38	6.59
S2BD-LW	218	11	2.43	0.731	2.02
Total	272	42	56.2	8.68	24.04

3.3.3 Facemask Stiffness Test Construct Validation

Construct validity for a testing procedure describes the ability of the test procedure to differentiate between groups that are known to be different. In the case of football facemasks, it is assumed that the impact performance of different facemasks will be different, and this section explores whether facemask stiffness is effective in differentiating between facemask styles. Figure 3.7A shows effect that contact location has on the stiffness of each facemask. For the S3BD, S2BD, and 360-2BD-LW facemask styles, stiffness for the chin and mouth contact locations was higher than the stiffness measured at the nose contact location. For the 360-2BD-LW, SF-3BD, and S2EG facemask styles, the stiffness measured at the nose was similar to the stiffness measured at the mouth contact

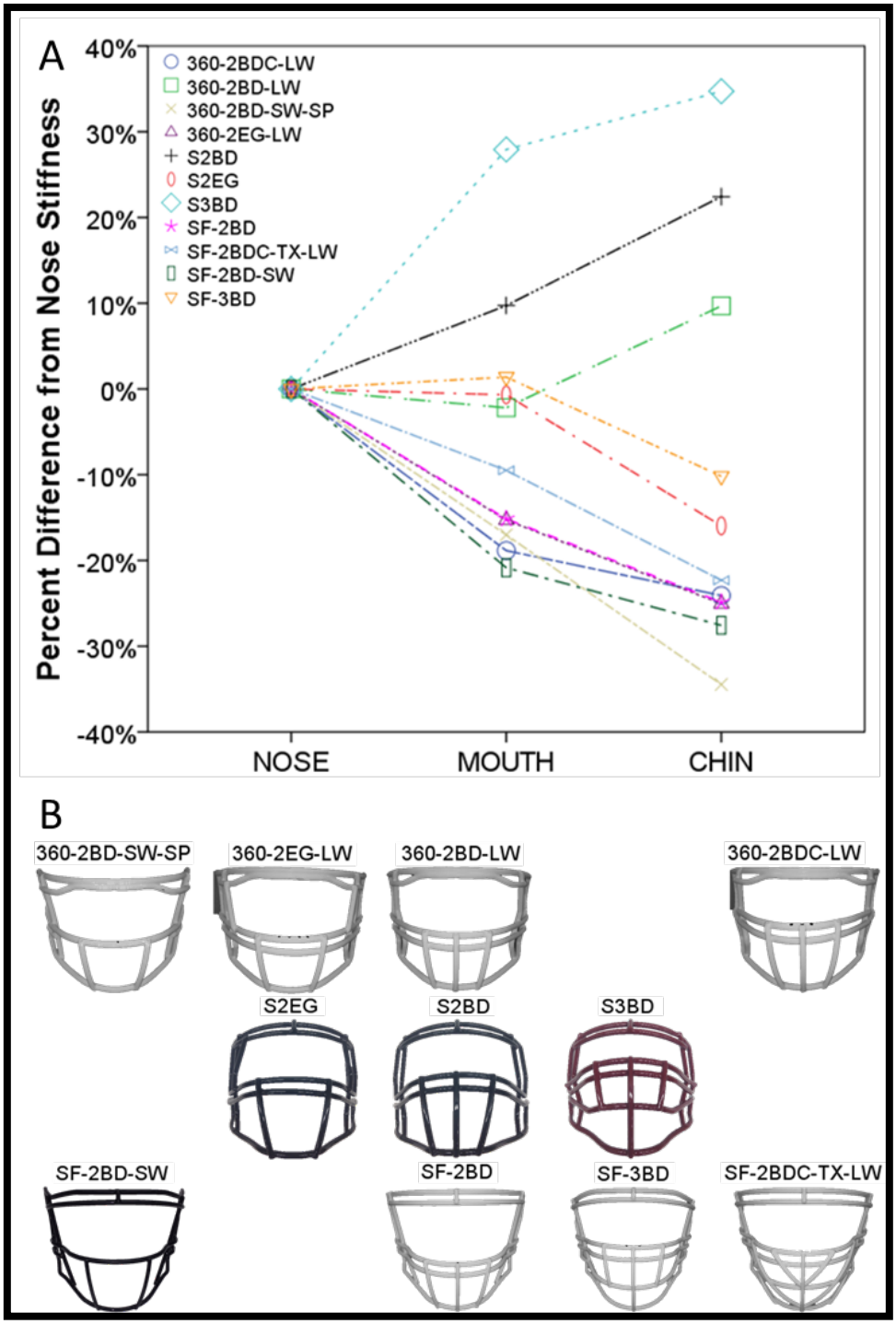

Figure 3.7: The effect of contact location on facemask stiffness (A). The mask geometries of the facemask measured to demonstrate the construct validity of stiffness as a metric to differentiate facemask performance (B).

location. For the 360-2BDC, 360-2BD-SW-SP, 360-2EG-LW, SF-2BD, SF-2BDC-

TX-LW, and SF-2BD-SW facemask styles, the stiffness measured at the mouth was less than the stiffness measured at the nose, and the stiffness measured at the chin was less than the stiffness measured at the mouth. To fully characterize a facemask, stiffness must be measured at multiple locations, as there is not a trend across all three contact locations consistent across all facemask styles used.

The construct validity of stiffness as a metric used to differentiate facemask styles is presented in Figure 3.8. For all new facemasks tested (Table 3.1), stiffness measured at the nose contact location ranged from 90 N/mm to 431 N/mm. Each letter in Figure 3.8 represents a group identified by the Tukey's post hoc analysis used to determine statistically significant group differences in stiffness based on facemask style. The range of stiffness values associated with existing facemask styles in Figure 3.8 indicates that stiffness is a valid metric to be used to differentiate facemask styles.

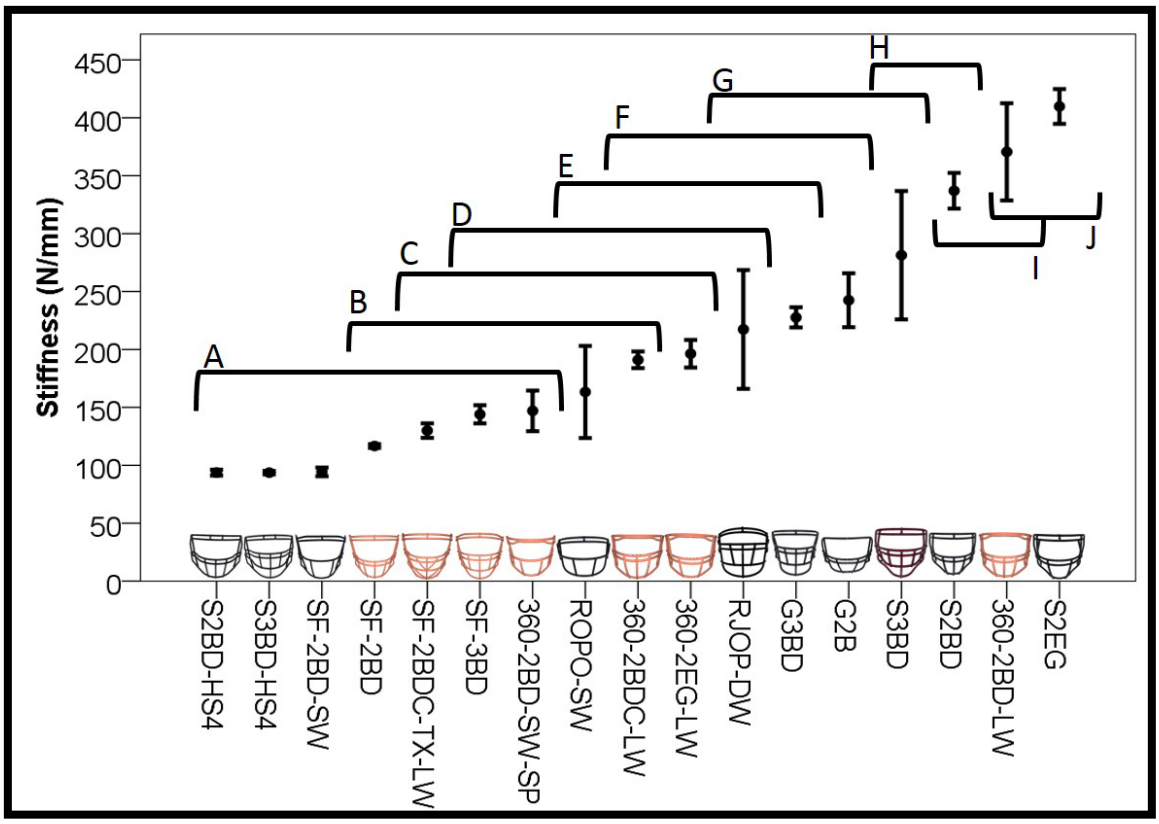

Figure 3.8: The spectrum of stiffness measured on new masks of various styles. Error bars represent 1 standard deviation.

3.4 Discussion

The purpose of this research was to explore the validity and reliability of a stiffness test in evaluating facemask performance in American football protective headgear systems. Previous work by Rush et al. has attempted to explain the role that the football facemask has in a protective helmet system [83,105]. Rush et al. showed, using a traditional NOCSAE drop tower to compare the impact performance of a helmet system with and without a facemask, that the presence of a facemask can increase or decrease impact severity experienced by a test headform, depending on the helmet used during testing. Thus, when evaluating facemask performance using the NOCSAE drop tower, the helmet used affects the ability of the test to differentiate facemask performance across facemask styles. For this reason, a need exists to establish a novel method used to characterize facemasks that removes the dependence on the rest of the helmet system.

There were three goals for this article: 1.) to determine an input deflection for a facemask stiffness test that is non-destructive according to established NOCSAE standards and is effective in demonstrating stiffness differences across facemask styles; 2.) to establish the reliability of a facemask stiffness measurement procedure; and 3.) to establish the construct validity of a stiffness test that requires stiffness measurements at three contact locations. An input deflection of 5 mm is effective in producing stiffness measurements across facemask styles similar to the stiffness measurements produced at higher input

deflections (Figure 3). Deflecting facemasks 5 mm is also effective in preventing permanent damage to a facemask above an acceptable permanent deformation threshold. NOCSAE document 087, “The Standard Method of Impact Test and Performance Requirements for Football Faceguards,” states “Deformed guards must be discarded. Any bar bent more than 1/8 inch (3.175 mm) from its normal shape at any point constitutes deformation” [49]. Both vertical and horizontal bending resulting from a stiffness test using an input deflection of 5 mm are less than 3.175 mm (Figure 2). Thus, goal 1 was accomplished.

The reliability of the proposed facemask stiffness measurement procedure is shown in Figure 4. For a single mask tested 10-20 times, the coefficient of variation (CoV) for the resulting stiffness measurements was between 1.1% and 3.3%. For comparison, when using a pendulum impactor to generate head impacts, Jadischke et al. measured a CoV of 1% for peak linear acceleration (PLA, g) measured during three impacts to the facemask region of a Riddell Revolution helmet at both 4.2 m/s and 5.1 m/s [107]. Also using a pendulum impactor to impact the facemask region, Cobb et al measured PLA CoV between 1-10% [108] In a separate study using a pneumatic ram impactor, Jadischke et al. measured a CoV of 3% in PLA when impacting the location where the facemask attaches to the helmet system at 9.3 m/s [64]. When impacting the facemask directly at various impact velocities, Jadischke et al. measured a PLA coefficient of variance between 1-5% for non-centric impacts, and between 2-15% for centric impacts [64]. For severity index measurements, Jadischke measured a CoV

between 2-29%. Also using a pneumatic ram, Post et al. measured a CoV for PLA of 5% and 4% for impacts to the front or facemask locations, respectively [29]. For front impacts to helmets with facemasks from different generations of use, Viano et al. measured PLA CoV between 0-21%, with higher CoV occurring on samples that were impacted 12-16 times, as opposed to samples impacted 2-4 times [60]. Based on previous work using two different methods to evaluate the impact performance of a helmet system that includes a facemask, the reliability of the stiffness measurement procedure presented presently is comparable to the current paradigm.

In an analysis of the response of an athlete's jaw upon head impact in American football, Craig identified three impact locations that involve the facemask that are correlated with head injury risk, and that the linear acceleration response of an impacted helmeted headform is different for each location [50]. The impacts generated by Craig using a pneumatically-driven linear impactor feature the entire helmet system, as well as a biofidelic neckform, and it is not clear whether the difference in the acceleration response of the headform is related to the structural properties of the facemask or to the structural properties of other helmet or test system components. The stiffness measured for each of the 11 different facemask styles at the three contact locations summarized in Figure 1C is presented in Figure 5 as a percent difference from the stiffness measured at the nose location to show that the relationship between the stiffness at the nose, mouth and chin locations depends on the facemask geometry. For two mask

styles, the S2BD and the S3BD, the chin location is the stiffest part of the mask, and the mouth is stiffer than the nose locations. For three mask styles, the S2EG, the SF3BD, and the 360-S2BD-LW, the stiffness at the nose and mouth were similar, but the chin stiffness was much different, greater for the 360-2BD-LW, lesser for the S2EG and the SF3BD. For the other six facemask styles, the facemask stiffness was greatest at the nose, and least at the chin, with the mouth stiffness being greater than the chin and less than the nose.

Current methods used to evaluate facemask impact performance are dictated by NOCSAE document 087 [49]. This standard was designed to ensure that facemasks did not put an athlete at additional risk for severe traumatic brain injury. However, the use of a NOCSAE drop tower to differentiate facemask performance has been limited, as evidenced by the data presented in Chapter 2. Rush et al. also used a NOCSAE drop tower in an effort to explain how a helmet performs with and without a facemask attached. These findings demonstrated that the impact severity of a helmeted headform is both increased and decreased with the presence of a facemask, depending on the helmet used [83,105]. This demonstrates the need to establish a testing system that differentiates the potential performance of facemasks without confounding facemask performance with helmet performance. Stiffness has been demonstrated to be a valid metric to be used to compare facemasks across a spectrum of facemask styles and materials in Figure 6. The focus of future research will elucidate the optimal

stiffness for a facemask, now that a stiffness measurement procedure for football facemasks has been documented.

The most recent update to ND 087 includes a section describing a method to measure the stiffness of football facemasks.[102] The NOCSAE method differs from the method presented in this dissertation in three major ways. First, the NOCSAE method requires the applied deformation of the mask to exceed 3 inches, which will permanently destroy the facemask beyond re-use, as evidenced by the data presented in Figure 2.16. Secondly, under the NOCSAE method, the facemask is rigidly fixed in one orientation, which limits the contact locations available, and further promotes the permanent destruction of the mask beyond reuse. Finally, the NOCSAE method applies a load at a rate of 254 mm/min, which is about 2.5 times faster than the method presented in this dissertation. The implication of loading rate on structural stiffness was briefly examined when the structural stiffness protocol was first being developed. However, only loading rates less than 100 mm/min were explored. Loading the mask at a rate of 50 mm/min and 100 mm/min did not have a meaningful effect on the structural stiffness measured for the facemask. It is unclear how increasing the loading rate will affect the measured structural stiffness. However, data presented in Figure 5 shows the necessity of measuring stiffness in different mask orientations. Rigidly constraining the mask to one orientation limits the understanding of mask behavior, which can be detrimental to the design process. Finally, rigidly constricting the facemask and deforming the mask more than 3

inches will permanently flatten the mask beyond use. In order to save environmental and financial resources, a stiffness test that can differentiate between mask structures without preventing continued use of the mask, such as the test presented in this dissertation, is ideal.

One limitation of this research is that no effort was made to explain why stiffness differs across facemask styles. The geometry of the 11 facemask styles, broken down into columns based on similarity of facemask geometry for different materials is shown in Figure 5B. However, it is not obvious based on visual assessment why certain masks are stiffer at the nose than the chin, and others experience maximal stiffness at the chin when compared to the mouth or nose. In addition, not all materials currently used to manufacture facemasks were included in this study. Future work will evaluate the structural stiffness of titanium masks in addition to the steel masks evaluated in the present study. The spectrum of facemask nose stiffness that exists for commonly used facemask styles is summarized in Figure 6. Johnson et al. postulated that facemask stiffness may be driven by the quantity of vertical bars in a facemask design, which was shown to be optimal for reducing brain injury risk [82]. Future research can use the proposed stiffness test procedure in an effort to inform future facemask designs that take facemask stiffness into account.

One consideration that must be made when interpreting the results of the current study is the isolation of the facemask from the helmet system. Now that a process has been proposed that can differentiate masks based on their structure

and material, future research must establish a relationship between the structural stiffness and facemask impact response. The relationship between a valid stiffness measurement and the impact response of a facemask will inform future computational modelling efforts that could allow for quick iterations of facemask structural designs, material decisions, and even the design of hardware used to attach the facemask to the helmet. The present study sets a foundation for future work in evaluation football facemask impact performance.

In summary, the novel facemask stiffness method demonstrated in this work can now be used for the non-destructive evaluation of facemasks by reconditioners, and by facemask manufacturers to differentiate the potential impact performance of novel facemask designs.

3.5 Final Conclusions and Future Considerations

To summarize the above text, the conclusion of this line of research inquiry presented in this dissertation is threefold: 1.) The existing method to evaluate facemask performance using the twin-wire drop tower is insufficient to determine the role a facemask plays in the protective capacity of the helmet system. 2.) A non-destructive, repeatable, quasi-static method is possible to measure football facemask structural stiffness, which is differentiable across facemask designs. 3.) A need exists to relate facemask structural stiffness to impact response characteristics of a facemask, but this need was not met by modifying a cushion impact test system as described in Appendix D.

Based on the results using the NOCSAE drop tower to evaluate the role a facemask has on the helmet system performance, a novel methodology is necessary to expose the effect design criteria (bar material, bar placement, mass, etc) of a facemask has on its capacity to mitigate head impact trauma. This novel methodology must generate a repeatable stimulus to the facemask and use continuous metrics that differentiate the performance of the mask based on specific design criteria. Ideally, the novel methodology should not generate permanent damage to the facemask to allow the use of tested facemasks on the field and reduce evaluation waste. The design criteria of a novel method to evaluate the performance of facemask design is the subject of Chapter 3 of this document.

Now that a process has been proposed that can differentiate masks based on their structure and material, future research must establish a relationship between the structural stiffness and facemask impact response. The relationship between a valid stiffness measurement and the impact response of a facemask will inform future computational modelling efforts that could allow for quick iterations of facemask structural designs, material decisions, and even the design of hardware used to attach the facemask to the helmet. The present study sets a foundation for future work in evaluation football facemask impact performance. In summary, the novel facemask stiffness method demonstrated in this work can now be used for the non-destructive evaluation of facemasks by reconditioners,

and by facemask manufacturers to differentiate the potential impact performance of novel facemask designs.

Based on the data presented in Appendix D, it was deemed that the current iteration of the modified cushion impact test system was not effective in generating the appropriate and translatable impact characteristics for each facemask design. Even though impact inputs were deemed reliable and repeatable, the impact response, especially impactor platen acceleration and coefficient of restitution of the facemask expressed large variance. The lack of separation based on facemask design in several impact response metrics indicates the insufficiency of this system to properly generate impacts to the facemask as well as characterize the impact response of a facemask. The lack of apparent correlation between the structural stiffness of the facemask and the impact characteristics (duration, deflection, permanent spreading, coefficient of restitution, and impactor platen linear acceleration) requires a re-evaluation of the system used to generate impacts to a facemask as well as the metrics chosen to characterize the impact response of football facemasks. Future work in this field will require an appropriate system, apparatus, and methodology to generate repeatable impacts to a facemask to characterize facemask impact response that will inform future design decisions in the field of football head impact safety.

The order of operations performed in the research outlined in this dissertation flies in the face of common methodologies used to evaluate three-dimensional designs. In a traditional mechanical engineering research pipeline, it

is common to begin with a three-dimensional computational model and use laboratory testing to validate the performance of this model to evaluate football facemasks, in this case. By starting with a laboratory test system, this research group has opened the door for the need for computational modelling that aligns with the results of the quasi-static structural stiffness test. In this manner, future facemask manufacturers will be able to ensure that facemask design considerations are validated without the risk of evaluation waste that results from permanently damaging mask prototypes.

For future generations of graduate students operating in the Clemson Headgear Impact Performance Lab (CHIP Lab), there is momentum to carry from this project to advance the field of headgear impact performance. Future research in both a laboratory and computational setting will continue this line of research a draw a stronger connection between design criteria (material, bar placement, etc) and predicted or simulated impact response of the facemask as a component of the full helmet system. The work presented in this dissertation served as this laboratory's first foray into the field of headear impact performance assessment but will certainly not be the last. As the page turns from this line of experimentation to the next, it is clear that the foundation for groundbreaking work in this field from this laboratory group has been established by the work presented herein.

References

1. Mueller, FO, Colgate B. Annual Survey of Football Injury Research 1931-2008. 2009:1689-1699. doi:10.1017/CBO9781107415324.004.
2. Kucera, KL, Klossner, D, Colgate, B, Cantu R. Annual Survey of Football Injury Research 1931-2015. *Natl Cent Catastrophic Sport Inj Res*. 2016.
3. Irick E. *NCAA Sports Sponsorship and Participation Rates Report: 1981-1982-2012-2013*.; 2013.
4. Anzell AR et al. Changes in height, body weight and body composition in American football players from 1942 to 2011. *J Strength Cond*. 2013;27(2):277-284.
5. Secora, CA, Latin, RW, Berg, KE, Noble J. Comparison of Physical and Performance Characteristics of NCAA Division I Football Players: 1987 and 2000. *J Strength Cond Res*. 2004;18(2):286-291. doi:10.1177/0192513X12437708.
6. Gennarelli TA, Pintar FA, Yoganandan N. Biomechanical Tolerances for Diffuse Brain Injury and a Hypothesis for Genotypic Variability in Response to Trauma. *Annu Proc / Assoc Adv Automot Med*. 2003;47:624-628. http://www.ncbi.nlm.nih.gov/pmc/articles/PMC3217573/.
7. King AI. Fundamentals of Impact Biomechancis: Part I - Biomechanics of the Head, Neck, and Thorax. *Annu Rev Biomed Eng*. 2000:55-81. doi:10.1016/B978-1-4557-5134-1.00001-9.
8. Rowson S, Bland M, Campolettano E, et al. Biomechanical Perspectives

on Concussion in Sport. *Sports Med Arthrosc*. 2016;24(3):100-107.

9. Gennarelli T, Thibault L. Biomechanics of acute subdural hematoma. *J Trauma*. 1982;22(8):680-686.
10. Harmon KG, Drezner JA, Gammons M, et al. American Medical Society for Sports Medicine position statement: concussion in sport. *Br J Sports Med*. 2013;47(1):15-26. doi:10.1136/bjsports-2012-091941.
11. Langlois J a, Rutland-Brown W, Wald MM. The epidemiology and impact of traumatic brain injury: a brief overview. *J Head Trauma Rehabil*. 2006;21(5):375-378. doi:00001199-200609000-00001 [pii].
12. Guskiewicz KM, Weaver NL, Padua DA, Garrett WE. Epidemiology of concussion in collegiate and high school football players. *Am J Sports Med*. 2000;28(5):643-650.
13. Matava MJ, Görtz S. The University of the National Football League : How Technology , Injury Surveillance , and Health Care Have Improved the Safety of America ' s Game. *J Knee Surg*. 2016;29:370-378.
14. Talavage TM, Nauman EA, Breedlove EL, et al. Functionally-Detected Cognitive Impairment in High School Football Players without Clinically-Diagnosed Concussion. *J Neurotrauma*. 2014;31(4):327-338. doi:10.1089/neu.2010.1512.
15. Kawata K, Rubin LH, Takahagi M, et al. Subconcussive Impact-Dependent Increase in Plasma S100β Levels in Collegiate Football Players. *J Neurotrauma*. 2017;34(14):2254-2260. doi:10.1089/neu.2016.4786.

16. Wilson MJ, Harkrider AW, King KA. The effects of visual distracter complexity on auditory evoked p3b in contact sports athletes. *Dev Neuropsychol*. 2014;39(2):113-130. doi:10.1080/87565641.2013.870177.

17. Churchill NW, Hutchison MG, Di Battista AP, Graham SJ, Schweizer TA. Structural, functional, and metabolic brain markers differentiate collision versus contact and non-contact athletes. *Front Neurol*. 2017;8(AUG):1-11. doi:10.3389/fneur.2017.00390.

18. Mayinger MC, Merchant-Borna K, Hufschmidt J, et al. White matter alterations in college football players: a longitudinal diffusion tensor imaging study. *Brain Imaging Behav*. 2017:1-10. doi:10.1007/s11682-017-9672-4.

19. Tremblay S, Henry LC, Bedetti C, et al. Diffuse white matter tract abnormalities in clinically normal ageing retired athletes with a history of sports-related concussions. *Brain*. 2014;137(11):2997-3011. doi:10.1093/brain/awu236.

20. Kutner KC, Erlanger DM, Tsai J, Jordan B, Relkin NR. Lower cognitive performance of older football players possessing apolipoprotein E ε4. *Neurosurgery*. 2000;47(3):651-658. doi:10.1097/00006123-200009000-00026.

21. Koerte IK, Mayinger M, Muehlmann M, et al. Cortical thinning in former professional soccer players. *Brain Imaging Behav*. 2016;10(3):792-798. doi:10.1007/s11682-015-9442-0.

22. Alosco ML, Kasimis AB, Stamm JM, et al. Age of first exposure to American football and long-term neuropsychiatric and cognitive outcomes. *Transl Psychiatry*. 2017;7(9):e1236. doi:10.1038/tp.2017.197.

23. Levy ML, Ozgur BM, Berry C, Aryan HE, Apuzzo MLJ. Birth and evolution of the football helmet. *Neurosurgery*. 2004;55(3):656-661. doi:10.1227/01.NEU.0000134599.01917.AA.

24. Hodgson VR. National Operating Comittee on Standards for Athletic Equipment football helmet certification program. *Med Sci Sport*. 1975;7(3):225-232.

25. Viano DC, Withnall C, Wonnacott M. Football helmet drop tests on different fields using an instrumented hybrid III head. *Ann Biomed Eng*. 2012;40(1):97-105. doi:10.1007/s10439-011-0377-3.

26. Myers T, Yoganandan N, Sances Jr A, Pintar F, Reinartz J, Battocletti J. Energy Absorption Characteristics of Football Helmets Under Low and High Rates of Loading. *Biomed Mater Eng*. 1993;3(1):15-24.

27. Bishop P, Norman R, Kozey J. An evaluation of football helmets under impact conditions. *Am J Sports Med*. 1984;12(3):233-236.

28. Beckwith JG, Greenwald RM, Chu JJ. Measuring head kinematics in football: Correlation between the head impact telemetry system and hybrid III headform. *Ann Biomed Eng*. 2012;40(1):237-248. doi:10.1007/s10439-011-0422-2.

29. Post A, Oeur A, Walsh E, Hoshizaki B, Gilchrist MD. A centric/non-centric

impact protocol and finite element model methodology for the evaluation of American football helmets to evaluate risk of concussion. *Comput Methods Biomech Biomed Engin*. 2013;5842(March 2013):37-41. doi:10.1080/10255842.2013.766724.

30. Walsh ES, Rousseau P, Hoshizaki TB. The influence of impact location and angle on the dynamic impact response of a Hybrid III headform. *Sport Eng*. 2011;13(3):135-143. doi:10.1007/s12283-011-0060-9.
31. Karton, Clara, Hoshizaki, Thomas B., Gilchrist MD. The Influence of Impactor Mass on the Dynamic Response of the Hybrid III Headform and Brain Tissue Deformation. *Mech Concussion Sport*. 2014:23-40.
32. Ahmadisoleymani SS, Yang J. American football helmet for preventing concussion , a literature review. *Procedia Manuf*. 2015;3(Ahfe):3796-3803. doi:10.1016/j.promfg.2015.07.882.
33. Fernandes F a., Sousa RJ a. D. Head injury predictors in sports trauma - A state-of-the-art review. *Proc Inst Mech Eng Part H J Eng Med*. 2015;229(8):592-608. doi:10.1177/0954411915592906.
34. Calvano NJ, Berger RE. Effects of selected test variables on the evaluation of football helmet performance. *Med Sci Sport*. 1979;11(3):293-301. http://www.ncbi.nlm.nih.gov/pubmed/522643.
35. Cobb BR, MacAlister A, Young TJ, Kemper AR, Rowson S, Duma SM. Quantitative comparison of Hybrid III and National Operating Committee on Standards for Athletic Equipment headform shape characteristics and

implications on football helmet fit. *Proc Inst Mech Eng Part P J Sport Eng Technol*. 2014;229(1):1754337114548245. doi:10.1177/1754337114548245.

36. Newman, James, Beusenberg, Marc, Fournier, Edmund, Shewchenko, Nicholas, Withnall C. Interlibrary Loan @ Ke ering University. In: *1999 International IRCOBI Conference on the Biomechanics of Impact*. Vol 108. ; 1999:17-36.

37. Newman JA, Beusenberg MC, Shewchenko N, Withnall C, Fournier E. Verification of biomechanical methods employed in a comprehensive study of mild traumatic brain injury and the effectiveness of American football helmets. *J Biomech*. 2005;38(7):1469-1481. doi:10.1016/j.jbiomech.2004.06.025.

38. Hernandez F, Shull PB, Camarillo DB. Evaluation of a laboratory model of human head impact biomechanics. *J Biomech*. 2015;48(12):3469-3477. doi:10.1016/j.jbiomech.2015.05.034.

39. Chu JJ. An Investigation of the NOCSAE Linear Impactor Test Method Based on In Vivo Measures of Head Impact Acceleration in American Football. *J Biomech Eng*. 2009;132(1):11006. doi:10.1115/1.4000249.

40. Bartsch A, Benzel E, Miele V, Morr D, Prakash V. Hybrid III anthropomorphic test device (ATD) response to head impacts and potential implications for athletic headgear testing. *Accid Anal Prev*. 2012;48:285-291. doi:10.1016/j.aap.2012.01.032.

41. Dressler, Daniel M., Dennison, Christopher R., Cripton PA. Development of an Advanced Football Helmet to Provide Increased Protection against Concussion. *Mech Concussion Sport STP 1552*. 2014:84-101. doi:10.1520/STP155220120172.

42. Viano DC, Pellman EJ, Withnall C, Shewchenko N. Concussion in professional football: Performance of newer helmets in reconstructed game impacts - Part 13. *Neurosurgery*. 2006;59(3):591-605. doi:10.1227/01.NEU.0000231851.97287.C2.

43. Pellman EJ, Viano DC, Withnall C, Shewchenko N, Bir CA, Halstead PD. Concussion in professional football: Helmet testing to assess impact performance - Part 11. *Neurosurgery*. 2006;58(1):78-95. doi:10.1227/01.NEU.0000196265.35238.7C.

44. Viano, David C., Pellman EJ. Concussion in Professional Football: Biomechanics of the Striking Player-Part 8. *Neu*. 2004;56(2):266-281.

45. Feng T, Aono K, Member S, Covassin T. Self-Powered Monitoring of Repeated Head Impacts Using Time-Dilation Energy Measurement Circuit. *IEEE Trans Biomed Circuits Syst*. 2015;9(2):217-226.

46. Pellman, Elliot J., Viano, David C., Tucker, Andrew M., Casson, Ira R., Waeckerle JF. Concussion in Professional Football: Reconstruction of Game Impacts and Injuries. *Neurosurgery*. 2003;53(4):799-814.

47. Viano DC, Casson IR, Pellman EJ. Concussion in professional football: Biomechanics of the struck player - Part 14. *Neurosurgery*.

2007;61(2):313-327. doi:10.1227/01.NEU.0000279969.02685.D0.

48. Berger, R E, Calvano N. Evaluation of Product Safety Test Methods: Protective Headgear. *J Safety Res*. 1979;11(1):14-19.

49. NOCSAE. Standard Method of Impact Test and Performance Requirements for Football Faceguards. *(ND)087-12m15a*. 2015;(September).

50. Craig MJ. Biomechanics of Jaw Loading in Football Helmet Impacts. 2007.

51. Cournoyer, J, Post, A, Rousseau, P, Hoshizaki B. The ability of American football helmets to manage linear acceleration with repeated high-energy impacts. *J Athl Train*. 2016;51(3):258-263.

52. Post A, Blaine Hoshizaki T. Rotational Acceleration, Brain Tissue Strain, and the Relationship to Concussion. *J Biomech Eng*. 2015;137(3):30801. doi:10.1115/1.4028983.

53. Zhang L, Yang KH, King AI. A Proposed Injury Threshold for Mild Traumatic Brain Injury. *J Biomech Eng*. 2004;126(2):226. doi:10.1115/1.1691446.

54. Jadischke, Ron, Viano DC, Mccarthy J, King AI. The Effects of Helmet Weight on Hybrid III Head and Neck Responses by Comparing Unhelmeted and Helmeted Impacts. *J Biomech Eng*. 2016;138:1-10. doi:10.1115/1.4034306.

55. Bartsch a, Benzel E, Miele V, Prakash V. Impact test comparisons of 20th and 21st century American football helmets. *J Neurosurg*.

2012;116(1):222-233. doi:10.3171/2011.9.JNS111059.

56. Rowson S, Daniel RW, Duma SM. Biomechanical performance of leather and modern football helmets. *J Neurosurg*. 2013;119(3):805-809. doi:10.3171/2013.3.JNS121735.

57. Cummiskey B, Schiffmiller D, Talavage TM, Meyer JJ, Adams D, Nauman EA. Reliability and accuracy of helmet-mounted and head-mounted devices used to measure head accelerations. *J Sport Eng Technol*. 2016:1-10. doi:10.1177/1754337116658395.

58. Post A, Oeur A, Hoshizaki TB, Gilchrist MD. Differences in region-specific brain tissue stress and strain due to impact velocity for simulated American football impacts. 2014;228(4):276-286. doi:10.1177/1754337114527742.

59. Ivancic PC. Biomechanics of sports-induced axial-compression injuries of the neck. *J Athl Train*. 2012;47(5):489-497. doi:10.4085/1062-6050-47.4.06.

60. Viano DC, Halstead D. Change in size and impact performance of football helmets from the 1970s to 2010. *Ann Biomed Eng*. 2012;40(1):175-184. doi:10.1007/s10439-011-0395-1.

61. Viano DC, Withnall C, Halstead D. Impact performance of modern football helmets. *Ann Biomed Eng*. 2012;40(1):160-174. doi:10.1007/s10439-011-0384-4.

62. League NF. 2015 NFL Health and Safety Report. 2015.

63. Siegmund GP, Guskiewicz KM, Marshall SW, DeMarco AL, Bonin SJ.

Laboratory Validation of Two Wearable Sensor Systems for Measuring Head Impact Severity in Football Players. *Ann Biomed Eng*. 2016;44(4):1257-1274. doi:10.1007/s10439-015-1420-6.

64. Jadischke R, Viano DC, Dau N, King AI, Mccarthy J. On the accuracy of the Head Impact Telemetry (HIT) System used in football helmets. *J Biomech*. 2013;46:2310-2315. doi:10.1016/j.jbiomech.2013.05.030.

65. Siegmund, GP, Guskiewicz, KM, Marshall, SW, DeMarco, AL, Bonin S. A Headform for Testing Helmet and Mouthguard Sensors that Measure Head Impact Severity in Football Players. *Ann Biomed Eng*. 2014;42(9):1834-1845. doi:10.1007/s10439-014-1052-2.

66. Campbell, K. R., M. J. Warnica, I. C. Levine, J. S. Brooks, A. C. Laing, T. A. Burkhart JPD. Laboratory Evaluation of the gForce Tracker TM , a Head Impact Kinematic Measuring Device for Use in Football Helmets. *Ann Biomed Eng*. 2016;44(4):1246-1256. doi:10.1007/s10439-015-1391-7.

67. Johnston JM, Ning H, Kim JE, et al. Simulation, fabrication and impact testing of a novel football helmet padding system that decreases rotational acceleration. *Sport Eng*. 2015;18(1):11-20. doi:10.1007/s12283-014-0160-4.

68. Ide TM, Infusino RJ, Kraemer N, Withnall CRP, Bayne TD. Football helmet. 2005. http://www.google.com/patents/US6934971.

69. Leon R. Helmet System. 2012. doi:10.1037/t24245-000.

70. Krzeminski DE, Fernando D, Gould TE, Rawlins JW, Piland SG.

Quantifying the effects of accelerated weathering and linear drop impact exposures of an American football helmet outer shell material. *Proc Inst Mech Eng Part P J Sport Eng Technol*. 2014;228(3):171-187. doi:10.1177/1754337114526587.

71. Nelson T, Cripton P. Inducing head motion with a novel helmet during head-first impact can mitigate neck injury metrics: an experimental proof-of-concept investigation using mechanical surrogates. In: *Proceedings of the 2008 International IRCOBI Conference on the Biomechanics of Impact*. Bern, Switzerland; 2008:1-8. http://ibrc.osu.edu/wp-content/uploads/2014/01/Nelson_Manuscript_2008.pdf.
72. Ramirez BJ, Gupta V. Evaluation of novel temperature-stable viscoelastic polyurea foams as helmet liner materials. *Mater Des*. 2018;137:298-304. doi:10.1016/j.matdes.2017.10.037.
73. Krzeminski DE, Fernando BMD, Curtzwiler G, Gould TE, Piland SG, Rawlins JW. Repetitive impact exposure and characterization of stress-whitening of an American football helmet outer shell material. *Polym Test*. 2016;55:190-203. doi:10.1016/j.polymertesting.2016.08.019.
74. Rossi A, Claiborne T, Thompson G, Todaro S. The Influence of Friction Between Football Helmet and Jersey Materials on Force: A Consideration for Sport Safety. *J Athl Train*. 2016;51(9):701-708.
75. Myers T, Yoganandan N, Sances Jr A, Pintar F, Reinartz J, Battocletti J. Energy absorption characteristics of football helmets under low and high

rates of loading. *Biomed Mater Eng*. 1993;3:15-24.

76. Honarmandi P, Sadegh AM, Cavallaro P V. Modelling and impact analysis of football player head with helmet toward mitigating brain concussion. *Int J Exp Comput Biomech*. 2015;3(4):267-299.

77. Johnston JM, Ning H, Kim JE, et al. Simulation, fabrication and impact testing of a novel football helmet padding system that decreases rotational acceleration. *Sport Eng*. 2015;18(1):11-20. doi:10.1007/s12283-014-0160-4.

78. Rowson S, McNeely DE, Duma SM. Force transmission to the mandible by chin straps during head impacts in football. *Biomed Sci Instrum*. 2008;44(April):195-199.

79. Zuckerman S, Reynolds B, Yengo-Kahn A, et al. A football helmet prototype that reduces linear and rotational acceleration with the addition of an outer shell. *J Neurosurg*. 2018:1-8. doi:10.3171/2018.1.JNS172733.

80. Krzeminski DE, Goetz JT, Janisse AP, et al. Investigation of linear impact energy management and product claims of a novel American football helmet liner component. *Sport Technol*. 2011;4(1-2):65-76. doi:10.1080/19346182.2012.691508.

81. MacAlister A, Young T, Daniel RW, Rowson S, Duma SM. Methodology for mapping football head impact exposure to helmet pads for repeated loading testing. In: *Biomedical Sciences Instrumentation*. Vol 50. ; 2014:242-247. http://www.scopus.com/inward/record.url?eid=2-s2.0-

84904902108&partnerID=tZOtx3y1.

82. Johnson KL, Chowdhury S, Lawrimore WB, et al. Constrained topological optimization of a football helmet facemask based on brain response. *Mater Des*. 2016;111:108-118. doi:10.1016/j.matdes.2016.08.064.

83. Rush GA, Rush GA, Sbravati N, et al. Comparison of shell-facemask responses in American football helmets during NOCSAE drop tests. *Sport Eng*. 2017;20(3):199-211. doi:10.1007/s12283-017-0233-2.

84. Rush GA, Prabhu R, Iii GAR, Williams LN, Horstemeyer MF. Modified Drop Tower Impact Tests for American Football Helmets. *J Vis Exp*. 2017;120. doi:10.3791/53929.

85. Decoster LC, Shirley CP, Swartz EE. Football face-mask removal with a cordless screwdriver on helmets used for at least one season of play. *J Athl Train*. 2005;40(3):169-173. doi:10.1016/S0162-0908(08)70277-0.

86. Swartz EE, Norkus SA, Cappaert T, Decoster LC. Football equipment design affects face mask removal efficiency. *Am J Sports Med*. 2005;33(8):1210-1219. doi:10.1177/0363546504271753.

87. Copeland A, Decoster L, Swartz E, Gattie E, Gale S. Combined Tool Approach is 100% Successful for Emergency Football Face Mask Removal. *Clin J Sport Med*. 2007;17:452-457.

88. EE S, LC D, SA N, TA C. The influence of various factors on high school football helmet face mask removal: a retrospective, cross-sectional analysis. *J Athl Train (National Athl Trainers' Assoc*. 2007;42(1):11-19.

http://proxy.library.adelaide.edu.au/login?url=http://search.ebscohost.com/login.aspx?direct=true&db=c8h&AN=106301542&site=ehost-live&scope=site.

89. Swartz EE, Mihalik JP, Beltz NM, Day MA, Decoster LC. Face mask removal is safer than helmet removal for emergent airway access in American football. *Spine J*. 2014;14(6):996-1004. doi:10.1016/j.spinee.2013.10.032.

90. Endres BD, Swartz EE, Tucker WS, Decoster LC. Head Acceleration, Time, and Difficulty During Helmet Removal With and Without Facemask Removal. *Athl Train Sport Heal Care*. 2015;7(6):224-231. doi:10.3928/19425864-20151029-03.

91. Knox KE, Kleiner DM. The efficiency of tools used to retract a football helmet face mask. *J Athl Train*. 1997;32(3):211-215.

92. Nakatsuka AS, Yamamoto LG. External foam layers to football helmets reduce head impact severity. *Hawaii J Med Public Health*. 2014;73(8):256-261. doi:10.1177/0363546515570622.

93. Pellman EJ, Viano DC, Tucker AM, et al. Concussion in Professional Football: Location and Direction of Helmet Impacts - Part 2. *Neurosurgery*. 2003;53(6):1328-1341. doi:10.1227/01.NEU.0000093499.20604.21.

94. Daniel RW, Rowson S, Duma SM. Head impact exposure in youth football. *Ann Biomed Eng*. 2012;40(4):976-981. doi:10.1007/s10439-012-0530-7.

95. Crisco JJ, Fiore R, Beckwith JG, et al. Frequency and location of head

impact exposures in individual collegiate football players. *J Athl Train*. 2010;45(6):549-559. doi:10.4085/1062-6050-45.6.549.

96. Crisco JJ, Wilcox BJ, Machan JT, et al. Magnitude of head impact exposures in individual collegiate football players. *J Appl Biomech*. 2012;28(2):174-183. doi:10.4085/1062-6050-45.6.549.

97. Schnebel B, Gwin JT, Anderson S, Gatlin R. In vivo study of head impacts in football: A comparison of National Collegiate Athletic Association Division I versus high school impacts. *Neurosurgery*. 2007;60(3):490-495. doi:10.1227/01.NEU.0000249286.92255.7F.

98. Daniel RW, Rowson S, Duma SM. Head Impact Exposure in Youth Football: Middle School Ages 12–14 Years. *J Biomech Eng*. 2014;136(9):94501. doi:10.1115/1.4027872.

99. Broglio SP, Eckner JT, Surma T, Kutcher JS. Post-concussion cognitive declines and symptomatology are not related to concussion biomechanics in high school football players. *J Neurotrauma*. 2011;28(10):2061-2068. doi:10.1089/neu.2011.1905.

100. Eckner JT, Sabin M, Kutcher JS, Broglio SP. No evidence for a cumulative impact effect on concussion injury threshold. *J Neurotrauma*. 2011;28(10):2079-2090. doi:10.1089/neu.2011.1910.

101. Broglio SP, Sosnoff JJ, Shin S, He X, Alcaraz C, Zimmerman J. Head impacts during high school football: A biomechanical assessment. *J Athl Train*. 2009;44(4):342-349. doi:10.4085/1062-6050-44.4.342.

102. Nocsae. Standard Method of Impact Test and Performance Requirements for Football Faceguards. *(ND)087-18m18*. 2018;(February).

103. Versace J. A review of the Severity Index. *Proc 15th Stapp Car Crash Conf SAE Pap No 710881*. 1971:771-796. doi:10.4271/710881.

104. Gadd CW. Use of a weighted impulse criterion for estimating injury hazard. *Proc 10th Stapp Car Crash Conferfence*. 1966;SAE Paper:164-174. doi:10.4271/660793.

105. Rush GA, Prabhu R, Rush GA, Williams LN, Horstemeyer MF. Modified Drop Tower Impact Tests for American Football Helmets. *J Vis Exp*. 2017;(120). doi:10.3791/53929.

106. Vaz S, Falkmer T, Passmore AE, Parsons R, Andreou P. The Case for Using the Repeatability Coefficient When Calculating Test-Retest Reliability. *PLoS One*. 2013;8(9):1-7. doi:10.1371/journal.pone.0073990.

107. Jadischke R, Viano DC, McCarthy J, King AI. The Effects of Helmet Weight on Hybrid III Head and Neck Responses by Comparing Unhelmeted and Helmeted Impacts. *J Biomech Eng*. 2016;138:101008. doi:10.1115/1.4034306.

108. Cobb BR, Zadnik AM, Rowson S. Comparative analysis of helmeted impact response of Hybrid III and National Operating Committee on Standards for Athletic Equipment headforms. *J Sport Eng Technol*. 2016;230(1):50-60. doi:10.1177/1754337115599133.

109. Schnebel B, Gwin JT, Anderson S, Gatlin R. In vivo study of head impacts

in football: A comparison of National Collegiate Athletic Association Division I versus high school impacts. *Neurosurgery*. 2007;60(3):490-495. doi:10.1227/01.NEU.0000249286.92255.7F.

110. Bina AJ, Batt GS, DesJardins JD. A review of laboratory methods and results used to evaluate protective headgear in American football. *Proc Inst Mech Eng Part P J Sport Eng Technol*. 2018:175433711875936. doi:10.1177/1754337118759360.
111. Bina AJ, Batt GS, Desjardins JD. Development of a non-destructive method to measure football facemask stiffness. 2018:1-11. doi:10.1177/1754337118812351.
112. Rowson B, Terrell EJ, Rowson S. Quantifying the effect of the facemask on helmet performance. *Proc Inst Mech Eng Part P J Sport Eng Technol*. 2018;232(2):94-101. doi:10.1177/1754337117707859.

APPENDICES

Appendix A
Protocol for the Use and Maintenance of the NOCSAE Drop Tower

Below is the step-by-step procedure that was followed any time the NOCSAE Drop Tower was used for experiments found in this dissertation. The source of this procedure was NOCSAE Document 087, titled “Standard Method of Impact Test and Performance Requirements for Football Faceguards.” Specifically, Section 9 (Section 10 for the 2019 version of the standard), which outlines the procedure for evaluating reconditioned facemasks, was the inspiration for this protocol. The calibration procedure and data set from the course of this dissertation work is also included below. The headform was calibrated any time the headform impact location was changed. During the course of this dissertation, the NOCSAE Drop Tower was used to evaluate 1,040 reconditioned facemasks, 11 novel helmet prototypes, and 3 protective headgear systems designed for use in soccer.

CHIP LAB PROTOCOL
Written by: Alex Bina
8/31/17

Test PROTOCOL: STANDARD METHOD OF IMPACT TEST AND PERFORMANCE REQUIREMENTS FOR FOOTBALL FACEGUARDS (NOCSAE DOC ND087-12M15)

Summary of Methods and Materials

According to Section 10 of NOCSAE Document (ND) 087, titled "Recertification Procedure for Metal Faceguards", the NOCSAE linear drop tower (figure 1) is used to drop each faceguard twice, once from approximately 3 feet and once from approximately 5 feet. A faceguard is rejected according to two failure modes:

1. 3 foot fail: A faceguard is rejected if, after the 3 foot drop, the nose of the headform contacts either the faceguard or the impact surface.
2. 5 foot fail: A faceguard is rejected if, after the 5 foot drop, the recorded severity index of the impact is above 1200.

If a faceguard is rejected based on failure mode 1, the test should be repeated on a fresh guard of the same faceguard model. If face contact continues with the fresh face guard, no guards of that model/batch should be recertified until the problem is more appropriately understood.
If a faceguard is rejected based on failure mode 2, no guard of that model/batch should be recertified.

A test is considered non-compliant according to two non-compliant modes:

A. The impact velocity of the drop is out of the appropriate range. For the 3 foot drop, the impact velocity must be between 13.89-14.31 ft/s. For the 5 foot drop, the impact velocity must be between 17.94-18.48 ft/s.

B. The impact of a drop resulted in a restorable structural failure. The most common examples of a restorable structural failure are unbuckling of the chin strap or the jaw pads.

If a noncompliant test permanently damages the faceguard (through bending or spreading), the guard must be discarded and the test is considered Null. If the guard is not permanently damaged by the noncompliant test, the guard may be retested.

Step by Step Procedure

1. Receiving Masks
    - **a.** Incoming masks must be weighed and sorted based on helmet to ensure all masks are properly labeled and to plan out testing strategy
    - **b.** Once sorted, all available helmets must be equipped with appropriate mask before testing begins
2. Drop Tower Pre-Test Calibration
    - **a.** Before testing occurs, ensure all joints (headform to neck collar, neck collar to drop carriage, impact anvil) and guide wires are tightly secured.
    - **b.** Before testing occurs, unhelmeted NOCSAE headform must be raised and dropped from 18 inches 3 times to impact the forehead (Figure 2)
        - **i.** Make sure forehead is in contact w/ 0.5 in rubber pad ("modular elastomer programmer"), but the headform nose is not.
        - **ii.** Ensure velocity gate is in proper position by resting headform on impact pad and lowering the velocity gate to <0.5 in above drop carriage velocity flag. This position should be marked on velocity gate guide rod as "18 in"
    - **c.** For each 18 inch drop, the date, impact velocity, Severity Index (SI) and linear acceleration (g) must be recorded in the appropriate table (see Appendix A for example of appropriate table)
3. Drop Tests
    - **a.** Place helmet with facemask attached onto NOCSAE headform.
        - **i.** Secure chin strap at all four locations as evenly and tightly as possible
        - **ii.** Ensure brow of helmet is aligned with brow of headform
        - **iii.** Ensure facemask is securely attached to helmet shell
    - **b.** Place contact indicator lotion on nose of headform, taking care to avoid lotion placement on any part of facemask, chin strap or facemask
    - **c.** Raise helmeted headform to 3 ft
    - **d.** Reset velocity gate, Severity Index calculator BEFORE DROP
    - **e.** Press release button to drop helmeted headform
    - **f.** Enter appropriate data into testing spreadsheet (see appendix B for example of column headers).
    - **g.** Check inside of facemask and brow of helmet for lotion
        - **i.** If lotion on facemask, chinstrap or helmet brow, enter "Y" for face contact in spreadsheet (and for 3 ft drop fail)

h. Raise the helmeted headform off the impact pad in order to adjust helmet and chin strap, if necessary, to ensure proper helmet placement on headform
i. Reset velocity gate (“arm”) and Severity Index calculator
j. Raise helmeted headform to 5 foot drop height marker
k. Press release button to drop helmeted headform
l. Enter impact velocity, SI and linear acceleration into spreadsheet
m. Remove helmet from headform
n. Repeat a-m for rest of helmets equipped with facemask to be tested.

4. Drop Tower Post-Test Calibration
    a. After one round of testing for available helmets (12-16 tests), remove all headgear from headform and repeat steps 2.a-c.
    b. Compare impact data from Pre-check test to the data from 4.a. Tests valid if % difference between pre and post test calibration drops (18 in) is <7%. If >7%, previous tests invalidated and drop tower, headform, and accelerometer all much be observed for sources of error.

Appendix B
Headform Calibration, Pre and Post System Checks

Headform Calibration

Every time the headform is removed from the drop carriage, headform calibration procedures, as outlined in ND101-00m14a, must be performed. Headform calibration is performed by dropping the headform attached to the drop carriage from a height necessary to generate the impact velocity provided by Southern Impact Research Center headform calibration pad report. For the calibration used in this procedure, the headform was dropped from 56 inches to generate the 17.2 +/- 0.1 ft/s onto the 3 inch thick (Modular Elastomer Programmer) MEP calibration pad. The drop was performed three times so that the average SI is 1200 +/- 2%. The voltage for the y-component of the triaxial accelerometer was adjusted in order for the SI to be in the proper range.
Location: Front

		DROP 1			DROP 2			DROP 3			AVERAGE		
DATE	VOLTAGE (V)	DROP VEL (ft/s)	SI	PEAK G	DROP VEL (ft/s)	SI	PEAK G	DROP VEL (ft/s)	SI	PEAK G	DROP VEL (ft/s)	SI	PEAK G
5/3/2017	0.900	17.3	1224	186	17.21	1213	182	17.21	1179	182	17.24	1205	183
5/24/2017	0.916	17.22	1188	172	17.21	1239	175	17.44	1208	173	17.29	1212	173
6/5/2017	0.875	17.4	1205	183	17.4	1183	182	17.35	1188	181	17.38	1192	182
8/8/2017	1.179	16.53	1215	183	16.65	1228	187	16.64	1199	183	16.61	1214	184
8/14/2017	1.320	17.21	1215	173	17.41	1222	171	17.36	1218	175	17.33	1218	173
9/1/2017	0.770	17.21	1211	168	17.41	1224	169	17.26	1224	171	17.29	1220	169
3/16/2018	0.850	17.41	1241	181	17.41	1188	178	17.3	1118	173	17.37	1182	177
6/26/2018	1.064	17.27	1187	172	17.28	1176	172	17.29	1281	174	17.28	1215	173

Pre- and Post-System Check Procedure Summary:

Every time the NOCSAE drop test system (Figure 1) is used, the bare NOCSAE headform is dropped in triplicate from 18 inches onto the NOCSAE ½ inch MEP pad before and after testing. For each of the 3 pre- and post-testing drops, the severity index, peak acceleration and impact velocity are recorded and averaged. If the post-testing (labelled A in table below) average severity index is within 7% of the pre-testing (labeled B in table below) average severity index, the testing is valid. If the post-testing average severity index differs from the pre-testing average severity index by more than 7% (labelled in red in Table 5), the testing is invalid and must be repeated.

DROPS	DATE	VELOCITY (ft/s)		SEVERITY INDEX		PEAK g	
1-14	5/10/2017	8.29	5%	613	2%	165	4%
	5/10/2017	8.67		603		158	

Appendix C
Necessary Data for each Drop Test

Data Column Headers:

TEST #	TEST DATE	HELMET MNF	HELMET	HELMET CODE	MASK MNF	MASK STYLE	MASS (g)	RECOND CLIENT	RECOND DATE	LAB TEMP. (

Data Group 1: This data describes the mask and helmet being tested as well as the test conditions. This data can be entered either before or after the three foot drop.

3 FT VEL (13.89-14.31 FT/	3 FT CONTA	3 FT FAIL?	NUM. CHIN	NUM. JAW

Data Group 2: This data should be entered after the three foot drop, indicating whether any chin strap or jaw pad fails occurred. If so, 3 ft drop should be repeated until no chin strap or jaw pad failure occurs. Drop data should only be recorded on drops without chin strap or jaw pad failures.

5 FT VEL (17.94-18.4	5 FT SI NOCSA	5 FT PEAK G	5 FT FAIL?	NUM. CHIN	NUM. JAW

Data Group 3: This data should be entered after the five foot drop, indicating whether any chin strap or jaw pad fails occurred. If so, 5 ft drop should be repeated until no chin strap or jaw pad failure occurs. Drop data should only be recorded on drops without chin strap or jaw pad failures.

ANY FAIL?	SPREADING?	No. CHIN FAILS	No. JAW FAILS	NOTES

Data Group 4: This data reports any failures that occurred, whether for the 3 ft or 5 ft drops. The total number of chinstrap and jaw pad failures should be entered here, as well as any notes from the drop tester.

Appendix D
Preparation and Validation for Dynamic System for Facemask Evaluation

Iterative design of facemasks with respect to geometry, material, or manufacturing process, has been difficult without a rapid method for specific component evaluation. In addition, measuring the effect of repeated impacts to the facemask is not possible without confounding effects introduced by the rest of the helmet system on the measured impact response. Thus, a need exists for an evaluation process that evaluates the impact response of an individual football facemask as a middle step in the helmet design process. Understanding how facemasks of different materials, geometries, manufacturing process, or age differ in their impact response will improve the ability of equipment managers, coaches, parents, and athletes in choosing protective equipment most appropriate for the safety of the athlete. Chapter Three presented a method that has been effective in differentiating facemasks based on their structural stiffness. Not only is structural stiffness effective in differentiating across different facemask designs and materials, but the process has a minimal permanent effect on the shape of the facemask, which ensures the continued use of the facemask as after testing has been performed. Informal research (unpublished) revealed that the structural stiffness of the facemask has no relationship to the impact response of the facemask on a helmet during simulated head impacts using a

NOCSAE Drop Tower. Thus, to demonstrate that structural stiffness is a predictor of the impact response of a facemask, a novel method for impacting a facemask for the sole purpose of facemask evaluation is proposed.

The goal of this appendix is to summarize preliminary work on a novel method that can be used to evaluate the impact response of a football facemask without the noise introduced by the rest of the helmet system. This summarizes the overview of the proposed dynamic impact test apparatus, method, and theoretical background and indicates the reliability of the proposed dynamic impact protocol as well as the validity of using the dynamic impact test to relate facemask structural stiffness to impact performance. By the end of this appendix, it will be clear that further work in this area is needed to inform the decisions of future facemask designers, manufacturers, and users based not only on the facemasks visual appeal, but, more importantly, their performance upon impact.

Methods:

There are several components that must be included to ensure a reliable and valid facemask impact evaluation. For the purposes of this chapter, evaluation reliability refers to the repeatability of generating the same results when using the same inputs. For a dynamic impact test, each impact of the same severity should generate the same response so that differences in response are related solely to the differences in facemask characteristics, such as age, geometry, material, or manufacturing process. To ensure reliability, the orientation of the facemask

must be easily controlled. Variance in facemask orientation results from differences in facemask geometry. For instance, from Chapter 3, Figure 3.7B presents several different facemask geometries made from similar materials manufactured by the same process, with the same impact history. These facemasks represent four different helmets, and each of the helmets require a different attachment angle. The differences in attachment angle of these facemask styles require an apparatus that allows for variety in facemask support angles. To accomplish variable facemask orientations, the dynamic impact test apparatus must include a fixture that has six degrees of freedom prior to impact but can lock into position to ensure rigid constraint at the facemask attachment interface. Figure D1 summarizes the needs of the facemask attachment apparatus before and during impacts.

The dynamic impact system was created by modifying a drop impact cushion testing apparatus. The system was used to evaluate both the coefficient of restitution, the deflection of the impactor, and the plastic deformation (“permanent spreading”) of the facemask. The theory behind the dynamic impact system is that relationship between these dynamic impact facemask characteristics and the facemask stiffness measured via the quasi-static methodology outlined in Section 3 would be linear, making the quasi-static evaluation system an effective, repetitive, non-damaging method for to characterize modern and future facemask materials and geometries.

The first decision made in establishing a dynamic system for facemask evaluation was the boundary conditions for each facemask. Three methods were proposed for facemask boundary conditions within the cushion drop-impact apparatus:

1.) “fully restricted”

2.) “ground support”

3.) “helmet clips”

The fully restricted system is presented in Figure D.2C. This system can be further adapted to accommodate the “ear hole” clip placements to generate head impacts that better relate to scenario 3, the “helmet clip” boundary condition. The

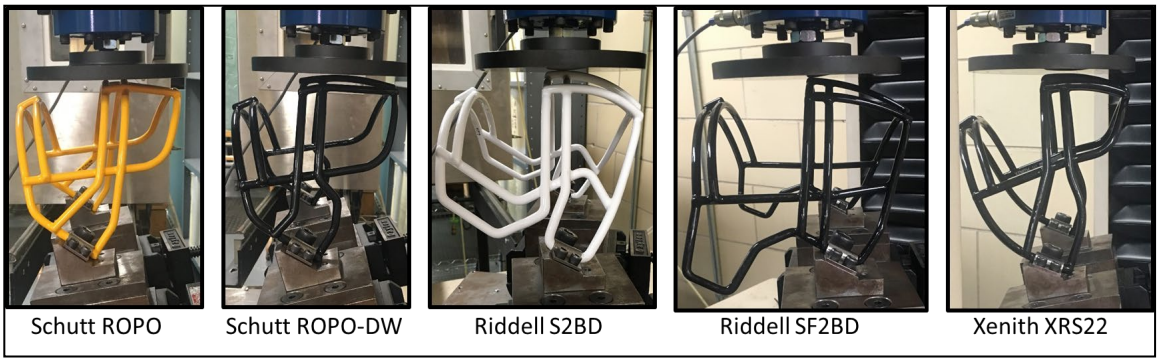

Figure D.1: Five different facemask geometries that represent four different helmet attachment angles. The differences in facemask attachment angles require a dynamic impact test apparatus fixture that has 6 degrees of freedom prior to impact. Impact location on the facemask is also variable between mask styles, since the location of horizontal bars across the nose location differs across mask styles. Difference in horizontal bar location further outlines the need for a dynamic impact test apparatus to be variable in 6 degrees of freedom prior to impact.

fully restricted method would prevent any translation of the ends of the facemask traditionally attached to a helmet shell. The fully restricted method would treat the

facemask as a spring and evaluate the spring characteristics of the mask materials and geometry exclusively. It was determined that a starting point for evaluating impact performance of a facemask is to fully constrict the connection locations using a “fully restricted” boundary condition. The fully restricted boundary condition would feature diminished ecological validity but would most likely generate the most repeatable impact characteristics of the facemask with the least amount of impact noise.

In addition to the method used to constrict the facemask, the locations of facemask constriction were of concern. Traditionally, during the helmet design era between 2012 and 2019, facemasks were fixed to the outer shell of a helmet using either a 2x2 method (two locations at the forehead of the helmet, two locations near the ear holes) or a 4 side method (all four connections on the side of the helmet, two on the upper crown of the head, two lower and closer to the ear holes). Early designs for the dynamic cushion test modifications attempted to fix the facemask at both the side and forehead locations. However, in order to closer simulate the boundary conditions of the quasi-static test, the forehead connection locations were abandoned. This decision also holds merit as more recent helmet designs have abandoned the forehead connection location between facemask and helmet. The evolution of facemask boundary conditions can be found in Figure D.2.

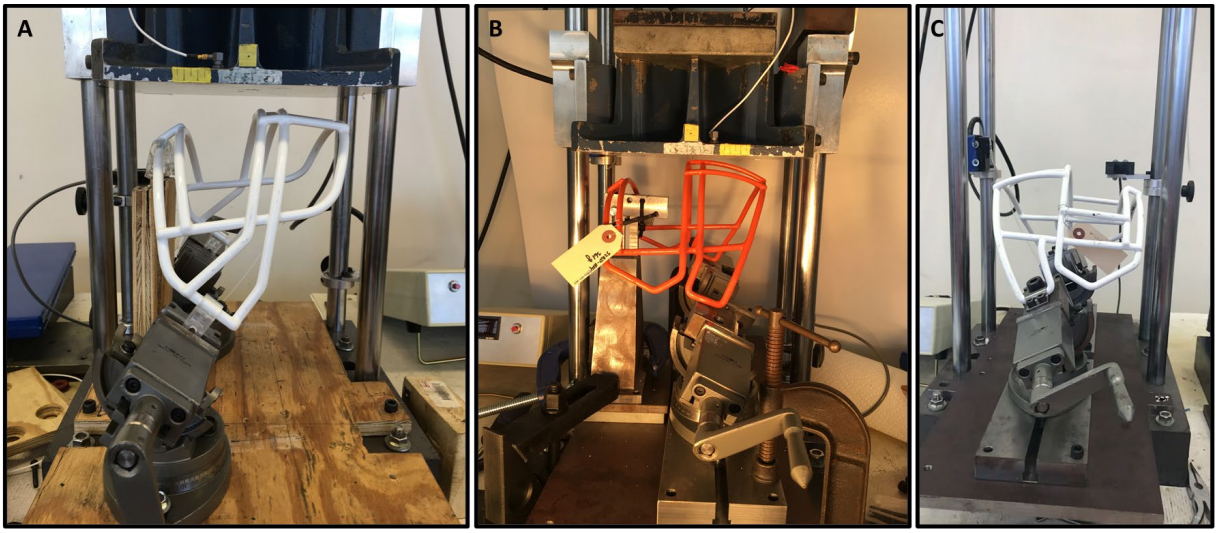

Figure D.2: A.) The first boundary conditions proposed to fix a facemask upon impact using the dynamic cushion tester featured helmet clips bound by two angle vices and a vertical support structure to support the forehead clip locations for the facemask. B.) A rigid method to "fully restrict" the facemask connection upon impact also features a vertically adjustable forehead support structure that was abandoned due to increased noise upon impact. C.) The final impact boundary conditions (fully restricted, no forehead support) used for the duration of impact testing.

Other considerations for a dynamic impact evaluation system were:

1.) Impact mass and velocity (energy transfer)

2.) Impact drop height (to dictate impact velocity)

3.) Impact platen geometry

The goal of impacts using the modified cushion test system is to generate impacts to the facemask that most represent previous impact conditions found both on the field and used in laboratory study. Previous on-field research has demonstrated that the average force applied by the striking player (which includes the torso, head, and neck mass) during concussive impacts were 7,642 ± 2,259 N, and the force applied to the "striking neck" was 6,372 N ± 2,486 N.[44]

The helmet plus a facemask commonly weighs between 1.3[54] and 1.9 kg, and the head and neck form commonly used in laboratory testing weights 4.38 kg[44] making the average range of head, helmet, and facemask impact mass between 6.04 and 6.73 kg.[54] Other studies estimated an appropriate torso mass to weight 5x the mass of the head (roughly 21.9 kg).[43] In this same research series, the authors used a 43.4 kg mass to estimate the “striking player” during impacts.[42] Another laboratory impact study used a 95 kg torso and a 5 kg head.[101] However, the limitations of the cushion test system prevented an impactor mass greater than 14.84 kg, which meant that impact mass would only affect the impact energy transfer based on the allowed vibrations of the impactor following impact (greater mass would be less impacted by the impact vibrations of the system). The manipulation of impact velocity (and thus, drop height) to generate the proper energy transfer to the impacted facemask would be the focus of early pilot testing.

In terms of impact energy transfer, Bartsch et al used 27 J for “low impact severity, 50-54 J for medium impact severity, and 67-89 J for high impact severity.[40, 55] As discussed by Bartsch et al, the reason for a range of impact energy transfer is the result of an increase in impact noise at higher impact velocities. As evidenced by the above, a lack of consensus exists for impact conditions to simulate dynamic impact performance in a laboratory setting.

The first set of pilot drops were performed to confirm the appropriate drop height using a consistent impact mass (14.84 kg). A high-speed camera

(Olympus i-Speed 3 Series) operating at a frame rate of 10,000 fps with a 50 mm 1:2.5 lens was used to calculate the impact duration, deflection upon impact, and inbound and outbound velocity of the impact platen. The drop heights and estimated impact energy and impact velocity are recorded in Table D.1.

Table D.1: Estimated impact conditions for Cusion Drop Tester.

Energy (J)	Impact Velocity (m/s)	Drop Height (m)
27	1.96	0.185
52	2.73	0.357
78	3.33	0.536
125	4.23	0.859
209	5.47	1.436

The protocol to use the high speed camera to measure the impact velocity was to pause the video on the frame upon which the impactor platen first made contact with the facemask, then rewind ten frames before impact was generated. The i-Speed software would then calculate the velocity the impactor indicator point was travelling during the final ten frames prior to impact, and this would be the impact velocity. To calculate the impact deflection, the video file was paused at the frame upon which the impactor platen changed direction in the vertical axis. The i-Speed software then calculated, based on the relationship between displacement and pixels established for each data collection session, the distance the impactor platen indicator point traveled during the downward trajectory of the impactor platen when in contact with the facemask. The impactor platen outbound velocity was calculated during the ten frames following the

frame upon which the impactor platen began to travel in an upward trajectory. Permanent spreading was measured using a pair of calipers to measure the distance between the furthest two points on the facemask in the horizontal direction and subtracting this distance from the identical distance measured prior to impact.

Once the protocol for using the dynamic cushion test system was established, a series of assessments were performed on facemasks that also had quasi-static data, presented in Chapter 3. The same facemasks that were used during quasi static testing were used in the dynamic impact evaluations because it was determined, as outlined in Chapter 3, that the quasi-static test did not result in permanent damage to the facemask.

Results

The reliability assessment of the proposed stiffness test was performed by repeating the stiffness measurement process outlined in section 3.2.2 on a single mask style, and calculating its coefficient of variance. One previously used and reconditioned mask of three different styles were used for the reliability testing: G2B and S2BD-LW (Riddell, BRG Sports, Elyria, OH) and NJOP (Schutt Sports, Litchfield, IL). The stiffness testing was performed at the “nose” location (Figure 1C) 11 times for the S2BD-LW mask, 10 times for the G2B mask, and 21 times for the NJOP mask. The stiffness measured for each style is represented in Figure 3.6 as a box and whisker plot. The box represents the interquartile range of stiffness for each mask style, and the whiskers represent 1.5x the 3rd and first

quartile, respectively. The coefficient of variance for each mask style subgroup was also calculated by dividing the standard deviation by the subgroup mean and is reported in Figure 3.6. The repeatability coefficient for each mask stiffness was measured and is recorded in Table 3.2.[106]

Like the process of determining reliability of the method proposed to measure the structural stiffness of a football facemask, to determine the reliability of the dynamic impact test, one must evaluate the ability of the test to expose the facemask to the same input and result in the same output. The reliability of the dynamic impact test can then be compared to the reliability of the manufacturing process to then highlight the discrepancies in dynamic impact performance as being potentially the result of a noisy test. One method to measure the reliability of the manufacturing process for facemasks is to measure the coefficient of variance of the facemask for each style. The mass of each of the 10 facemasks for each of the 11 facemask styles is summarized in Figure D.3. The coefficient of variance in the facemask mass within each facemask style ranged from 0.39% (SF2BDC-TX) to 1.4% (TROPO). The variance in facemask mass was not related to the average facemask mass for each style. Facemasks that fit the Riddell SpeedFlex helmet had the lowest average coefficient of variance in facemask mass (0.46%) while the facemasks that fit the Schutt XP helmet had the highest average coefficient of variance in facemask mass (0.917%).

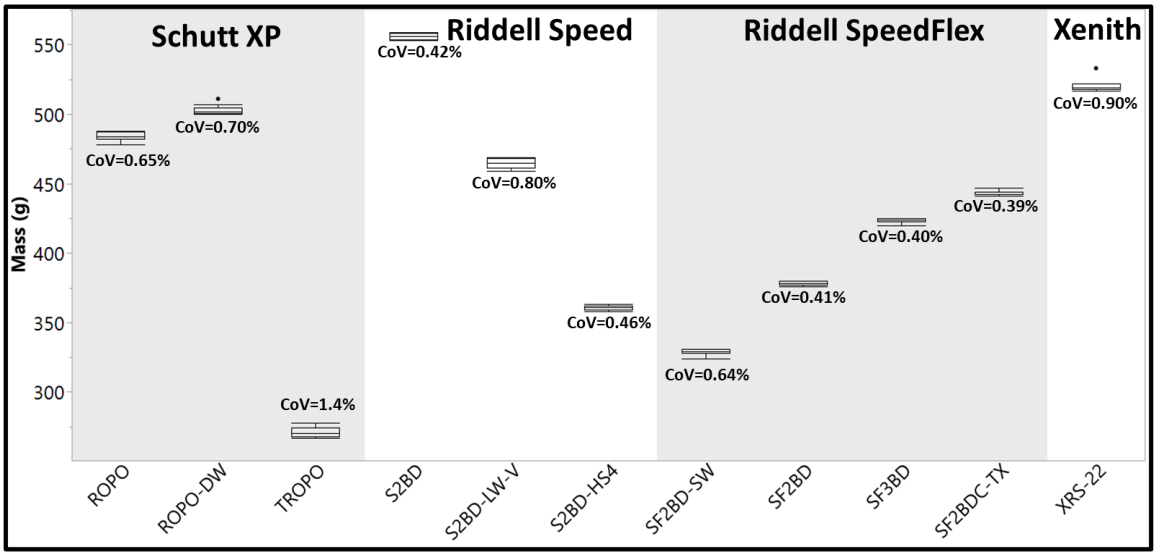

Figure D.3: Mass differences based on facemask design and material, with coefficient of variance within a facemask design included.

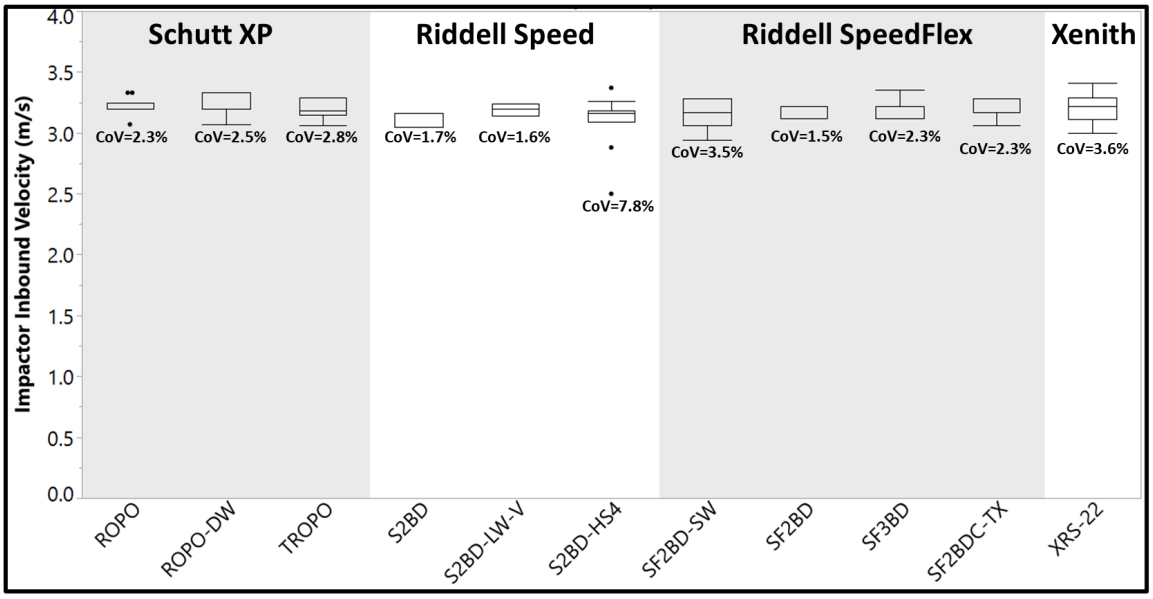

Figure D.4: Reliability of impact velocity used to evaluate the relationship between impact response and quasi-static stiffness characteristics of facemasks.

The ability of the dynamic impact test to generate reliable input velocity is summarized in Figure D.4. After impacting ten masks of each of the 11 facemask styles, the average impact velocity of the dynamic impact test platen was 3.18 m/s (+/- 0.11 m/s) and the average coefficient of variance was 3.5%. Two impacts, both to the S2BD-HS4, were performed with an input velocity less than 3.0 m/s. Without these two impacts, the average impact velocity was 3.18 m/s (+/- 0.0863 m/s) and the average coefficient of variance was 2.7%, and the coefficient of variance for the remaining 8 impacts was 2.4%, a decrease from the original 7.8% coefficient of variance for all ten impacts to the S2BD-HS4 facemask style. Further explanation for the two impacts less than 3.0 m/s can be found in the discussion section 4.3.4.

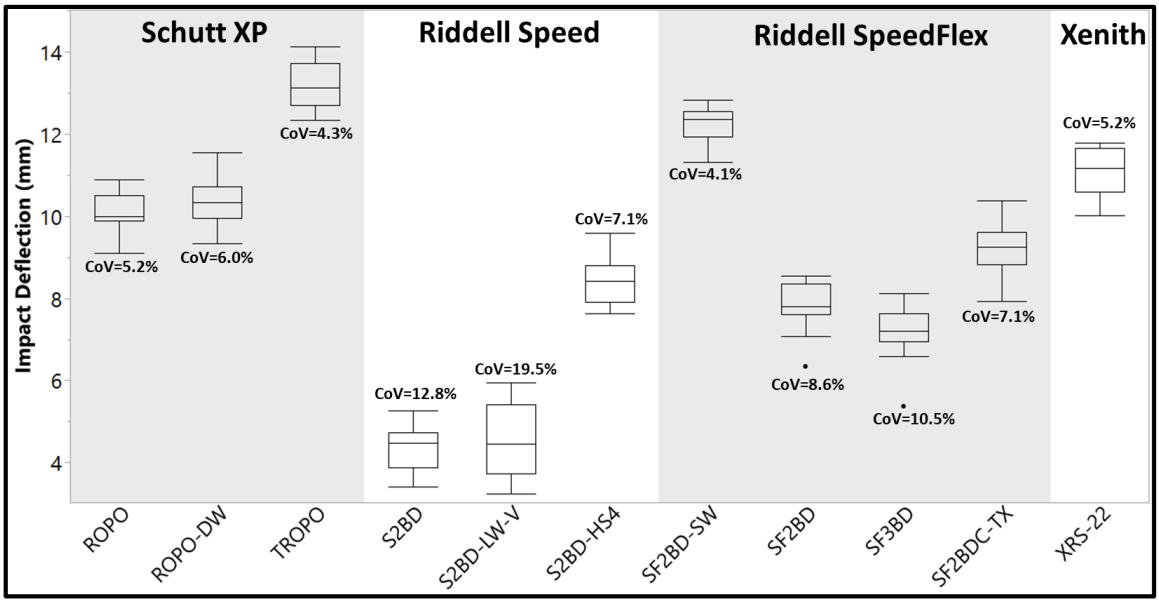

Figure D.5: Impact deflection variance within facemask impact response.

The variance in the impact deflection, impact duration, and impactor acceleration will be the result of the variance in facemask dynamic impact performance, the ability of the test to generate reliable impacts to the facemask, and the variability in the degrees of freedom allowed by the dynamic impact test apparatus. The average duration of the impacts to the ten facemasks for each of the 11 facemask styles is summarized in Figure D.6. The largest coefficient of variation occurred for the SF2BDC-TX (5.1%), the SF2BD-SW (7.5%), and the XRS-22 facemasks (12.0%). For the rest of the facemask styles, the coefficient of variation of the impact duration ranged from 0.65% (SF2BD) to 2.6% (ROPO). Impact duration ranged from 11.2 ms to 19.6 ms, with an average duration of 14.4 ms (+/- 1.84 ms).

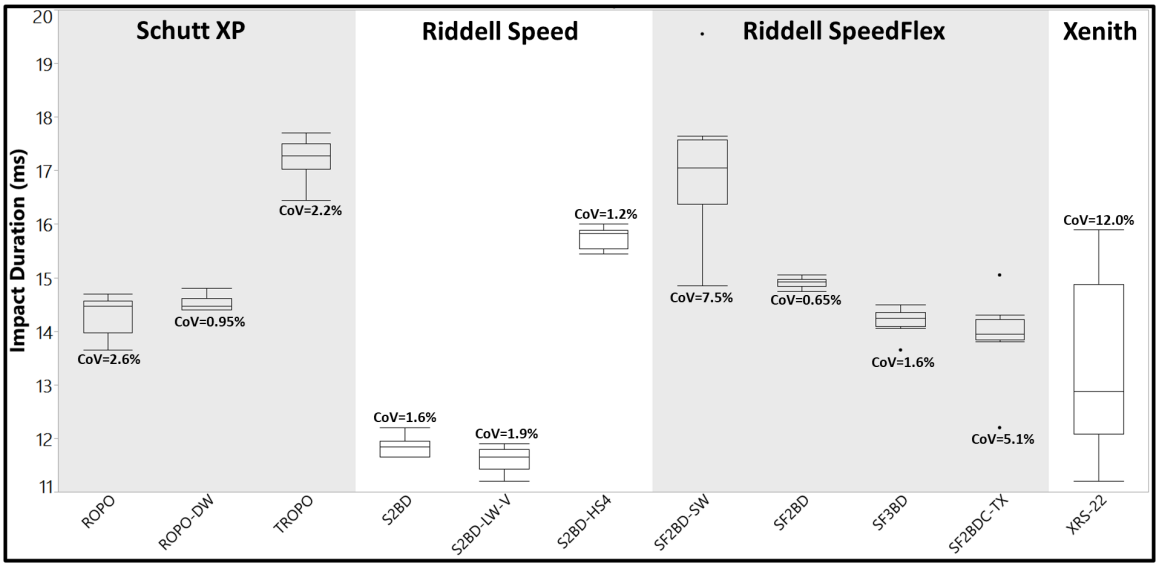

Figure D.6: Impact duration variance within facemask impact response.

The variation of the impactor acceleration for each impact to the ten facemasks of all 11 facemask styles is summarized in Figure D.7. The impactor acceleration for the 110 impacts ranges from 47.1 g to 83.3 g, with a mean of 64.8 g (+/- 9.14 g). The largest coefficient of variance for impactor acceleration is 12.9% (S2BD) and the smallest coefficient of variance for impactor acceleration is 3.0% (SF2BD).

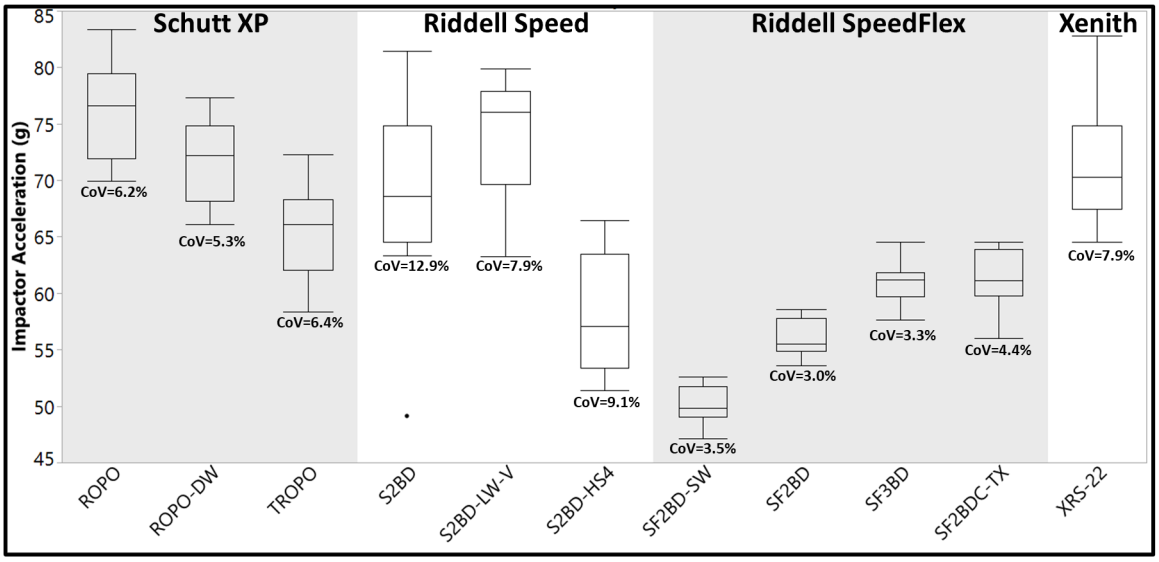

Figure D.7: The variance of acceleration of the impactor platen upon impact within a facemask style/material.

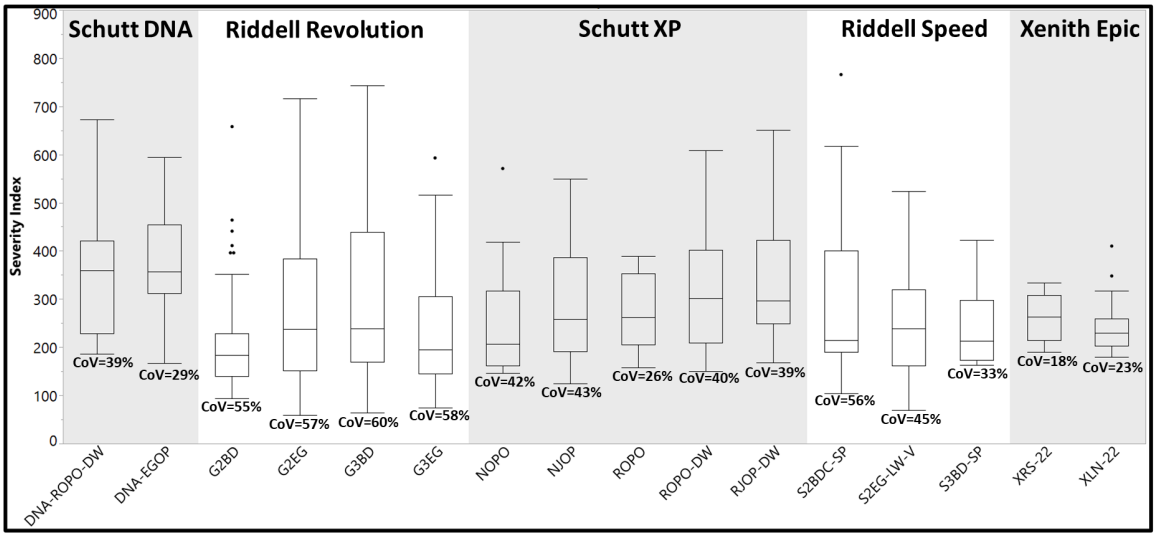

Figure D.8: For comparison to the dynamic cushion impactor test, the variance of the severity index measured using the NOCSAE drop tower is displayed in this figure.

For comparison to the reliability of the dynamic impactor test, the reliability of the NOCSAE twin-wire drop tower test is summarized in Figure D.8. The severity index of 975 impacts with an impact velocity of 5.46 m/s (+/- 3%) are presented in Figure 2.7. These impacts occurred using a biofidelic headform fitted with a helmet and facemask system. This data is further examined in Section 2.3.1. The coefficient of variation of the severity index of the 975 impacts from 5 feet range from 18% (XRS-22) to 60% (G3BD).

The ability to use this modified cushion tester to differentiate the impact performance of facemasks based on design criteria was deemed inappropriate. For example, the impact duration for each facemask is summarized in Figure D.9. The data demonstrated in Figure D.9 there is no clear facemask design

characteristic that seems to drive impact duration. For instance, group A contains a titanium ROPO style mask and a Single Wire Speedflex mask that is constructed with traditional carbon steel. Group C, on the other hand, contains five facemask styles of various vertical bar numbers, all of which are the traditional carbon steel material. Finally, Group E contains two facemasks, one using the hollow tube light weight material, and another using traditional carbon steel material. If impact duration was an appropriate metric to differentiate facemask impact characteristics, a pattern based on facemask material or bar location would be identified, but it is clear this pattern does not exist. Similar results (unreported here) were found for all impact metrics (impact deflection, impactor platen acceleration, facemask coefficient of variation, and permanent facemask spreading).

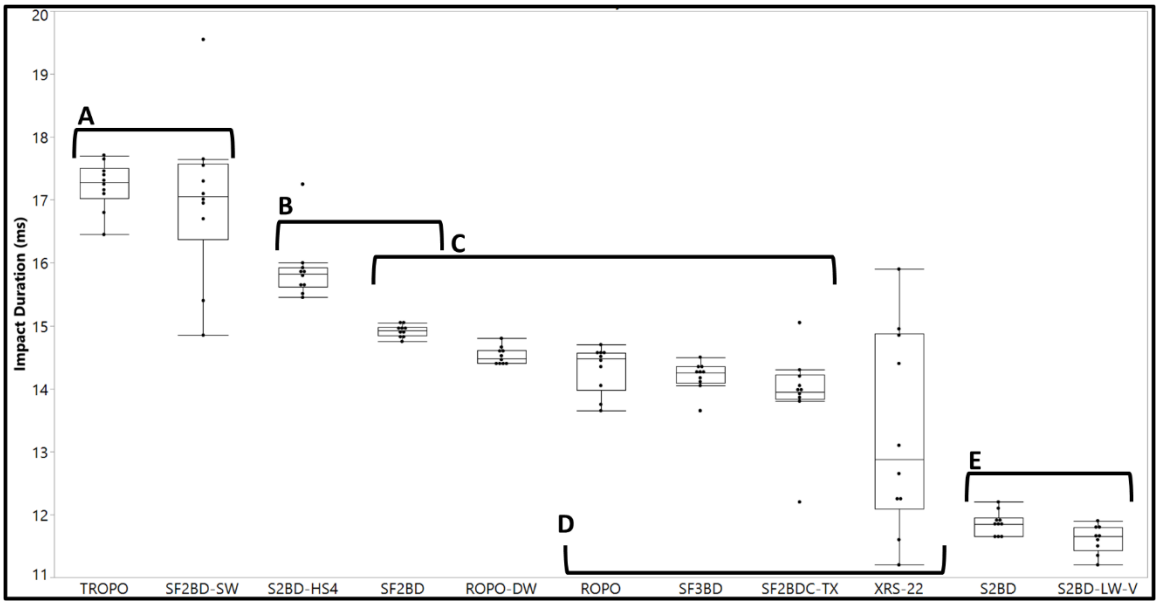

Figure D.9: The statistical significance of differences in the impact duration for each facemask style/material. Each letter designates a group that is statistically significantly different than other group. For instance, facemasks in group C are statistically different than the facemasks in group E.

Despite a dubious ability to differentiate facemask design based on performance upon impact, an attempt was also made to draw a linear relationship between any impact performance metric (impact duration, impact deflection, impactor platen linear acceleration, facemask coefficient of restitution, and permanent facemask spreading) and the facemask structural stiffness measured in Chapter 3. The relationship between the impact duration and structural stiffness is represented in Figure D.10. Almost 60% of the variance in facemask structural stiffness was explained by variance in the impact duration. No other impact metric expressed an r^2 value greater than 0.5, (most were <0.20). The lack of validity of the cushion test methodology to connect to the non-damaging quasi-static results to characterize facemasks based on structural stiffness inspired this

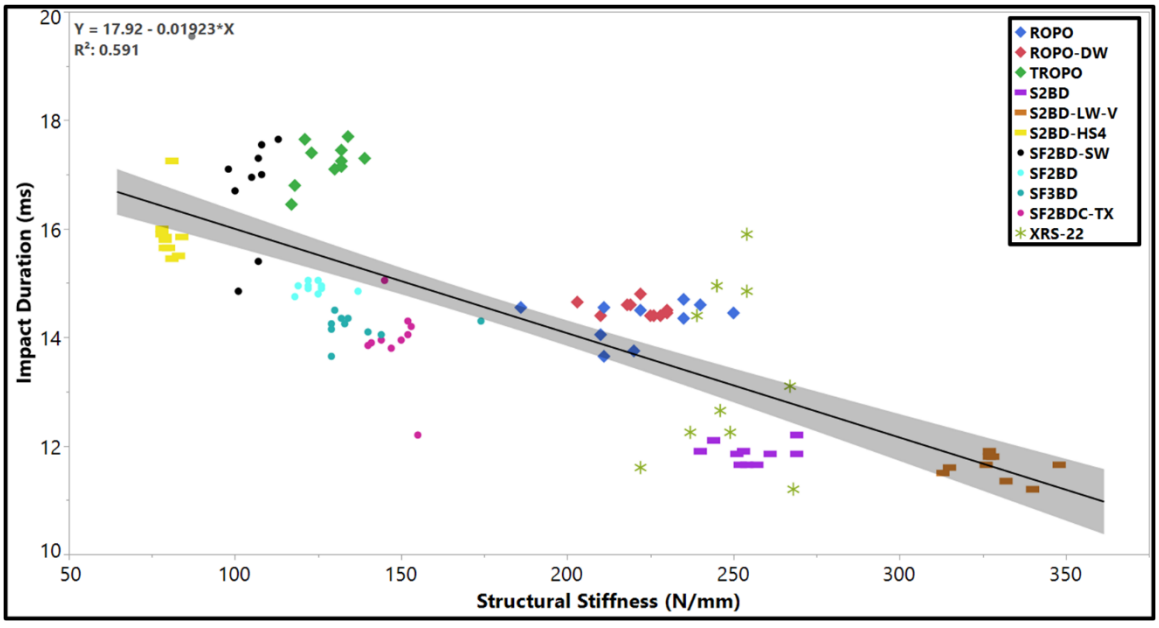

Figure D.10: The linear relationship between structural stiffness and the impact deflection for each of the 11 facemask styles/materials.

research group to postulate the need for a different system to impact facemasks for design characterization.

Based on the above data, it was deemed that the current iteration of the modified cushion impact test system was not effective in generating the appropriate and translatable impact characteristics for each facemask design. Even though impact inputs were deemed reliable and repeatable, the impact response, especially impactor platen acceleration and coefficient of restitution of the facemask expressed large variance. The lack of separation based on facemask design in several impact response metrics indicates the insufficiency of this system to properly generate impacts to the facemask as well as characterize the impact response of a facemask. The lack of apparent correlation between the structural stiffness of the facemask and the impact characteristics (duration, deflection, permanent spreading, coefficient of restitution, and impactor platen linear acceleration) requires a re-evaluation of the system used to generate impacts to a facemask as well as the metrics chosen to characterize the impact response of football facemasks. Future work in this field will require an appropriate system, apparatus, and methodology to generate repeatable impacts to a facemask to characterize facemask impact response that will inform future design decisions in the field of football head impact safety.

Contact Information

DEPARTMENT OF FOOD, NUTRITION, AND PACKAGING SCIENCES
College of Agriculture, Forestry & Life Sciences
223 Poole Agricultural Center Box 340370
Clemson, SC 29634-0370
Phone: 864.650.7936 FAX: 864.656.0331

DEPARTMENT OF BIOENGINEERING
College of Engineering and Science
301 Rhodes Engineering Research Center
Clemson, SC 29631-0905
Phone: 864.656.7276 FAX: 864.656.4466